POLYTECHNIC UNIVERSITY OF MARCHE
Ph.D. Course

Biomedical sciences

Replicative capacity and phenotypic sensitivity to antiretroviral compounds of HIV-1 strains from recently infected and chronically treated patients

Ph.D. student
Dr. Sara Caucci

Tutor
Prof. Stefano Menzo

XXXII cycle

1. Introduction

Since over 35 years ago, when it was identified as a new syndrome, the infection by Human Immunodeficiency Virus (HIV) has expanded to a pandemic. The high number of deaths associated to the infection represents one of the most challenging health issues worldwide, with implications in global economic and political stability. The HIV targets and destroys immune cells and impairs the function of the immune system, as infected individuals gradually become immunodeficient. Immunodeficiency results in increased susceptibility to a wide range of infections, cancers and other diseases that people with healthy immune systems can fight off. The most advanced stage of HIV infection is Acquired Immunodeficiency Syndrome (AIDS), which can take from 2 to over 15 years to develop depending on the individual. AIDS is defined by the development of certain cancers, infections, or other severe clinical conditions that become the major sources of morbidity and mortality for these patients (Knipe DM *et al*., 2013, Fields Virology).

The annual number of global deaths from AIDS-related illness among people living with HIV has declined from a peak of 1.9 million in 2004 to 770 000 in 2018. Since 2010, AIDS-related mortality has declined by 34% according to Joint United Nations Programme on HIV/AIDS (UNAIDS) in 2018.

The World Health Organization (WHO) estimates that 37.9 million people living with HIV at the end of 2018 globally of whom 2.5 million living in Europe. Africa is the most affected continent, with 25.7 million HIV infected people (Figure 1.1) (https://www.who.int/en/news-room/fact-sheets/detail/hiv-aids). In Italy 130 000 people live with HIV and new HIV infections and AIDS-related deaths decrease from 2005 to 2017 according to data from UNAIDS 2018 (https://www.unaids.org/sites/default/files/media_asset/unaids-data-2018_en.pdf).

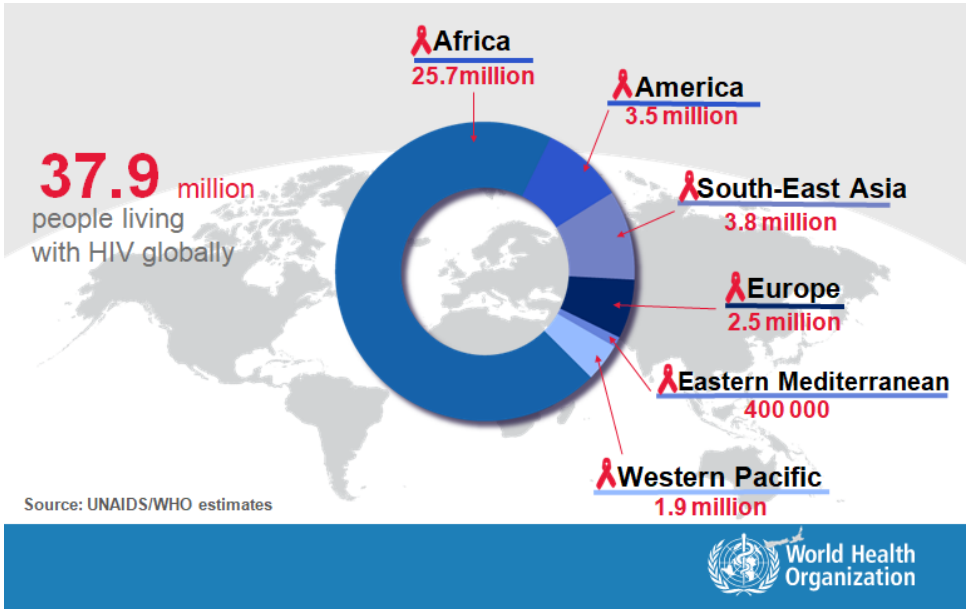

Figure 1.1: people living with HIV by WHO region in 2018 (from https://www.who.int/hiv/data/en/).

Thanks to the expansion of antiretroviral therapy (ART) HIV infections globally continue to decline in 2018. A recent study published in 2019 shows that the risk of HIV transmission through sex, where condoms are not used is virtually zero when HIV viral load is suppressed through correct antiretroviral treatment. The 2018 report by UNAIDS shows that new infections decline from a peak of 3.4 million in 1996 to 1.7 million in 2018 globally. Available data suggest that 54% of new HIV infections globally are among "high risk" populations and their sexual partners. High risk populations include: men who have sex with men (MSM), people who inject drugs, sex workers and their clients, and transgender people (https://www.who.int/en/news-room/fact-sheets/detail/hiv-aids). An HIV vaccine will probably be necessary to end the HIV pandemic but global HIV-1 genetic diversity is a major obstacle.

After zoonotic transmission from non-human primates to humans at the beginning of the 20th century, HIV-1 group M diversified into distinct subtypes: A, B, C, D, F, G, H, J, K and, recently, L. Recombinants between subtypes are: circulating recombinant forms (CRFs) or unique recombinant forms (URFs). A recent study reports the global prevalence of different HIV-1 subtypes and recombinants. Subtype C is the most prevalent

clade with 46,6% of global HIV-1 infections. Subtype B is responsible for 12,1% of infections, followed by subtype A (10,3%), CRF02_AG (7,7%), CRF01_AE (5,3%), subtype G (4,6%) and subtype D (2,7%). The contribution to global HIV-1 infections of recombinants, including CRFs and URFs, is 22,8%. Subtype C has the highest prevalence in southern Africa. During 2005–15, subtype B increased , subtypes A and D were stable, and subtypes C and G and CRF02_AG decreased globally (Figure 1.2) (Hemelaar J. *et al.*, 2019).

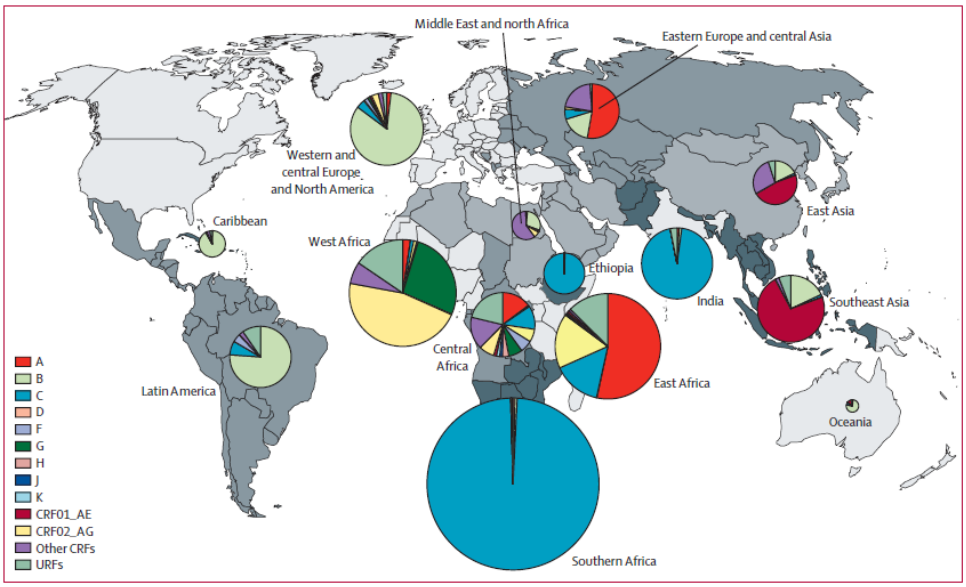

Figure 1.2: regional distribution of HIV-1 subtypes, CRFs and URFs, 2010-2015; countries forming a region are shaded in the same color on the world map and the surface area of each pie-chart corresponds to the number of people living with HIV in each region (from Hemelaar J. et al., 2019).

Surveillance of the global molecular epidemiology of HIV-1 remains crucial for the design, testing, and implementation of HIV vaccines (Paraskevis D., *et al* 2019). Actually HIV vaccine is under study but UNAIDS has developed the ambitious 90-90-90 strategy with the objective to end the AIDS epidemic by 2030 by achieving the following three targets: 90% of all people living with HIV know their status, 90% of all people diagnosed with HIV receive sustained ART and 90% of all people on ART are virally suppressed.

In 2018, 79% of people living with HIV knew their status. About 8.1 million people didn't know that they were living with HIV. Among people who knew their status, 78% were accessing treatment. And among people accessing treatment, 86% were virally suppressed (Figure 1.3) (https://www.unaids.org/en/resources/documents/2017/20170720_Global_AIDS_update_2017).

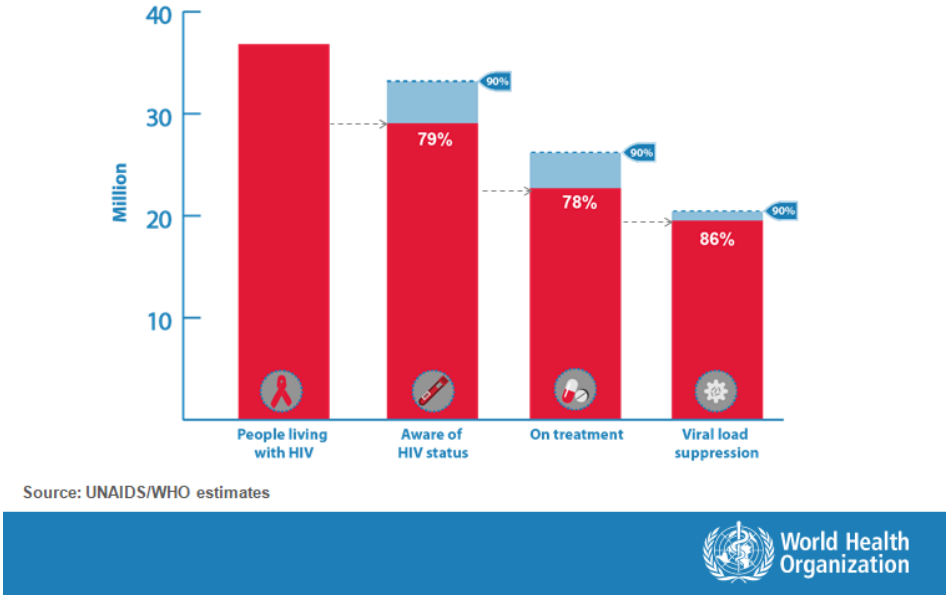

Figure 1.3: the UNAIDS 90–90-90 strategy in 2018 (from https://www.who.int/hiv/data/en/).

2. HIV life cycle

HIV-1 directly infects the $CD4^+$ T lymphocytes, $CD4^+$ cells of the macrophage lineage and some populations of dendritic cells. HIV-1 uses the CD4 cellular receptor and a chemokine receptor as coreceptor, CCR5 or CXCR4, during entry into susceptible cells. The HIV life cycle is complex, with a duration and viral production depending on the target cells type and cell activation. It can be divided into several steps: attachment, entry, reverse transcription, integration, protein processing and maturation (Figure 2.1). The first step is the interaction between the envelope glycoprotein of the virus (gp120) and specific host-cell surface receptors (CD4 T-cell receptor) of the host cell (binding or attachment). This interaction produces a conformational change in gp120, which allows it to bind to the chemokine co-receptor, either CCR5 or CXCR4. The HIV envelope and host cell membrane fuse (fusion). Fusion creates a pore through which the viral capsid enters the cell. Following entry into the cell, the viral reverse transcriptase (RT) enzyme catalyzes the conversion of viral RNA into proviral DNA. The proviral DNA becomes part of the pre-integration complex, which enters the nucleus. The proviral DNA is then incorporated into the host-cell genome using the HIV integrase (IN) enzyme (integration). HIV viral polyproteins are then expressed using host cell machinery. New HIV proteins and HIV RNA move to the surface of the host cell and assemble into immature noninfectious virus and it leaves the host cell by a process called budding. During the process of budding, HIV acquires the outer layer and envelope and releases protease (PR) enzyme. PR is responsible for the post-translational processing and nicks the long *gag-pol* polyproteins in the noninfectious, immature and non-competent virus, creating the mature infectious virus (maturation) (Warnke D. *et al.*, 2007).

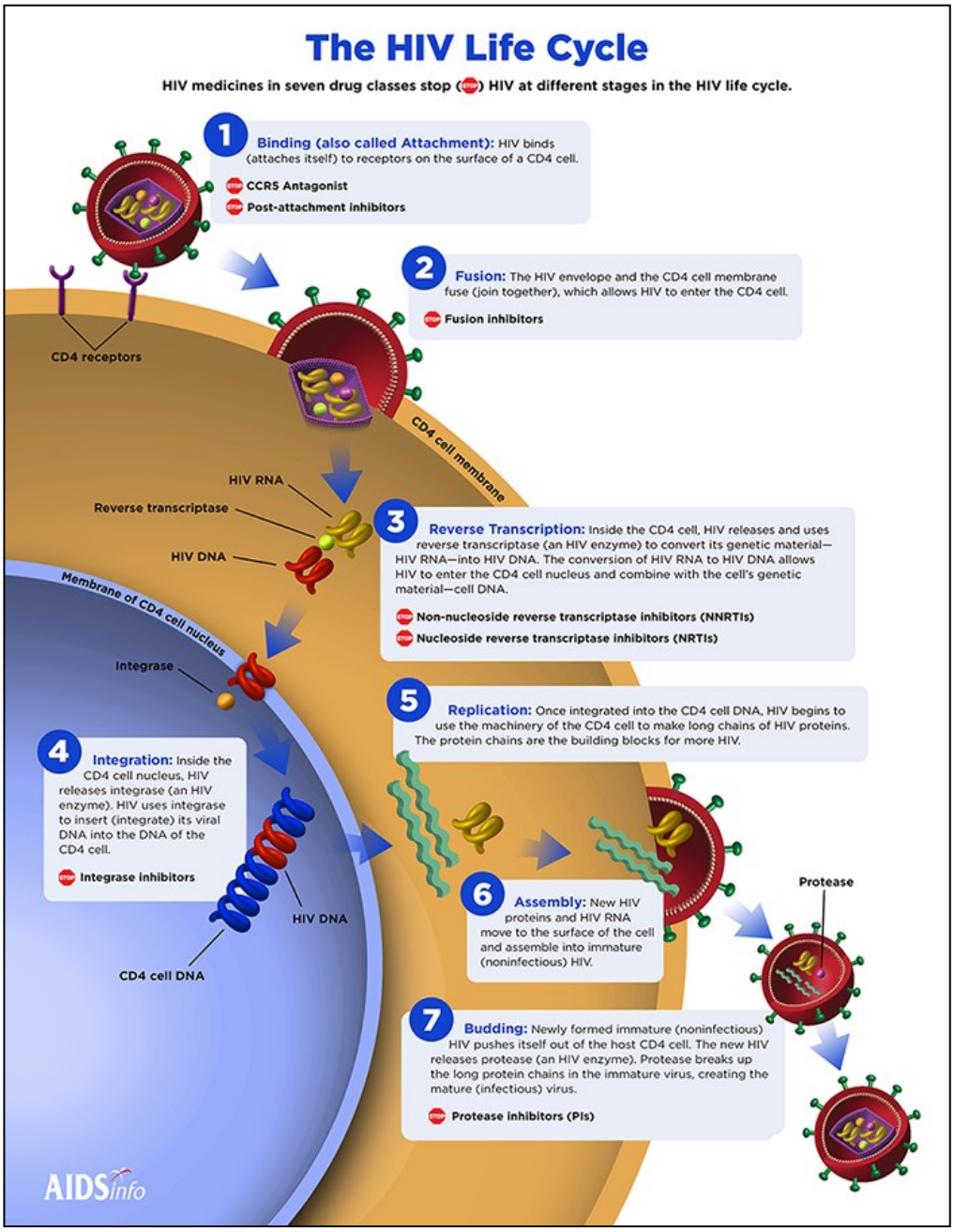

Figure 2.1: the HIV life cycle and antiretroviral targets. It was divided in seven stages: binding, fusion, reverse transcription, integration, replication, assembly, budding. (from Dionne B., 2019).

3. Antiretroviral Therapy

HIV was discovered in 1982, but the first treatment strategy was introduced 5 years later. Only in 1987 the Food and Drug Administration (FDA) approved the first antiretroviral drug: the nucleoside reverse transcriptase inhibitor, zidovudine (AZT). Since then ART has progressed significantly and different antiretrovirals with different mechanisms of action were developed that target major step in the HIV life cycle as described above (Dionne B., 2019). Monotherapy with AZT remained the standard of care for 4 years until the early 1990s, when other drugs were approved by the FDA and dual antiretroviral therapy was implemented. Patients receiving monotherapy or dual therapy initially experienced decreases in viral load, increases in CD4 count and improvement in quality of life. Subsequently the therapy caused adverse effects like viral rebound and decreased CD4 counts as a result of treatment failure due to development of resistant virus.

In the mid-1990s the concept of highly active antiretroviral therapy (HAART) was developed, thanks to the introduction of other classes of inhibitors (protease inhibitors and non-nucleoside reverse transcriptase inhibitors): a treatment using three or more antiretroviral drugs in combination, that led to significant declines in HIV-associated morbidity and mortality improving survival, expectancy and quality of life for HIV-infected patients. Furthermore the following improvements were achieved: slower disease progression, decreased opportunistic infections, decreased viral loads, and increased CD4 counts. Early HAART often consisted of complex dosing schedules, strict food requirements, treatment-limiting adverse effects, and the need to take 16–20 pills/day. These treatments often led to patient non adherence, with subsequent treatment failure and development of resistant strains.

After decades of intensive research on antiretroviral compounds, current ART is generally well tolerated with

manageable adverse effects and low pill burdens. The optimization of HAART in the setting of viral suppression has become more commonplace as many people living with HIV are living longer and healthier lives. HAART optimization, also known as treatment simplification, minimizes pill burden, toxicities, drug-drug interactions, and potentially costs (Pandit N.S. *et al.*, 2019). Understanding the dosage forms, adverse effects, and drug interactions of antiretrovirals allows clinicians to choose the most appropriate regimen for their patients. The factors considered selecting an initial regimen include comorbidity (liver disease, depression, cardiovascular disease), pregnancy status, adherence potential (dosage regimen, pill burden, and dosing frequency), food restrictions (dosing with regard to meals), adverse drug effects and potential drug-drug interactions. The goal of therapy is to decrease the patient's viral load rapidly to undetectable levels and increase the patient's CD4 count, which may be limited by the patient's ability to produce CD4 cells.

Current guidelines recommend ART for all HIV-infected individuals to reduce the risk of disease progression and to prevent transmission of HIV. Thanks to the expansion of ART, HIV infections globally continue to decline in 2018. 23.3 million people living with HIV are accessing ART, up from 7.7 million in 2010. In Italy, 88% of people living with HIV were on treatment in 2017. Currently, there are 30 FDA approved antiretroviral drugs classified in 6 categories based on their different mechanisms of action. In addition, there are 25 fixed dose combination (FDC) that contain 2 or 3 drugs in a single-pill form. The last one Dovato, was approved in April 2019 and contains dolutegravir and lamivudine (Figure 3.1).

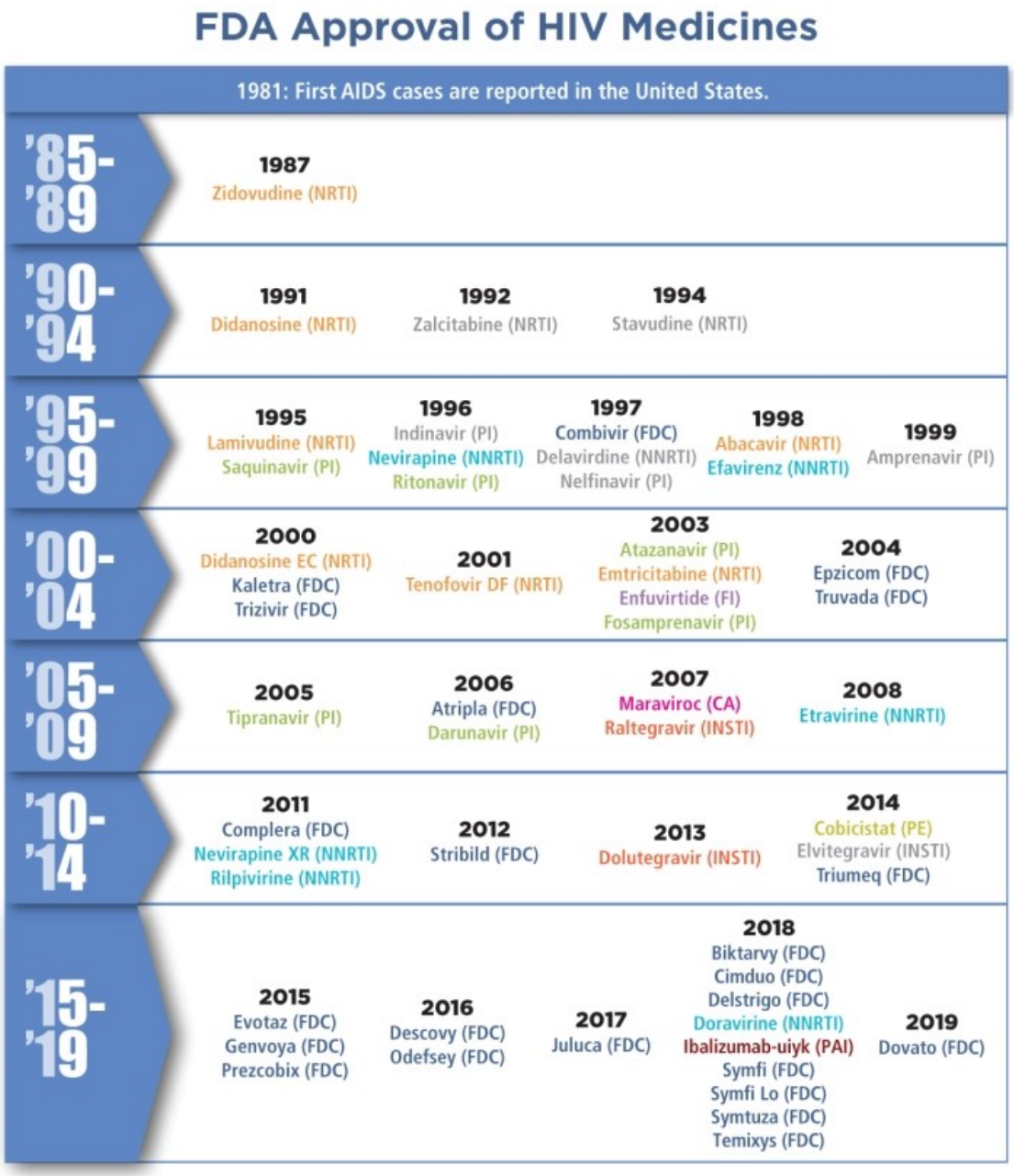

Figure 3.1: a timeline with all the FDA approval dates for HIV medicines, categorized by drug class: CA(CCR5 Antagonist), FDC (Fixed-Dose Combination), FI (Fusion Inhibitor), INSTI (Integrase Inhibitor), NNRTI (Non-Nucleoside Reverse Transcriptase Inhibitor), NRTI (Nucleoside Reverse Transcriptase Inhibitor), PE (Pharmacokinetic Enhancer), PI (Protease Inhibitor), PAI (Post-Attachment Inhibitor) (from https://aidsinfo.nih.gov/understanding-hiv-aids/infographics/25/fda-approval-of-hiv-medicines).

3.1 Nucleoside Reverse Transcriptase Inhibitors

Nucleoside and nucleotide reverse transcriptase inhibitors (NRTIs) were the first antiretroviral drugs to be approved: zidovudine (AZT; 1987), didanosine (ddI; 1991), zalcitabine (ddC; 1992), stavudine (d4T; 1994), lamivudine (3TC; 1995), abacavir (ABC; 1998), tenofovir (TDF; 2001) and emtricitabine (FTC; 2003).
Generally NRTIs are still commonly used as a "backbone" of therapy. The characteristic is the structural similarity of these drugs to the different deoxyribonucleotide triphosphates (dNTPs); they differ by the replacement of the hydroxy (-OH) group in the 3' position by another group that prevents binding of the next dNTP. Thus, NRTIs interfere with RT activity by competing with the natural substrates and being incorporated into viral DNA to act as chain terminators in the synthesis of proviral DNA. To exert their antiviral activity, NRTIs must first be intracellularly phosphorylated by cellular kinases. TDF is the only nucleotide reverse transcriptase analog because it already contains a phosphate molecule in its structure and doesn't require phosphorylation by cellular enzymes for its antiviral activity. HIV can develop resistance mutations to NRTIs and are listed in figure 3.2A. The common adverse effect of NRTIs is mitochondrial toxicity, which is responsible for the clinical syndromes of lactic acidosis with hepatic steatosis, peripheral neuropathy, and lipoatrophy (Warnke D. *et al*., 2007).

3.2 Non-nucleoside Reverse Transcriptase Inhibitors

Non-nucleoside reverse transcriptase inhibitors (NNRTIs) bind directly and noncompetitively to the RT enzyme at the allosteric site causing a conformational change in HIV-1 RT, which reduces its ability to bind to dNTPs and blocks DNA polymerase.

NNRTIs approved by FDA for the treatment of HIV until 2007 were: nevirapine (NVP; 1996), delavirdine (DLV; 1997) and efavirenz (EFV; 1998). Subsequently second-generation NNRTIs approved by FDA were developed to retain activity in the presence of certain high-level resistance mutations to the first-generation NNRTIs: etravirine (ETR; 2008), rilpivirine (RPV; 2011) and the last one approved in 2018 doravirine (DOR).
Resistance mutations to NNRTIs were observed both *in vitro* and *in vivo* and are listed in figure 3.2B. Most NNRTIs can cause rash and can be associate with hepatotoxicity the first six week of initiation therapy. The first-generation NNRTI NVP has a higher risk of causing of Stevens-Johnson syndrome and the second-generation NNRTIs are commonly associated with central nervous system (CNS) side effects, ranging from dizziness to hallucinations, insomnia, nightmares, and depression (Schauer G.D. *et al*., 2014).

3.3 Protease Inhibitors

Protease inhibitors (PIs) bind to PR and prevent cleavage of *gag-pol* polyproteins in infected cells, which cause the release of structurally disorganized and noninfectious viral particles. There are 10 PIs currently approved for clinical use: saquinavir (SQV; 1995), ritonavir (RTV; 1996), indinavir (IDV; 1996), nelfinavir (NFV; 1997) and amprenavir (APV; 1999) among first-generation PIs; the newer agents are fosamprenavir (FPV; 2003), atazanavir (ATV; 2003) tripranavir (TPV; 2005) and darunavir (DRV; 2006) that is the most recently approved.
DRV has a high barrier to resistance, requiring multiple point mutations to select for resistance; in addition, it retains activity against many viral isolates with extensive PI resistance (Figure 3.2C). The inhibitory effect of PIs on each other's metabolism leads to the evaluation of specific combinations that provide an advantageous pharmacokinetic profile, may delay or

prevent the onset of resistance, and allow for the dose reductions and the less toxicity. For example kaletra is a combination of lopinavir (LPV) and RTV approved in 2000 by FDA. The PIs have more metabolic effects than other antiretrovirals, causing insulin resistance and hyperlipidemia, although these side effects are less common or less severe with the newer agents.

3.4 Entry Inhibitors

The entry inhibitors include three classes with different mechanisms of action. They are often used for patients with multiple drug resistance mutations to other classes because of lower efficacy or administration challenges (higher pill burden or parenteral formulation)(Dionne B., 2019).
Three classes are:

- Postattachment Inhibitor (PAI)
- CCR5 Antagonist (CA)
- Fusion Inhibitor (FI)

3.4.1 Postattachment Inhibitors

Several advantages for HIV therapy with a monoclonal antibody are: unique mechanism of action, ability to restore CD4 T cell counts, minimal mechanisms for acquired resistance, and low potential for toxicities compared to alternative antiretroviral agents. Ibalizumab-uiyk (IBA, brand name Trogarzo) is the only PAI currently approved by the FDA in March 2018 for HIV multidrug resistant patients who have failed other regimens. It is a humanized monoclonal antibody that binds to domain 2 of CD4 T cell, which blocks HIV from fusing with the host cell without impairing CD4-mediated immune function. Traditionally, when the HIV envelope gp120 binds to CD4 T cell extracellular domain 1, a conformational shift occurs that

causes the V1 and V2 loops to expose the V3 loop, which converts the trimer from the closed state to an open state. The binding mechanism of IBA induces steric hindrance, which prevents these conformational changes within the complex of the CD4 T cell and the HIV envelope gp120. This subsequently inhibits the interaction of gp120 with the CXCR4 and CCR5 co-receptors via the V3 loop, as well as the rearrangement of the gp41 domain, which prevents viral fusion and entry into the CD4 T cell. An advantage is no significant drug-drug interactions. In addition, it should be used in combination with other antiretrovirals to prevent the emergence of drug resistance (Beccari M.V. *et al*., 2019).

3.4.2 CCR5 Antagonists

Maraviroc (MCV; brand name Selzentry) is the only CA approved by FDA in 2007 for use in antiretroviral treatment-experienced patients with CCR5-tropic HIV-1, detectable viral loads, and resistance to multiple antiretroviral drugs. MCV binds to the chemokine coreceptor CCR5 on the surface of $CD4^+$ cells, blocking the HIV surface protein gp120 from interacting with the CCR5 co-receptor. This is not the only, HIV can use CXCR4 or both (dual-tropic) as co-receptors for cell entry. Thus patients, before initiation MCV regimen, must perform virus tropism testing because this drug is not effective for CXCR4 or dual-tropic virus. Virological failure is significantly associated with a switch from CCR5 to dual-tropic or CXCR4 tropic virus.
The most common MCV adverse events are diarrhea, nausea, fatigue and headache. Many studies reveals that MCV significantly reduces HIV viral load and increases $CD4^+$ cell count when combined with an optimized background ART (Dau B. *et al*., 2009).

3.4.3 Fusion Inhibitors

Enfuvirtide (T-20) was the first FI to be approved by the FDA for treatment of HIV in 2003. It is a linear peptide homologous to a segment of the heptad repeat 2 region of gp41. It binds to the heptad repeat 1 region of gp41 and blocks the formation of the 6-helix bundle hairpin structure necessary for fusion of the viral and CD4 cell membranes (Zhang X. *et al*., 2019). In the last years, studies to develop new FI peptides against HIV-1 were performed, but unfortunately, T20 remains the only membrane FI available for treatment of HIV-1 infection in treatment-experienced patients. T20 is a salvage therapy for patients who experienced virological failure due to other compounds, but the emergence of drug resistance has significantly limited its application (Figure 3.2D). T20 is administered as a subcutaneous injection of 90 mg twice daily and injection site reactions are the most common adverse events reported. The manifestations includes erythema, induration, ecchymosis, nodules, cysts, symptoms of pruritus, pain or discomfort. For patients unable to tolerate the injection site reactions, intravenous infusion of T20 may be an option (Neijzen R.W. *et al*., 2016).

3.5 Integrase Inhibitors

An important step in the treatment of people living with HIV was the debut of the integrase strand transfer inhibitors (INSTIs) in 2007. Their mechanism of action is to prevent the integration of viral DNA (provirus) into the human cellular genome by inhibition of the catalytic activity of the IN enzyme. IN catalyzes the insertion of the viral DNA into the cellular DNA through two independent steps: 3′ processing and strand transfer. In the cytoplasm, IN binds to the specific sequences in the long terminal repeats (LTRs) of the viral cDNA to form the pre-

integration complex. IN catalyzes the removal of the two conserved nucleotides from the 3′-ends of both strands of the viral cDNA exposing the active 3′-hydroxyl group. In the nucleus, IN ligate the 5'-ends of the viral cDNA to the host chromosomal DNA by a process called strand transfer. INSTIs inhibit strand transfer through competitive binding to the enzyme's active site. INSTIs not only displace the 3′-end of the viral DNA from the active site, but also chelate the divalent cation (Mg2+ or Mn2+) that is required for IN enzymatic activity (Anstett K. *et al*., 2017). Current guidelines recommend INSTIs as components of frontline in conjunction with an optimized NRTI backbone as part of all initial regimens in treatment-naïve patients and of drug-switch ART formulations. The power for this recommendation is based on several factors: high efficacy, greater tolerability and fewer drug-drug interactions compared to other antiretrovirals such NNRTIs or PIs (Brooks K.M. *et al*., 2019).

There are currently four INSTIs approved by FDA for the treatment of HIV infection: raltegravir (RAL), elvitegravir (EVG), dolutegravir (DTG) and bictegravir (BIC). Cabotegravir (CAB) is the newer INSTI currently in phase III clinical trials. The first-generation INSTI (RAL and EVG) are susceptible to virological failure through the development of resistance mutations. RAL was the first INSTI approved by FDA in 2007 and EVG was only available in FDC with cobicistat, FTC, and tenofovir disoproxil (Stribild; 2012) or with cobicistat, FTC, and tenofovir alafenamide (Genvoya; 2015). The second-generation INSTIs (DTG and BIC) present higher barriers to the development of viral drug resistances than first-generation compounds. DTG was approved in 2013 and BIC is currently only available in a fixed-dose single-tablet regimen with FTC and tenofovir alafenamide commercially available as Biktarvy, approved in 2018 (Engelman A.N., 2019).

3.5.1 Raltegravir and resistance pathways

RAL, brand name Isentress, is the first INSTI approved by the FDA in 2007 in USA and, in combination with other antiretroviral drugs, is used in both treatment-naïve and treatment-experienced HIV infected patients. The recommended dose is 400 mg twice daily; however, 800 mg twice daily is recommended when it is co-administered with rifampin. Although many studies shown the clinical efficacy of RAL, adverse events, like emergence of resistance, treatment failure, drug toxicity and drug-drug interactions have been demonstrated.

The large randomized phase III study STARTMRK, compared the safety and efficacy of twice daily RAL-based regimen against EFV-based regimen in treatment-naïve patients over a period of 5 years. The optimized background therapy (OBT) in both treatment groups included TDF and FTC. At week 48, 86% of patients RAL-based treatment achieved a viral load of less than 50 copies/ml compared to 82% of patients on EFV. Patients in the RAL treatment shown better virologic suppression compared to those on EFV at week 240. RAL treatment also increase CD4 cell count more than EFV treatment with significantly fewer adverse effects.

Randomized phase III trials, BENCHMRK-1 and -2 date examined the long-term efficacy and safety of twice daily RAL in patients who are INSTI-naïve and have triple class HIV resistance mutations. This study compared RAL to placebo, each in combination with an OBT. In the BENCHMRK-1 trial at week 48, the proportions of patients with an HIV-1 RNA level below 50 copies/ml were 65% (RAL) and 31% (placebo). Similar results were obtained in the BENCHMRK-2 trial, at week 48 HIV-1 RNA levels below 50 copies/ml are achieved in 60% of RAL recipients compared with 35% of placebo recipients. At 5 years after study entry, RAL recipients experienced a mean increase in CD4

count of 183 cells/mm^3, and 42% of patients achieved an HIV-1 RNA level less than 50 copies/ml (Hicks C. *et al*., 2009).

In vitro studies shown potent activity of RAL against HIV-1, with a 95% inhibitory concentration (IC95) in human T lymphoid cell cultures of 31±20 nM. Other studies shown that RAL inhibits the strand transfer function of HIV-1 IN with potency in the low nanomolar range. The 50% inhibitory concentration (IC50) of 2–7 nM for strand transfer inhibition was determined by *in vitro* experiments using purified IN enzyme (Ramkumar K. *et al*., 2010).

The low genetic barrier of HIV-1 IN against RAL compromises its *in vivo* susceptibility. Rapid development of resistance were observed in both *in vitro* and clinical studies. The mutations observed in the HIV-1 IN coding sequence that contribute to RAL resistance (evolved either in cell culture or in subjects treated with RAL) generally includes an amino acid substitution (primary mutation) at either Y143 (change to C, H, or R) or Q148 (change to H, K, or R) or N155 (change to H) plus one or more additional substitutions (secondary mutation): L74M, E92Q, Q95K/R, T97A, E138A/K, G140A/S, V151I, G163R, H183P, Y226C/D/F/H, S230R, and D232N) (Figure 3.2E). (https://www.accessdata.fda.gov/drugsatfdadocs/label/2017/022145s036,203045s013,205786s004lbl.pdf). Primary mutations impose a severe cost in replicative capacity but secondary mutations can restore it with high levels of resistance: in particular T97A for Y143 and G140A/S or E138A/K for Q148 mutation. However, the secondary mutation associated to N155H, E92V, does not restore the viral fitness (Park T.E. *et al*., 2015). The Y143 pathway is specific to RAL and is not selected by any other INSTI. The reason is that residue Y143 interacts directly with the oxadiazole ring of RAL in crystal structure (IN in complex with RAL) forming a interaction that is abrogated when this position is mutated. This is not the case with the Q148 and N155 pathway, which disturb the geometry of the IN active site, disrupting the binding of INSTIs. N155H pathway is also

selected with moderate frequency both *in vitro* and *in vivo* in response to RAL and generally emerges first, and is eventually replaced by the Q148H mutation, usually in combination with G140S (Anstett K. *et al*., 2017).
Current Department of Health and Human Services (DHHS) guidelines continue to recommend RAL-based regimens as first-line in treatment-naïve patients; however, the current International Antiviral Society-USA (IAS-USA) guidelines have relegated this regimen to an alternative status. RAL is approved for use in combination with other antiretroviral agents for the treatment of HIV-1 infection in treatment-experienced adult patients who show evidence of viral replication and multidrug-resistant HIV-1 viral strains. The utility of RAL remains limited by the lower genetic barrier especially in patients with a history of poor adherence and current lack of a FDC.(Brooks K.M. *et al*.,2019).

3.5.2 Dolutegravir and resistance pathways

DTG, brand name Tivicay, is the first second-generation INSTI and was approved in 2013. DTG acts by impairing the function of the HIV IN-DNA complex to which it is chemically synthesized to bind. It is rapidly absorbed achieving maximal blood concentration hours after ingestion and requires once-daily administration without pharmacological enhancement (Kandel C.E. *et al*., 2015). DTG is administered 50 mg once daily in treatment-naïve or treatment-experienced INSTI naïve. Twice daily DTG dosing is also used in INSTI-experienced patients with certain INSTI-associated resistance mutations or clinically suspected INSTI resistances.
The efficacy of DTG in treatment-naïve HIV infected patients is supported by data from three clinical trials: SPRING-2, SINGLE and FLAMINGO (Park T.E. *et al*.,2015).

The SPRING-2 study was a randomized phase III trial that compares the efficacy and safety of DTG and RAL each combined with TDF/FTC or ABC/3TC. After 48 weeks, 88% of patients in the DTG arm achieved an HIV RNA level below 50 copies/ml, compared with 85% in the RAL arm. This noninferiority was maintained through 96 weeks in 81% of patients assigned to DTG and 76% patients assigned to RAL. The SPRING-2 study established DTG's noninferiority and similar tolerability to RAL.

The SINGLE study is a randomized phase III trial that compared the efficacy and safety of DTG with ABC/3TC against EFV/TDF/FTC. In this study, DTG was superior to the NNRTI-based regimen, with 88% of patients in the DTG group achieving HIV-1 RNA levels below 50 copies/ml compared with 81% in the EFV group after 48 weeks. The superiority of DTG persisted at 144 weeks. DTG treatment also led to a significant increase in $CD4^+$ cell count and to a shorter time of virological suppression than EFV (Shah B.M. *et al*., 2014).

The FLAMINGO study compared DTG to DRV, each administered with co-formulated TDF/FTC or ABC/3TC in treatment-naïve individuals. At 48 weeks, there was 90% of patients receiving DTG and 83% receiving DRV who achieve viral load below 50 copies/ml. DTG's noninferiority and statistical superiority was maintained at 96 weeks to the comparator regimen.

Two studies investigate the efficacy and safety of DTG in treatment-experienced patients.

The phase III VIKING trials (VIKING-3 and VIKING-4) evaluated the efficacy of DTG in treatment-experienced patients with preexisting INSTI resistance in virological failure and demonstrate that DTG maintains activity against RAL and EVG resistant virus.

The SAILING trial compares the safety and efficacy of DTG to RAL in combination with investigator-selected background therapy. At 48 weeks, participants in the DTG group were significantly more likely to achieve virologic suppression (HIV

RNA level below 50 copies/ml). Additionally, virologic failure due to INSTI resistance mutations was significantly less common with DTG, and no phenotypic resistance to DTG was reported (Brooks K.M. *et al*., 2019).

In vitro studies shown DGT inhibits the strand transfer function of HIV-1 IN with a IC50 of 2,7–12.6 nM using purified IN enzyme. Other studies shown that DGT exhibits antiviral activity against laboratory strains of wild-type HIV-1 with mean IC50 values of 0,5 nM to 2,1 nM in peripheral blood mononuclear cells (PBMCs) and MT-4 cells (https://www.accessdata.fda.gov/ drugsatfda_docs/ label/2018/204790s016s018lbl.pdf).

Resistance mutations to DTG (Figure 3.2E) were observed both *in vitro* and clinical studies but these were infrequent and had minimal clinical effects. Some *in vitro* experiments revealed that the most common mutation was R263K that led to low-level resistance to DTG. This mutation causes a deviation in spatial positioning of R262 in the subunits of IN (Park T.E. *et al*.,2015). Other mutations emerged in cell culture starting from different wild-type HIV-1 strains: E92Q, G118R, S153F/Y or G193E. The latter confers decreased susceptibility to DTG. Mutant viruses containing the Q148R/H substitutions with the additional mutations (T97A, E138K, G140S, and M154I) confer decreased susceptibility to DTG (https://www.accessdata.fda.gov/ drugsatfda_docs/label/2018/204790s016s018lbl.pdf). Others studies suggested that HIV-1 with primary mutations at codon 155 or codon 143 remain susceptible *in vitro* to DTG. All these data are consistent with DTG susceptibility reported in clinical isolates (Canducci F. *et al*., 2011). The most common INSTI resistance mutations in patients treated with DTG are R263K, G118R, N155H and Q148H/R. The highest level of reduced susceptibility occurs in viruses containing Q148H/K mutations in combination with G140S and/or E138K mutations. Y143R and N155H pathway isolates shown no reduction in the susceptibility to DTG (Rhee S.Y. *et al*.,2019).

Observational studies and case reports have called attention to potential concerns over CNS and cardiovascular adverse effects in patients receiving DTG. CNS adverse effects consisting of worsening depression, anxiety, insomnia and suicidality. However DTG-based regimens have become one of the most frequently employed regimens in both treatment-naïve and treatment-experienced patients. DTG has fewer drug-drug interactions, higher genetic barrier to resistance, good tolerability, effective virological suppression and once-daily administration (Brooks K.M. *et al*., 2019).

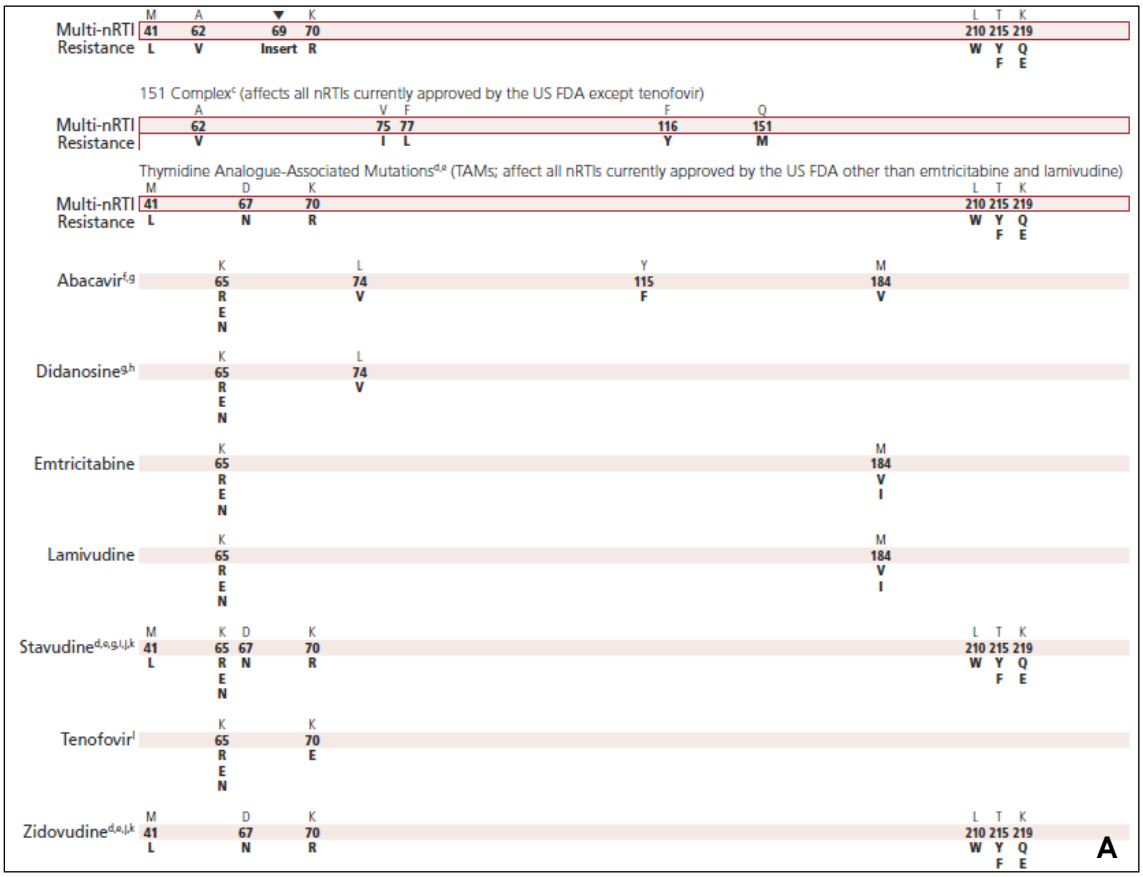
Multi-nRTI Resistance
M 41 L
A 62 V
▼ 69 Insert
K 70 R
L 210 W
T 215 Y F
K 219 Q E
151 Complex[c] (affects all nRTIs currently approved by the US FDA except tenofovir)
A 62 V
V 75 I
F 77 L
F 116 Y
Q 151 M
Thymidine Analogue-Associated Mutations[d,e] (TAMs; affect all nRTIs currently approved by the US FDA other than emtricitabine and lamivudine)
D 67 N
Abacavir[f,g]
K 65 R E N
L 74 V
Y 115 F
M 184 V
Didanosine[g,h]
Emtricitabine
M 184 V I
Lamivudine
Stavudine[d,e,g,i,j,k]
Tenofovir[l]
Zidovudine[d,e,j,k]
A

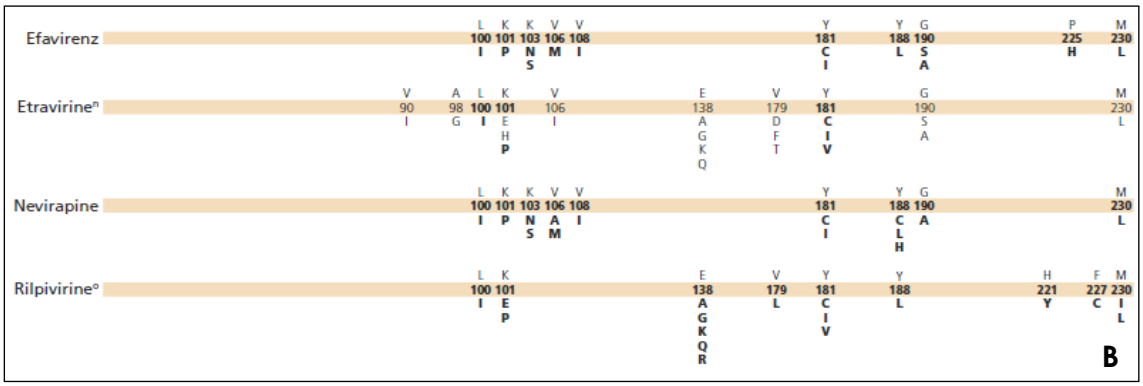
Efavirenz
L 100 I
K 101 P
K 103 N S
V 106 M
V 108 I
Y 181 C I
Y 188 L
G 190 S A
P 225 H
M 230 L
Etravirine[n]
V 90 I
A 98 G
E 138 A G K Q
V 179 D F T
G 190 S A
Nevirapine
Y 188 C L H
Rilpivirine[o]
H 221 Y
F 227 C
B

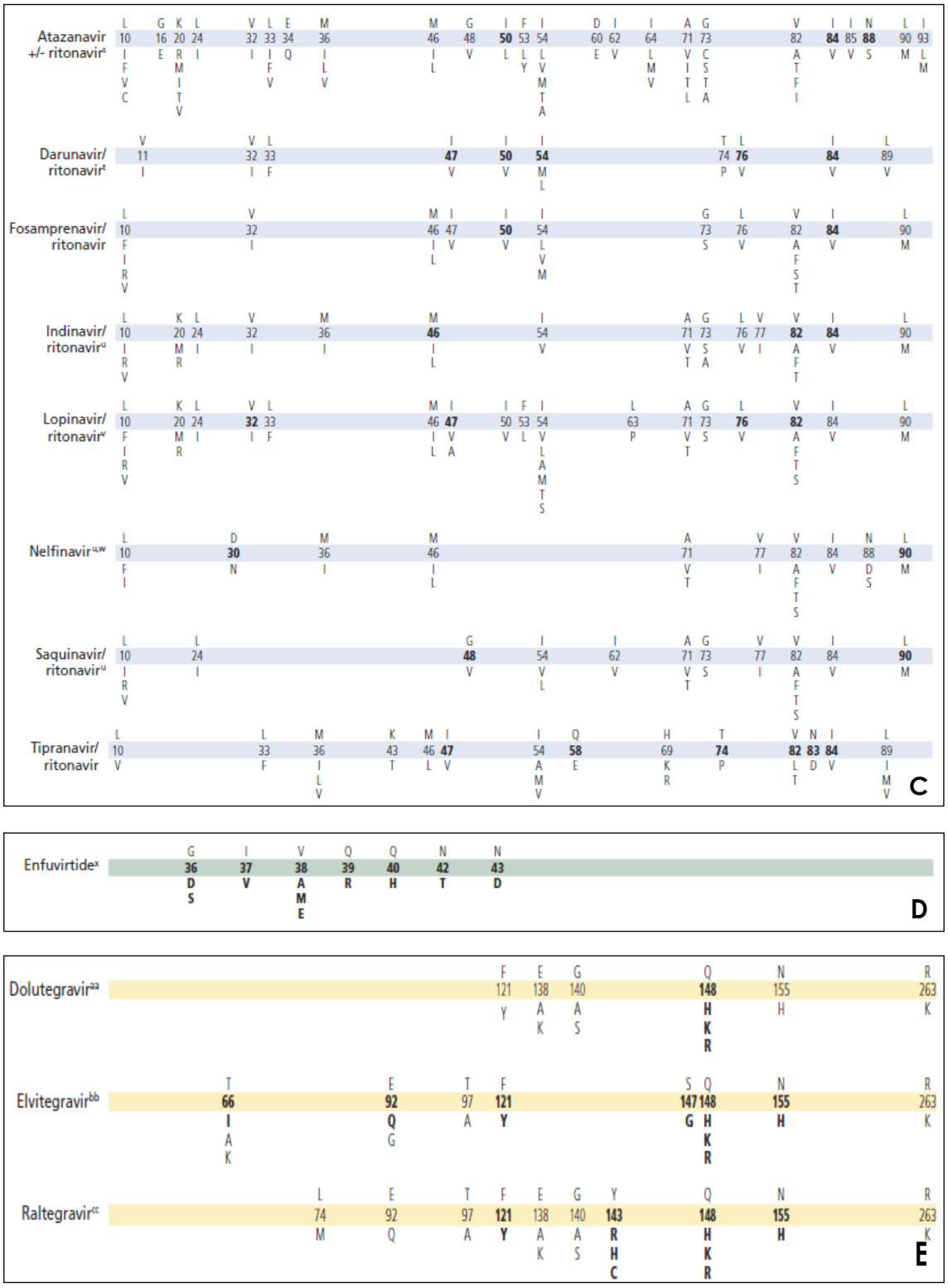

Figure 3.2: Resistance mutations to antiretroviral drugs: **A.** mutations in reverse transcriptase gene associated with resistance to NRTIs; **B.** mutations in reverse transcriptase gene associated with resistance to NNRTIs; **C.** mutations in protease gene associated with resistance to PIs; **D.** mutations in the envelope gene associated with resistance to FI; **E.** mutations in the IN gene associated with resistance to INSTIs (from Wansing A.M. *et al.*,2017).

4. Treatment failure and drug resistance mutations

Currently ART suppresses HIV-1 replication and improves or maintains immune function and quality of life. The ability of antiretrovirals to suppress or reduce HIV RNA below the level of quantification is known as antiviral potency and is used as a measure of treatment success (Kuritzkes D.R., 2004). However this success is not always observed in clinical practice and numerous and complex factors contribute to treatment failure in HIV-1 infections. Treatment failure is related:

1. to drug factors such as limited potency of regimen, low genetic barrier, sub-inhibitory plasma levels and pharmacological factors including drug–drug interactions that impair absorption or accelerate clearance;
2. to host-related factors as poor adherence (because of the complexity or tolerability of certain regimens), limited recovery capacity of the immune system and prior drug experience;
3. to viral related factors: error prone reverse transcription and drug resistance mutations (Ammaranond P. *et al*., 2012).

The need of HIV-1 to evade ART and host immunity drives viral evolution. HIV has vast genetic diversity within and between individuals. Although individuals are usually infected with only a single or few original virus variants, an estimated 10^{10} variants are produced each day in untreated individuals, resulting in a vast array of virus variants, often called "quasispecies". The genetic diversity of the HIV-1 quasispecies in a single infected individual is comparable to the global annual genetic variation of the influenza virus (Smyth R.P. *et al*., 2012). This genetic diversity is driven by a high replication and mutation rate, the absence of a proof-reading mechanism during reverse transcription, the accumulation of proviral variants during the infection and a high recombination rate.

Concerning the high mutation rate, HIV-1 accumulates one mutation per genome/replication cycle (1.4×10^{-5} errors per

base pair). The most prominent source is the RT enzyme, which is error prone due to the lack of a proofreading capability during viral replication. The complexity of the HIV-1 quasispecies is also increased by the high recombination rate that occurs whenever more than one viral variant infects the same cell. Recombination can efficiently shuffle mutations within a quasispecies because it can rapidly assemble beneficial genetic combinations that would be difficult to generate by mutation alone and it can also effectively remove deleterious mutations that would otherwise reduce viral fitness. In addition, latent virus variants archived in the chromosomes of infected cells may periodically reactivate complicating the spectrum of virus variants within infected patients (Tang M.W. *et al*., 2012). Genetic diversity and inadequate therapy are critical to the generation of drug resistance mutations. When HIV-1 develops drug resistance mutations, it often pays a price in terms of reduced replicative capacity (RC, capacity of the virus to replicate efficiently) and pathogenicity with deleterious effects on viral fitness. The term viral fitness refers to the ability of a virus to adapt and replicate in a defined environment. Although naturally drug resistant viruses arise every day in untreated patients, these variants rarely rise to detectable levels because they are less fit than wild type viruses and decrease RC in the absence of selective drug pressure. In the presence of selective drug pressure by different antiretrovirals, the fixation of different drug resistance mutations in the viral population occurs when mutations increase viral fitness (Smyth R.P. *et al*., 2012). This viral population consequently becomes the dominant species (Arenas M., 2015). Indeed, in the presence of selective drug pressure, the resistant virus is more fit than wild type virus (Nijhuis M. *et al*., 2001).

Different factors contribute to the genetic barrier to resistance to antiretrovirals: the number of mutations necessary to confer resistance (for some antiretrovirals, multiple drug resistance mutations are required to reduce susceptibility, while for others

a single mutation is sufficient), the frequency at which the mutations develop and the effect of each mutations on viral fitness. For this reason, drug resistance mutations can be categorized as primary mutations that directly reduce drug susceptibility and accessory mutations that enhance viral fitness of variants containing primary mutations and contributes to further reductions in susceptibility.

Intrinsic antiviral potency and genetic barrier to resistance of antiretrovirals influence the ability to avoid virological failure. Most regimens used for first-line therapy are sufficiently potent to completely block HIV-1 replication and have a high genetic barrier to resistance to maintain long-term virological suppression (Clutter D.S., 2016). Others antiretrovirals are at risk of becoming partly or fully inactive because of the emergence of drug-resistant viruses. HIV in people receiving treatment can acquire drug resistance mutations and people can also be infected with HIV that is already drug resistant. WHO commonly classifies resistant mutations into two categories according to the origin of drug resistant virus strains *in vivo*:

- acquired HIV drug resistance (ADR) develops because of viral replication in the presence of antiretroviral drugs in treated individuals.
- transmitted HIV drug resistance (TDR) is defined as the presence of drug resistance mutation detected in antiretroviral–naïve infected individuals with a genotypic resistance test performed before starting therapy (https://www .who.int/hiv/ pub/drugresistance/ hivdr-report-2019/en/).

The acquisition or transmission of HIV-1 drug resistance hamper the success of therapy because patients have fewer treatment options and have an increased risk of morbidity and mortality, particularly in developing countries where choices for therapy are limited (Tang M.W., 2012).

4.1 Transmitted HIV drug resistance

TDR is a clinical and public health issue because may significantly compromise the outcome of first-line therapy, limiting the antiretroviral regimen options and leading to virological failure(Rhee S.Y. *et al.*,2015).
Despite the general decreasing trend of TDR in United States and Europe, an alarming increase has been noticed in several countries in the last few years. The prevalence of TDR depends on regional therapy history with treatment failures, transmission networks and human migration. In addition, an increase in non-B subtypes and CRFs can have an impact on TDR. This increase in non-B subtypes occurs in conjunction with epidemiological changes such as human migration from low-income to middle-income areas and the increase of HIV transmission rate among MSM, which contribute to 43% of new HIV-1 cases.
The overall prevalence is defined as the percentage of patients infected with a virus carrying any TDR mutation. The prevalence of TDR for the different drug classes (NRTIs, NNRTIs, PIs and INSTIs) is defined as the percentage of patients infected with a virus carrying any TDR mutation to a particular drug class. Patients can also be infected with multiclass resistant virus (for example virus with mutations associated with both NRTIs and NNRTIs) (Hofstra L.M. *et al*., 2016).
In the absence of selective drug pressure, many drug resistance mutations reduce HIV-1 replication fitness and recede to levels not detectable by standard genotypic resistance test. This occurs rapidly for the NRTI resistance mutation like M184V whereas has not been observed for NNRTI resistance mutations because do not impact fitness and stability. Therefore NNRTI resistance mutations are responsible for most cases of high level TDR.
The prevalence of TDR varies in different continents: in Europe and in North America ranges from 6% to 15% and is significantly increasing in southern and eastern Africa, particularly TDR to

NNRTIs, which are recommended in first-line antiretroviral regimens in these regions. The epidemiologic characteristics, TDR prevalence and link to each study publication can be accessed using an interactive map on the Stanford HIV Drug Resistance Database (HIVDB) website (Figure 4.1) (https://hivdb.stanford.edu/page/surveillance-map/).

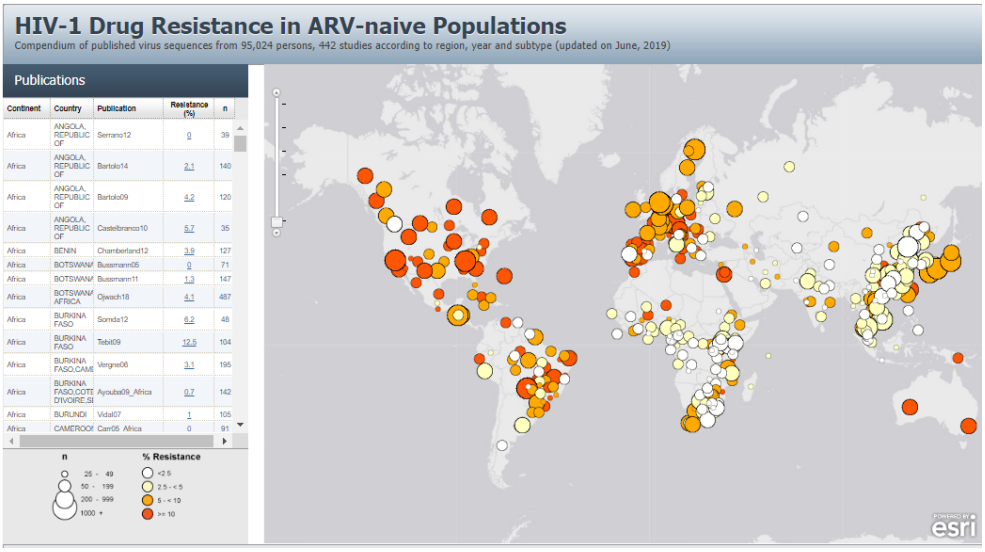

Figure 4.1: snapshot of an interactive map plotting the prevalence of transmitted drug resistance from 442 studies in 2019. Each study is represented by a circle. The size of the circle is proportional to the number of individuals in the study. The circle color indicates the prevalence of overall TDR in the study: white (<2,5%), pale yellow (2,5% to 4,9%), orange (5,0% to 9,9%), and red (>10,0%)(from https://hivdb.stanford.edu/page/surveillance-map/).

Studies conducted in countries in different continents highlighted that the overall TDR prevalence in sub-Saharan Africa (SSA), LMICs (low- and middle-income countries) of south and southeast Asia (SSEA), countries of the former Soviet Union (FSU), upper-income Asian countries, Latin America and Caribbean, Europe, and North America was 2,8%, 2,9%, 4,0 %, 5,6%, 7,6%, 9,4%, and 11,5%, respectively (Rhee S.Y. *et al.*, 2015). In China, diversity of subtypes, complex infected population structure, different medical treatment services and patient compliance contributed to the different TDR prevalence in various regions. Authors demonstrated that 11,1% of isolates

contained at least one NRTI or NNRTI resistance mutations while 2,0% of isolates were identified to be resistant to PIs (Xu Y. *et al*., 2018). The European surveillance program SPREAD is monitoring the TDR mutations in Europe since 2002 (Figure 4.2A). Hofstra L.M. and colleagues studied the prevalence of overall TDR from 2002 to 2010. This prevalence remained fairly stable and was around 8,3% in 2008–2010. NRTI resistance mutations were responsible for most cases of TDR (4,5%), followed by NNRTI mutations (2,9%) and PI mutations (2,0%). Authors linked the NRTI-related TDR with a longer exposure of subtype B to this drugs class and not to specific viral characteristics, especially before the introduction of combination therapy (Figure 4.2B)(Hofstra L.M. *et al*., 2016).

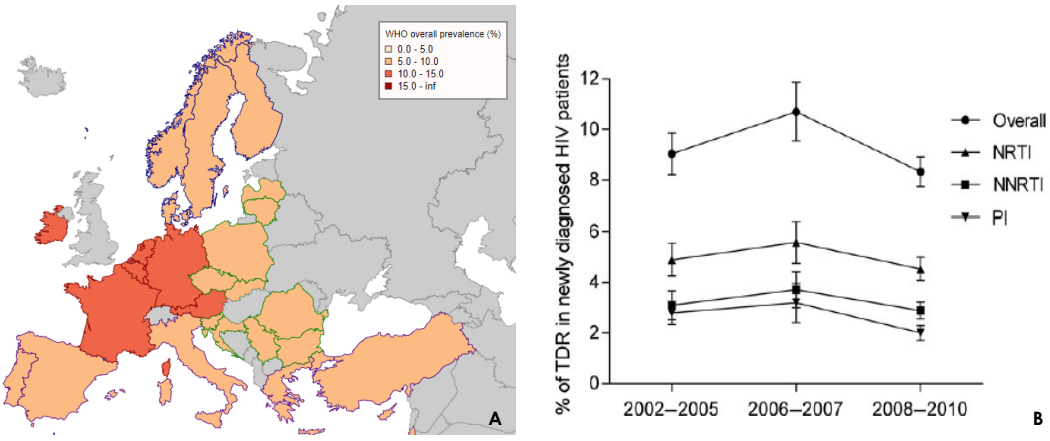

Figure 4.2: the prevalence of TDR in Europe: **A.** the colors indicates the prevalence of overall TDR, white (0,0% to 5,0%), pale yellow (5,0% to 10,0%), orange (10,0% to 15,0%), and red (>15,0%)(from https://spread.crp-sante.lu/); **B.** the lines indicates the prevalence of TDR from 2002 to 2010 (from Hofstra L.M. *et al.*, 2016).

The same decreasing trend of overall TDR prevalence has also been observed in Italy. An observational study analyzed the prevalence of overall TDR in three large Italian Cohorts. It was 12% in patients diagnosed with an acute or recent HIV infection from 2000 to 2010. NRTI, NNRTI and PI resistance mutations were detected in 7%, 7% and 3% of patients, respectively (Colafigli M. *et al*., 2012). Fabeni L. and colleagues characterized the dynamics and phylogenetic relationships of TDR and subtypes

among a large cohort of HIV-1 infected individuals diagnosed in Italy from 2000 to 2014. The overall prevalence of TDR in this period was 8,8%. TDR was higher in B subtype infected individuals than in those infected with non-B subtypes (9,7% vs 6,9%)(Fabeni L. *et al*., 2017). Other studies showed that subtype F1 was the most frequent non-B subtype in newly diagnosed individuals in Italy and was the major non-B subtype with higher TDR prevalence. This is in line with the important increase of non-B subtypes and CRFs reported in several European countries during the last decade (Franzetti M. *et al*., 2012). Franzetti M. and colleagues evaluated the genotypic results of naïve patients enrolled in the I.Co.N.A cohort in Italy between 2007 and 2014. The overall prevalence of TDR was 10,7% and the majority of patients was infected with a virus carrying TDR mutations to NNRTIs. In this study some evidence emerged about the possible increase of TDR in migrants (Franzetti M. *et al*., 2018).

Another study on data from the Antiviral Response Cohort Analysis (ARCA; http://www.dbarca.net), an Italian nationwide HIV drug resistance database, showed declining TDR in newly infected patients in Italy in 2016 compared with 2006 (7,3% vs 14,5%, respectively). The prevalence of overall TDR was 10,3%: 6% patients carried mutations to NRTIs, 4,4% to NNRTIs, 2,3% to PIs and 0,2% to INSTIs. The objectives of Rossetti B. and colleagues were to analyze the prevalence of TDR between 2006 and 2016 in Italy as previously described, to identify factors predictors of TDR and to investigate which resistance mutations were the most frequently transmitted by drug class (Figure 4.3). The factors predictors were viral subtype B, lower viral load at genotyping, clinical site located in northern Italy and earlier calendar year at genotyping (Rossetti B. *et al*., 2018).

The DHHS, IAS-USA and European guidelines recommend genotypic resistance testing before starting therapy because surveillance of TDR is essential to inform treatment policy making and guidance in the global fight against HIV/AIDS.

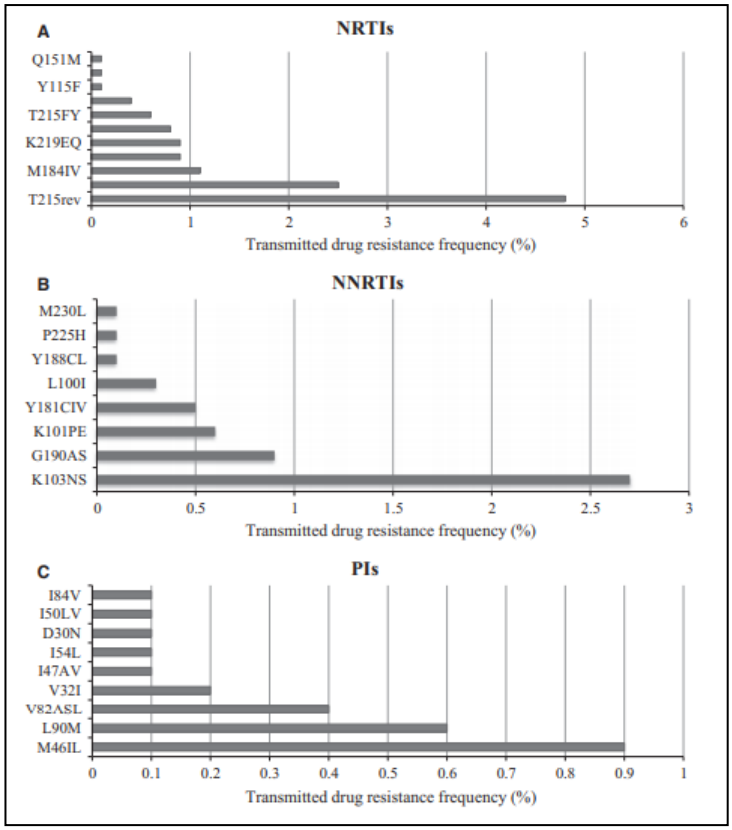

Figure 4.3: TDR mutations frequency in Italy by drug class: **A**. NRTIs; **B**. NNRTIs; **C**. PIs (from Rossetti B. *et al*., 2018).

4.2 Phenotypic and Genotypic Resistance Tests

The two categories of assays for resistance testing are genotypic and phenotypic assays. These tests are important tools for managing decisions related to therapy initiation or regimen modification following treatment failure. Properly used, they can lead to improved virologic outcomes for patients infected with HIV-1.

Phenotypic resistance test measure viral replication in cell culture in the presence of serial antiretroviral dilutions. Susceptibility is usually reported as the antiretroviral concentration that inhibits HIV-1 replication by 50% (IC50) and as levels of fold-resistance, which are calculated by dividing the IC50 of the recombinant virus by the IC50 of a control wild type virus. As isolating and replicating HIV *in vitro* from clinical samples is often difficult, recombinant phenotypic strategies are usually employed. Recombinant viruses are created by inserting PCR-amplified patient virus gene (PR, RT, IN, envelope) into the backbone of a wild type laboratory clone. One commercial phenotypic assay is currently available: PhenoSense (Monogram Biosciences) while another Antivirogram (Virco) is no longer available. Phenotypic resistance testing has different advantages: it can measure drug susceptibility directly and the susceptibility arising from all drug mutations in the virus and it is recommended for new or investigational drugs, drug resistance research and complex clinical cases. There are also disadvantages for phenotypic assay, including its relatively limited availability, greater cost, and longer turnaround time for results. In addition the recombinant viruses and cells used in a phenotypic resistance test often do not reflect *in vivo* conditions (Clutter D.S. *et al*., 2016).

Genotypic resistance testing relies on detecting known drug resistance mutations in the targets of ART: PR, RT, IN and envelope glycoproteins. The standard approach to genotypic

resistance testing is direct polymerase chain reaction (PCR) dideoxynucleotides (Sanger) sequencing. There are different commercially available kits as the ViroSeq_HIV-1 Genotyping System (Abbot) (Tang M.W., 2012). Interpreting genotypic resistance test results can be complex because it is common for more than one nucleotide to be present in a given position on Sanger sequence electropherograms (mixture). There are some algorithms that aid with interpretation: the HIVDB, French National Agency for AIDS Research (ANRS), HIV Genotypic Resistance-Algorithm Deutschland (HIV-GRADE), and Rega. For example, HIVDB provides an online genotypic resistance interpretation program to help clinicians and laboratories interpret HIV-1 genotypic resistance test (http://hivdb.stanford.edu). The program accepts RT, PR and IN sequences submitted by the user and returns a list of penalty scores for each drug resistance mutation and an estimate of reduced susceptibility for each antiretrovirals (Clutter D.S., 2016). The primary limitation of Sanger sequencing is the detection of resistance mutations present in 15% to 20% of the viral population and the loss of potentially relevant information for effective ART combinations. Next-generation sequencing (NGS) is a newer technology for genotypic resistance test and is rapidly evolving toward increased robustness, decreased complexity, and reduced cost. NGS can detect minority variants at thresholds as low as 1%, thus identifying significantly more drug resistance mutations than traditional Sanger sequencing (McCluskey S.M., 2019). The numerous sequence reads, moreover, permits quantification of clonal viral variants from the same sample with higher sensitivity and lower cost than Sanger sequencing. NGS allows testing a sufficiently large number of samples in a single run and more regions of the HIV-1 genome at minimal additional cost. Academic centers and private companies are developing semi-automated bioinformatics analysis pipelines that will allow NGS analyses to

be performed by non-expert laboratory technicians (Günthard H.F. *et al.*, 2019).

Genotypic assays are used more frequently than phenotypic assays because they are less expensive and have a shorter turnaround time. However genotypic testing provides an indirect measure of susceptibility, as algorithms are used to correlate resistance mutations to an estimated reduction of a drug's effectiveness. There are differences in the access to genotypic diagnostic test between LMICs and high-income countries. In high-income countries, drug resistance testing is part of routine care and it can help clinicians prevent virological failure and accumulation of further drug resistance mutations by selecting the most efficacious regimens for each patients. In most LMICs, genotypic resistance testing is not available routinely for patients receiving antiretrovirals. This is associated with an increased risk of virological failure and an increase of the prevalence transmitted or acquired drug resistance mutations, difficult clinical cases and deaths. (Collier D.A., 2019).

5. Statement of purpose

Highly active antiretroviral therapy (HAART) has transformed the diagnosis of HIV infection "from a former death sentence into a chronic disease", as often written. However, no "cure" yet exists for HIV and patients must remain on therapy for the entire life which causes deleterious effects related to toxicity and could induce the development of drug resistance mutations. Resistant viral strains are circulating in the population and occasionally people can also be infected with virus that is already drug resistant. In Italy, similarly to other European countries, the prevalence of transmitted drug resistance (TDR) is 8-10%, relatively low. Some TDR strains revert to wild type while others maintain resistance mutations over time. It is still unknown whether the latter strains are responsible of incidental events or some of them may have acquired sufficient replicative capacity (RC) to sustain micro-epidemics of their own. Recent infection is generally considered the phase within 6 months from HIV-1 infection. During the initial phase of the infection, the virus has little time to evolve significantly from the original strain or quasispecie that is transmitted to the new host. Although currently antiretroviral therapy (ART) can control viral replication even in patients with TDR, the surveillance of TDR is essential to control HIV-1 infections. The analysis of the replicative characteristics of viral strains from recent infections could disclose the mechanisms affecting the initial evolutionary phases.

More recently, the introduction of the new class of inhibitors, integrase stand transfer inhibitors (INSTIs), has represented an important step for ART, and despite the use of raltegravir and elvitegravir has promptly led to the development of resistant viral strains, dolutegravir (and possibly bictegravir) display a remarkable genetic barrier to resistance. Resistance to older INSTIs *in vivo* has been extensively documented and is mostly associated with 3 main mutational pathways: Y143C/R,

Q148H/R/K or N155H. However, the mechanisms that drive the selection of a specific pathway are still poorly understood.

The aim of this study is:

- to understand the evolutionary dynamic of TDR by comparing the RC of viral strains from 4 categories of patients: recent infection without resistance mutations, recent infection with resistance mutations, non-recent infection without resistance mutations and non-recent infections with resistance mutations. A recombinant phenotypic resistance assay was specifically developed to test the RC conferred by the reverse transcriptase (RT) and protease (PR) genes from viral strains circulating in patients. This part of the present study aims at establishing the fitness of viral strains bearing resistance mutations (for both antiretroviral classes) responsible of primary infections and at investigating the evolutionary dynamics that underlies the selection of these strains during the first month of primary infections. The results from this study might finally contribute to the development of an epidemiological model based on the diffusion of TDR in chronically infected patients and their role on therapeutic failure.

- to investigate the influence of the viral genetic background of the integrase gene (IN) from patients who failed INSTIs therapy in selecting of a specific resistance pathway. A recombinant phenotypic resistance assay was developed to test the RC conferred by the basal sequences of the IN gene, the natural resistance pathway (observed *in vivo*) mutations and mutations of alternative resistance pathways, introduced by site-directed mutagenesis. The phenotypic studies were used to analyze the biological significance of accessory or compensatory mutations and the role of the genetic context in which these mutations arose. The viral fitness was evaluated in the absence and in the presence of increasing dilutions of raltegravir and dolutegravir to

calculate the 50% inhibitory concentration (IC50) of drugs. The comparison of RC of the different clones obtained *in vitro* will allow to verify whether the natural resistance pathway observed *in vivo,* was linked to the genetic background of the IN gene.

6. Materials and methods

6.1 Patients and clinical samples

The study was conducted in three sets of patients:

1. 40 HIV-1 viremic patients from two different clinical centers ("Ospedale Luigi Sacco" of Milan and "Ospedali Riuniti di Ancona") were enrolled for the study of the reverse transcriptase (RT) gene. 20 patients were recently infected (< 1 year) and naïve for antiretroviral treatment: 10 harbored a virus with RT resistance mutations and 10 wild type virus. The other 20 patients with a non-recent infection were divided as follow: 10 in treatment failure (mutated virus) and 10 naïve (wild type virus). The virological characteristics of each patient are described in table 6.1.

2. 18 HIV-1 viremic patients were selected for the study of the protease (PR) gene: 8 infected with a virus carrying resistance mutations and 10 without resistance mutations. The virological characteristics of each patient are described in table 6.2.

3. 5 patients from two different clinical centers ("Department of Biomedical Sciences and Human Oncology, University of Bari" and "Ospedali Riuniti di Ancona") were enrolled for the study of the integrase (IN) gene. These patients treated with integrase stand transfer inhibitors (INSTIs) and their viral isolates naturally developed drug resistance mutations (the G140S/Q148H mutation pathway, 2 patients; the N155H mutation pathway, 2 patients; the Y143R mutation pathway, 1 patient). Pre-therapy plasma samples were analyzed to obtain the basal sequence of the IN gene. The virological characteristics of each patient are described in table 6.3.

The viral HIV RNA was extracted from plasma samples using an automatic nucleic acid extractor based on the principle of magnetic microspheres (QIAsymphony, Quiagen, Germany).

RECENT INFECTION			NON-RECENT INFECTION		
Isolated without resistance mutations			Isolated without resistance mutations		
Samples	*RT MUT : NNRTI, NRTI, other*	*Copies/ml*	*Samples*	*RT MUT: NNRTI, NRTI, other*	*Copies/ml*
001	-	1.632	025	-	1.207.177
004	-	37.290	026	-	387.014
008	V90I	5.262.000	027	-	50.370
039	-	328.310	028	-	401.109
024	-	132.520	029	S68G	90.566
049	-	965.900	031	-	85.096
051	-	>10.000.000	032	-	66.714
013	-	1.100.000	044	S68G	1.105.796
015	-	17.330	045	-	230.558
033	-	121.351	046	-	184.483
Isolated with resistance mutations			Isolated with resistance mutations		
002	V118I, E138A	202.300	018	K103N	2.298.365
003	V118I, E138A	12.290	020	E138A	108.304
005	K101E, E138K	164.800	021	V75I, K103N, K238T	7.896
006	S68G, E138A	105.500	022	M184V	16.857
007	V118I,E138G	129.900	038	M41L, K103N, M184V, T215F	4.239
009	D67N, T69N, K103N, V118I, K219Q, K238T	498.300	041	M41L, E44D, D67N, T69D, K103N, V106I, V118I, L210W, T215D	9.131
010	K101E, Y181C	6.050	043	M41L, T215D	54.404
011	K103N	100.200	047	D67N, K103N, M184V, K238T	303.578
016	M184V	39.881	048	I32M, K101E, Y181I, M184V, G190A, T215F	347.000
050	K103N, V179I	9.944.147	052	S68G, T69N, K103R, Y181C, E138Q, V179D, T215D	7.012

Table 6.1: first set of patients enrolled in the study of RT and their virological characteristics.

RECENT INFECTION			NON-RECENT INFECTION		
Isolated without resistance mutations			Isolated without resistance mutations		
Samples	*PR MUT, accessory, other*	*Copies/ml*	*Samples*	*PR MUT, accessory, other*	*Copies/ml*
006	K20I	105.500	026	V82I	387.014
007	K20R, M36I	129.900	027	-	50.370
024	-	132.520	028	-	401.109
			029	-	90.566
033	-	121.351	031	L10I, A71V	85.096
			032	-	66.714
Isolated with resistance mutations			Isolated with resistance mutations		
039	L10V, V11I, K20I, L24I, L33F, M36I, K43T,M46I, I54V, T74P, V82A	328.310	023	L10V, V11L, K20V, V32I, L33F,M46IMVL, I47V, F53L, I54L, Q58E, A71V, G73S, V82F, L89V, L90M	7.581
			041	L10I, K20M, I54V, A71V, L90M	9.131
			058	K20T, L33F, I50L, V82L	1.985
			060	L10I, M46IM, I50V	
009	L10I, K20I, L24I, M36I, M46I, I54V, V82A	498.300	061	L10F, L33F, M46I, I54V, G73T, I84V, L90M	1.336
			062	L10T, K20I, M46I, A71V, G73S, L90M	562

Table 6.2: second set of patients enrolled in the study of PR and their virological characteristics.

Samples	Basal sequence	Resistant sequence
	INT MUT, accessory, other	*INT MUT, accessory, other*
036		G140S, Q148H
054	V72I/V	M50I ,V72I, G140S, Q148H
037	T125M/V	T97A, T125V, E138D, N155H
053	E157E/K, S230N	T97A, N155H,S230N
055		L74M, T97TA, Y143R,

Table 6.3: third set of patients enrolled in the study of IN and their virological characteristics.

6.2 HIV recombinant molecular clones: *pNLΔPROgfp*, *pNLΔRTgfp* and *pNLΔINTgfp*

The *pNL4-3mod*, HIV-1 X4 tropic molecular clone, was previously developed (Bagnarelli *et al.*, 2003) starting from the original molecular clone *pNL4-3,* obtained from Dr. Malcolm Martin at NIH (National Institutes of Health, Bethesda, MD, USA) and derived from the NY5-LAV clinical isolates (Akio Adachi *et al*., 1986). The *pNL4-3* was modified to reduce the HIV-1 flanking regions and to substitute the original pUC-18 vector with the pCR-Script SK (+) Amp vector.
The molecular clone *pNL4-3mod* was employed as a backbone for the construction of other HIV molecular clones suitable for phenotypic studies. The construction of HIV molecular clones was described in the results. These molecular clones carrying the complete HIV genome, were engineered with the green fluorescent protein (GFP) reporter gene to yield a nef/GFP fusion protein to quantitatively measure viral replicative capacity (RC). The 3 clones were subsequently developed with the following features (Figure 6.1) :

- *pNLΔRTgfp* vector: RT gene-deleted clone replaced with a Eco47III blunt-end restriction site for cloning exogenous RT genes;

- *pNLΔPROgf*p vector: PR gene-deleted vector clone replaced with a SmaI blunt-end restriction site for cloning exogenous PR genes;

- *pNLΔINTgfp* vector: IN gene-deleted vector clone with a Eco47III blunt-end restriction site for cloning exogenous IN genes.

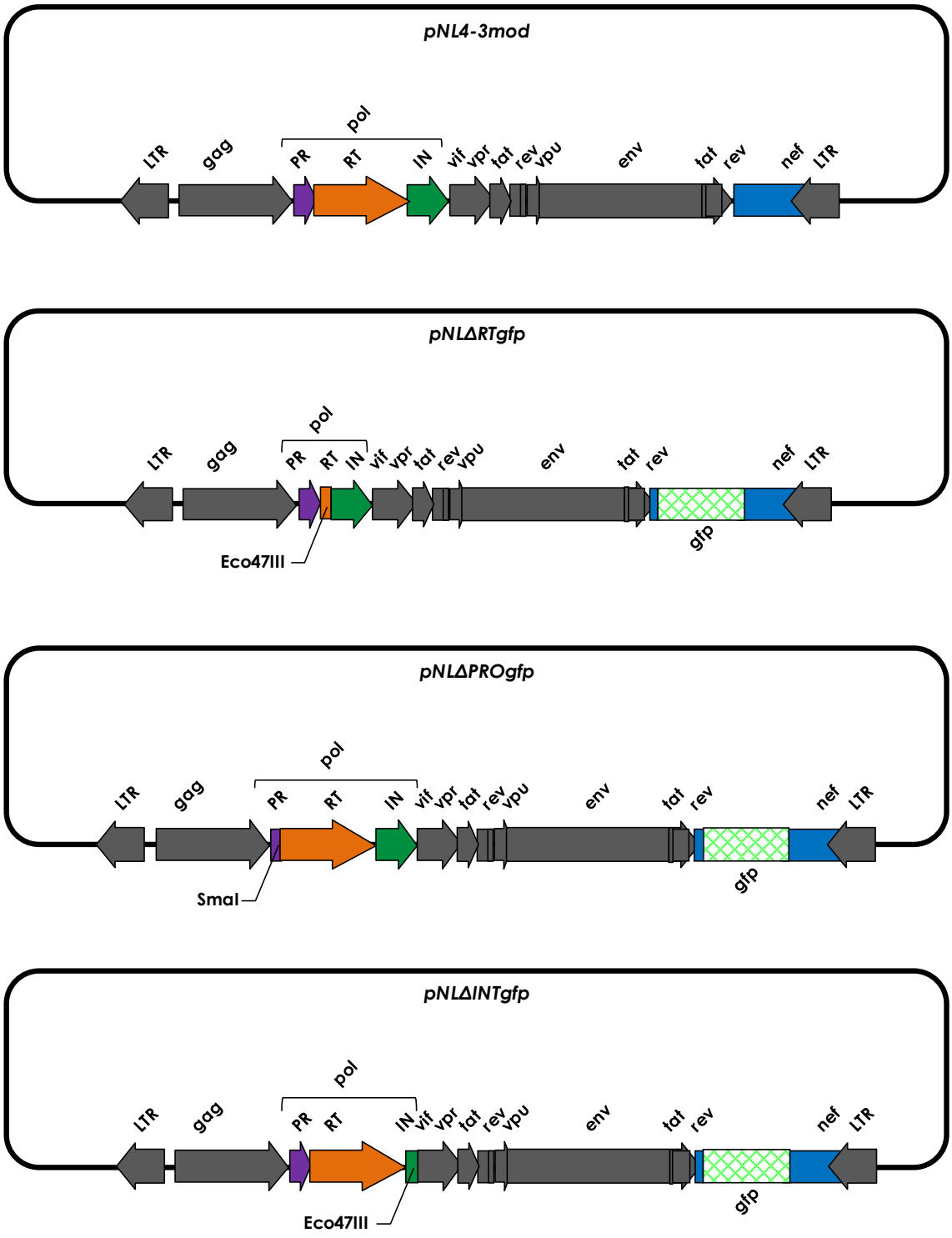

Figure 6.1: HIV recombinant molecular clones used in phonotypic assays.

6.3 Polymerase chain reaction amplification of HIV RT, PR and IN for production of chimeric viruses

The viral RNA from the patient's plasma was reverse transcribed in cDNA and amplified using the SuperScript One-Step RT-PCR kit for Long Templates (Invitrogen). RT-PCR reactions were performed in a final volume of 50 µl consisting of 25 µl of 2X Reaction Mix, 1,5 µl of RT/Platinum Taq, 1 µl of RNase Inibitor, 2 µl of sense primer (10 µM), 2 µl anti-sense primer (10 µM), 13,5 µl of autoclaved distilled water and 5 µl of RNA extract. The amplification program was as follows: an incubation of 45 minutes at 50°C, an incubation of 2 minutes at 94°C followed by 45 cycles of 15 seconds at 94°C, 30 seconds at 50°C, 2 minutes and 30 seconds at 72°C; and a final extension step of 10 minutes at 72°C. The sequence of the primers used in RT-PCR assay are listed in table 6.4. The PCR fragments were loaded on the polyacrylamide gel (10%) in TBE 1X, 184 Volts to evaluate the presence and the quality of samples. The pGEM DNA Molecular Weight Marker (Promega) was used as standard molecular weight.

Primer ID	Sequence (5'- 3')	Sense/Antisense	RT-PCR	Base pair of PCR products
PRs	TCAGATCACTCTTTGGCAACG	sense	Reverse Transcriptase	1761 bp
RTasCLOSMA	GAATCCTGCAAAGCTAGATGAATTGC	antisense		
PRs	TCAGATCACTCTTTGGCAACG	sense	Protease	337 bp
PRac	TGGCTTTAATTTTACTGGTAC	antisense		
INTESTs	GTAGCAAAAGAAATAGTAGCCAGC	sense	Integrase	893 bp
INTESTas	GTGGGATGTGTACTTCTGAACTTA	antisense		

Table 6.4: primers used for the RT-PCR of RT, PR and IN.

The next step was a nested PCR using the Pwo DNA Polymerase (Roche) to generate blunt-end PCR products and nested amplification primers. The PCR products obtained using the SuperScript One-Step RT-PCR kit were amplified in a final volume of 50 µl using 2,5 µl of each primers in the presence of 1X PCR buffer homemade (containing 100mM Tris HCl, 500mM KCl, 15mM $MgCl_2$), 1 µl dNTP mix and 2,5 U of Pwo DNA Polymerase (Roche). The amplification program was as follows: an initial denaturation step of 3 minutes at 94°C followed by 25-28 cycles of 30 seconds at 94°C, 30 seconds at 50°C, 2 minutes and 30 seconds at 72°C; and a final elongation step of 3 minutes at 72°C. The primer sequences used in the Nested PCR assay are listed in table 6.5. The PCR fragments were loaded on polyacrylamide gel (10%) in TBE 1X, 184 Volts to evaluate the presence and the quality of samples. The pGEM DNA Molecular Weight Marker (Promega) was used as standard molecular weight. Subsequently the products were ligated in the respective vectors where they competed the reading frame of the respective genes.

Primer ID	Sequence (5'- 3')	Sense/Antisense	Nested-PCR	Base pair of PCR products
RTsCLOECO	TTAGTAGAAATTTGTACAGAAATG	sense	Reverse Transcriptase	1305 bp
RTasCLOECO	GGGACAACTTTTTGTCTTCC	antisense		
PRs	TCAGATCACTCTTTGGCAACG	sense	Protease	337 bp
PRac	TGGCTTTAATTTTACTGGTAC	antisense		
INTEGRASIs	CATGCATGGACAAGTAGACTGTA	sense	Integrase	767 bp
INTEGRASIas	TTTCCTTGAAATATACATATGGTG	antisense		

Table 6.5: primers used for the Nested-PCR of RT, PR or IN.

6.4 Site-directed mutagenesis of IN gene

Mutagenesis of specific IN residues in the original IN gene was achieved by PCR. Primers bearing the mutated nucleotides, synthesized in the reverse and forward orientation, were used coupled with primer INTESTs or INTESTas (table 6.4), respectively, in two different amplification reactions. After PCR amplification, aliquots of the two products were mixed and amplified with the internal primers (INTEGRASIs and INTEGRASIas) (table 6.5) as described above. The primers used for mutagenesis experiments are listed in Table 6.6. The mutated IN genes were then inserted into the *pNLΔINTgfp* as described in the results.

Primer ID	Sequence (5'- 3')(mutaed nucleotides)	Sense/Antisense	Mutated residues
MUT140s	GCAGGAATTTAGCATTCCCTACAA	sense	G140S
MUT140as	TTGTAGGGAATGCTAAATTCCTGC	antisense	
MUT148s	CTACAATCCCCAAAGTCACGGAGT	sense	Q148H
MUT148as	ACTCCGTGACTTTGGGGATTGTAG	antisense	
Vs_155MUT	GGAGTAGTAGAATCTATGCATAAGAA	sense	N155H
Vas_155MUT	TTCTTATGCATAGATTCTACTACTCC	antisense	
Ts_155MUT	GGAGTAGTAGAATCTCTCCATAAAGA	sense	N155H
Tas_155MUT	TCTTTATGGCGAGATTCTACTACTCC	antisense	
PZ1MUT155s	GGAGTAGTAGAATCTATGCATAAAGA	sense	N155H
PZ1MUT155as	TCTTTATGCATAGATTCTACTACTCC	antisense	
036MUT155s	GGAGTAGTAGAATCTATACATAAAGA	sense	N155H
036MUT155as	TCTTTATGTATAGATTCTACTACTCC	antisense	

Table 6.6: primers used for site-directed mutagenesis of IN sequences.

6.5 Cloning strategies

6.5.1 Enzymatic digestion of *pNLΔRTgfp*, *pNLΔPROgfp* and *pNLΔINTgfp*

An enzymatic digestion reaction of *pNLΔRTgfp* vector was performed in 50 µl final volume with 2,5 µl of ECO47III (Promega), 5 µl of 10X buffer, 2,5 µl of vector and 40 µl of sterile water. The reaction was incubated for 2 hours at 37°C and then was loaded on agarose gel (1 %) in TBE 1X, 90Volts (cell size: 9,2 x 25,5 x 5,6 cm). Lambda DNA/EcoRI+HindIII Markers (Promega) was used as standard molecular weight marker. The same enzymatic digestion reaction was carried out for the *pNLΔINTgfp* vector. The *pNLΔPROgfp* vector was digested with SmaI (Promega) and the enzymatic digestion reaction was performed for 2 hours at 25°C. Different aliquots of the digested vectors were stored at -80°C for following experiments.

6.5.2 Ligation

Blunt-end PCR products (RT, PR and IN gene) were directly added to the digested vector, *pNLΔRTgfp*, *pNLΔPROg*fp and *pNLΔINTgfp* respectively. The ligation reaction (final volume 10 µl) was performed in the presence of 1X ligation buffer (Promega) containing Eco47III or SmaI (1,6 U) to improve the yield of the recombinant plasmid and 1 U of T4 DNA Ligase (Promega). The reactions were incubated at 20° C overnight.

6.5.3 Bacterial transformation

An aliquot of 2 µl of the ligation reaction was used to transform the JM109 high-efficiency Competent Cells (Promega) by the heat-shock method according to the manufacturer

instructions. After a short incubation on ice (10 minutes) the mixture of competent cells and plasmid was placed at 42°C for 40 seconds and then placed back on ice (2 minutes). 450 µl of SOC medium was added and the transformed cells were incubated at 37°C for 60 minutes with shaking. To isolate transformed colonies, transformed bacteria were plated on Luria Bertani agar plates (LB: 10 g/l Bacto-tryptone, 5 g/l Bacto-yeast extract, 5 g/l NaCl and 12 g/l Agar) supplemented whit ampicillin to a final concentration of 40 µg/ml. The plates were incubated at 37˚C overnight. Resistant colonies were confirmed by another step on LB agar plate containing the same concentration of antibiotic used for selection.

6.5.4 PCR screening of positive colonies

Single colonies were isolated and checked for the orientation of the inserted RT, PR or IN by PCR using specific primers. The sequences of the primers used in the PCR screening assay are listed in table 6.7. The sense primer hybridized on the vector before the junction with the inserted gene and the anti-sense primer was in the insert; only the colonies which had the correct orientation of the inserted gene allowed PCR amplification. Colonies from the second plate were picked up with a sterilized toothpick and directly transferred to the PCR tube as DNA templates. The PCR screening were performed in a final volume of 50 µl using 2,5 µl of each primers (10 µM) in the presence of 5µl of 10X Dream Taq Buffer, 1 µl dNTP mix and 1 U of Dream Taq DNA Polymerase (Thermo Fisher Scientific). The thermal cycle program consisted of an incubation of 94°C for 3 minutes followed by 25 cycles of 94°C for 30 seconds, 55°C for 30 seconds and 72°C for 1 minute and 30 seconds, and then incubation at 72°C for 3 minutes. Subsequently, PCR products were separated on 10% polyacrylamide gel electrophoresis.

Primer ID	Sequence (5'- 3')	Sense/Antisense	PCR-SCEENING
INTAGE4	ATTCTAAAAGAACCAGTACATG	sense	Reverse Transcriptase
RTSEQas	CTGGTTGTGCTTGAATGATTC	antisense	
PROTs	AAGCAGGAGCCGATAGACAAG	sense	Protease
PRac	TGGCTTTAATTTTACTGGTAC	antisense	
INSEQs	TAACCTACCACCTGTAGTAG	sense	Integrase
INT6as	TGTCTACTATTCTTTCCCCT	antisense	

Table 6.7: primers used for PCR screening of positive colonies.

6.5.5 Plasmid extraction

Bacteria bearing positive clones were expanded in 5 ml of LB broth with 40 µg/ml ampicillin at 37°C overnight with shaking. Plasmids were obtained by miniprep purification using Exprep Plasmid SV mini 200p (Gene All) according to the manufacturer instructions.

6.5.6 Restriction enzyme digestion

Plasmids were checked for integrity by restriction enzyme digestion using HindIII (five fragments expected) and BglII (six fragments expected). The restriction enzyme digestion was performed in a volume of 10 µl: 0.5 µl of restriction enzyme (HindIII or BglII), 1 µl of restriction enzyme buffer (Buffer E or Buffer D respectively), 1,5 µl of extracted plasmid and 7 µl of sterile water. The reaction was incubated at 37°C for 2 hours and 30 minutes. The samples were analyzed on agarose gel (1%) in TBE 1X, 90 Volts (cell size: 9,2 x 25,5 x 5,6 cm) to compare plasmids restriction profiles with a control sample. Lambda DNA/EcoRI+HindIII Markers (Promega) was used as molecular weight marker.

6.6 Sequences Analysis

The DNA sequencing was used to analyze the sequence for the patients genetic backbone and the desired mutations associated with antiviral resistance and to analyze the absence of insertions, deletions or unwanted artefactual mutations. Sequence analysis was performed using an ABI Prism 3100 Genetic Analyzer (Applied Biosystems-HITACHI). This was the latest generation of 16-capillary electrophoresis instruments based on the Sanger sequencing approach: a simple and rapid method allowing to determine nucleotide sequences in single-stranded DNA. This technique (commercialized by Applied Biosystems) is based on the incorporation of chain-terminating dideoxynucleotides by DNA polymerase during *in vitro* DNA replication (Sanger and Coulson, 1975).

Sequencing reactions were performed using a commercial kit (Big Dye Terminator v1.1 Cycle Sequencing Kit, Applied Biosystems) and contained 0,5 µl of DNA sample, 2 µl of Big Dye Terminator, 2µl of 5X Sequencing Buffer, 1 µl of Primer (100 µM) and sterile water to 10 µl final volume. The cycle conditions were 25 cycles at 95°C for 10 seconds, 50°C for 5 seconds, and 60°C for 2 minutes.

At completion of the sequencing reaction, the sequencing products were purified using the Big Dye X Terminator Purification Kit (Applied Biosystems) in 96-well plate directly. Specifically, the sequencing products were purified by addition of 45 µL of SAM Solution and 10 µL of Big Dye X Terminator solution. The 96-well plate was placed on a shaker at 2,000 rpm for 30 minutes, followed by a spin at 1,000 x g for 2 minutes. The RT in the recombinant molecular clones was sequenced using the primers POL4 and RTSEQas, the PR gene using PRs and PRac and the IN region was sequenced using the INTESTs, INT6s, INT6as, and INTESTas (table 6.8) in order to evaluate the specific sequence of the insert and the correct insertion in the vector. These sequences were analyzed using Sequencing analysis,

Seqscape and BioEdit programs. Subsequently the sequences were evaluated with a specific algorithm for the analysis of drug resistance mutations: HIVDB. These sequences of recombinant molecular clones were compared with the sequence of the viral quasispecies obtained from the plasma of the corresponding patients in order to select the most representative clones of the viral quasispecies in each patient.

Primer ID	Sequence (5'- 3')	Sense/Antisense	Sequencing PCR
POL4	CCAGGAATGGATGGCCCAAAAGTT	sense	Reverse Transcriptase
RTSEQas	CTGGTTGTGCTTGAATGATTC	antisense	
PRs	TCAGATCACTCTTTGGCAACG	sense	Protease
PRac	TGGCTTTAATTTTACTGGTAC	antisense	
INTESTs	GTAGCAAAAGAAATAGTAGCCAGC	sense	Integrase
INTESTas	GTGGGATGTGTACTTCTGAACTTA	antisense	
INT6s	CAGGGGAAAGAATAGTAGA	sense	
INT6as	TGTCTACTATTCTTTCCCCT	antisense	

Table 6.8: primer used for sequencing reaction of recombinant molecular clones.

6.7 Cell culture

To obtain recombinant viruses for infection experiments, eukaryotic cells were transfected using the HIV recombinant molecular plasmids. The TZM cells (engineered HeLa cell line expressing high levels of CD4 and co-receptors CCR5 and CXCR4) was maintained in Dulbecco's modified Eagle medium (DMEM) supplemented with 10% fetal calf serum (FCS) and an antibiotic-antimycotic cocktail (100 U/ml penicillin, 100 µg/ml streptomycin and 0.25 µg/ml amphotericin B). Cells were maintained in T25 tissue culture flasks; once a week the confluent monolayer was passed (1:5) using T25 flasks following trypsinization.

The U87/CXCR4 cell line was used to study the RC of the HIV-1 recombinant molecular clones. U87 (engineered human glioma cell line expressing CD4 and HIV co-receptor CXCR4)

was maintained in DMEM supplemented with 10% FBS and 0,5X generic antibiotics. 300 µg/ml geneticin and 1 µg/ml puromycin were added to maintain the expression of CD4 and co-receptor respectively. All cultures were incubated at 37°C in 5% CO_2 and 95% humidity.

6.7.1 Transfection

TZM cells were transfected with the recombinant plasmids by the non-liposomal reagent "FuGENE HD Transfection Reagent" (Promega). The day before transfection confluent cell monolayers were trypsinized, resuspended in coltured medium and counted using Burker's counting chamber. Cells were seeded in 24-well tissue culture plates at a density of 150000 cells/well/ml of DMEM 10% SCF medium and the plates were incubated overnight to allow the cell adhesion to the surface (Figure 6.2A). The medium in the well plate was discarded and washed with fresh medium twice. After washing, 500 µl of DMEM 10% SFC medium was added to each well. Cells were transfected with 26 µl solution containing 0,02 µg/µl of plasmid and 1,6 µl of Fugene. The solution was incubated at room temperature for 10 minutes, then added to the cells by pipetting 5 times. Following overnight incubation, 500 µl medium was added to each well for a final volume of 1 ml. The plasmid, in the cells, expressed viral genes, producing infectious virus particles that were released into the supernatant causing syncytia formation and cytopathic effect (CPE) (Figure 6.2B). After 72 hours, the supernatant containing infectious viruses, was harvested and centrifuged at 3000 *g* for 10 minutes and stored at -20 °C. The p24 antigen (HIV-1 capsid) was dosed by chemiluminescent immunoassay (ARCHITECT system, Abbott, USA), allowed to quantify the virus particles produced during transfections in the supernatant and to standardize infection of permissive cell line. The titer of infectious virus particles in the

supernatant of transfected cells was quite variable from sample to sample. Basing on the results of p24, the transfection supernatant was standardize to have the same titer of infectious virus particles for each samples.

6.7.2 Infection

The day before infection, U87 cells of co-receptors were plated in 96 well black plates with clear bottom (Corning Incorporated, Costar) at a density of 50000 cells/well in 150 µl of DMEM 10% FCS medium with geneticin and puromycin (Figure 6.2C). The cells were infected 24 hours later by 50 µl of a solution (minimum volume to cover the bottom of well) containing the transfection supernatant and the culture medium. Adsorption of virus was allowed to occur for 1 hours at 37°C, then 100 µl DMEM 10% FCS medium with geneticin and puromycin were added to obtain a final volume of 150 µl/well. Cultures were examined daily for syncytia formation and CPE (Figure 6.2D). The virus produced GFP-*nef* fusion protein which made infected cells fluorescent after 24 hours (Figure 6.2E) and fluorescent emission increased after 72 hours (Figure 6.2F). For this reason, the relative fluorescence values (RFV) were measured directly on the culture plate from day 1 to day 6 post-infection using the Fluoroskan Ascent (Thermo scientific). This instrument was a microplate fluorometer capable of measuring the emitted light of a different substances. In the fluorometer, a light source emitted light of an excitation wavelength; the sample absorbed light energy and instantaneously emitted light of a longer wavelength. The specific excitation wavelength for the GFP reporter gene was 485λ and emission wavelength was 510 λ. The emitted light was measured by a detector and data was transferred to PC. Subsequently the RC of recombinant viruses was determinate as described in the results.

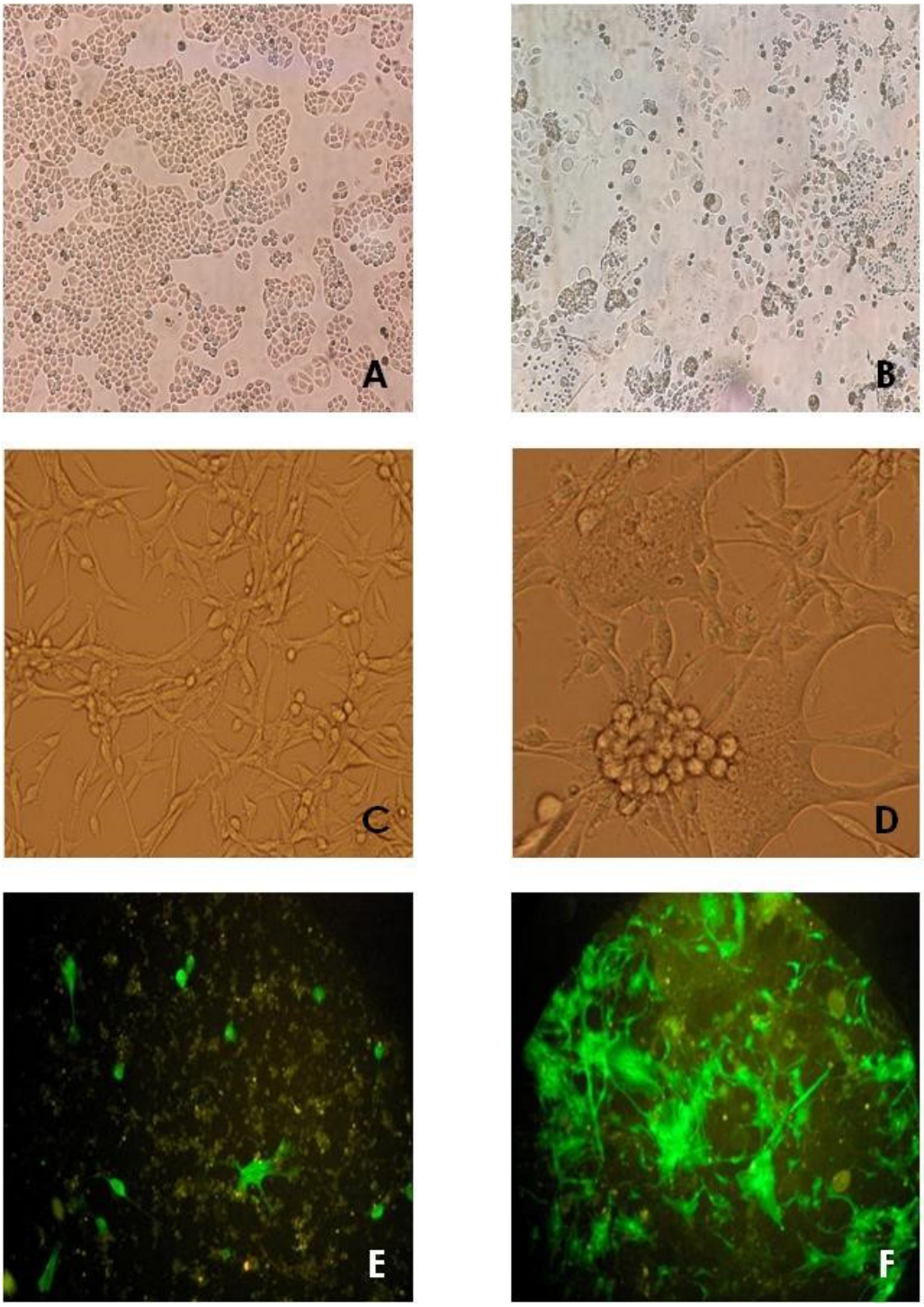

Figure 6.4: **A.** TZM cell line; **B.** TZM cell line 72 hours after transfection with syncytia formation and CPE; **C.** U87/CXCR4 cell line; **D.** U87/CXCR4 cell line 72 hours after infection with syncytia formation and CPE; **E.** U87/CXCR4 infected cells and fluorescent emission 24 hours after infection; **F.** increase of fluorescent emission 72 hours after infection.

6.8 Raltegravir and Dolutegravir dilution

The RC of IN recombinant molecular clones was evaluated under 2 different drug selective pressure: raltegravir (RAL) and dolutegravir (DTG). Antiretroviral drugs were provided free of charge by Immunology Laboratory (Ospedali Riuniti di Ancona).
A RAL tablet (400 mg) was dissolved in 5 ml dimethyl sulfoxide (DMSO) to obtain a concentration of 160 mM and then diluted 1:10000 to a final concentration of 16 µM. The latter solution was further diluted 1:3.3 and stored at -80°C at a final concentration of 4,8 µM.
A DTG tablet (50 mg) was dissolved in 3 ml dimethyl sulfoxide (DMSO) to obtain a concentration of 39,74 mM and then diluted 1:40 to a final concentration of 1 mM. The latter solution was further diluted 1:100 and stored at -80°C at a final concentration of 10 µM.
The drugs dilutions tested were selected basing on several *in vitro* studies. The RAL concentrations tested were: 0,1875 nM, 0,75 nM, 3 nM and 12 nM. The DTG concentrations tested were: 0,1875 nM, 0,75 nM, 3 nM, 12 nM and 48 nM.

7. Results

7.1 Development of HIV molecular vectors: *pNLΔRTgfp*, *pNLΔPROgfp*, and *pNLΔINTgfp*

Three molecular vectors were developed for this study.
The HIV-1 X4 tropic molecular vector, named *pNLΔPRO,* was obtained as described by Menzo *et al.(*2000). Briefly this molecular clone bears the deletion of the protease (PR) gene, replaced with a novel, unique SmaI restriction site in order to maintain the replication competence after the introduction of the exogenous HIV-1 PR-encoding ORF (open reading frame).
The HIV-1 X4 tropic molecular vector, named *pNLΔRT*, was obtained starting from *pNL4-3mod* (Bagnarelli *et al*., 2003) (Figure 7.1). The *pNL4-3mod* was digested using MscI blunt-end restriction enzyme to obtain a deletion of a portion of the *pol* gene including reverse transcriptase (RT) gene and gene encoding RNAseH enzyme. PCR-direct mutagenesis was used to obtain the RNAseH encoding sequence and to introduce a new Eco47III blunt-end restriction site for cloning exogenous RT genes. The RNAseH gene was amplified starting from *pNL4-3mod* vector using Pwo DNA Polymerase (Roche) and specific primers: RTasECO (5'-CCATCTTCCTGCTAATTTTAAGAG-3') bearing three nucleotides of MscI restriction site and PRsECO (5'-
CCATTGACAGAAGAAAAAATAAAAGCGCTAACGGACACAA
C-3') bearing a deletion encompassing 1305 nucleotides of the RT region, Eco47III restriction site and three nucleotides of MscI restriction site for in frame insertion into the vector. The mutagenized fragment was verified by sequencing analysis and ligated into the MscI digested *pNL4-3mod* vector, obtaining the final construct named *pNLΔRT*. The *pNLΔRT* molecular vector bears the deletion of the RT gene, the introduction of a novel, unique Eco47III restriction site and no

other modification compared to the original molecular clone sequence, thus being replication-competent after the introduction of the HIV-1 RT-encoding ORF .

The molecular clone *pNL4-3mod* was also employed as a backbone for the construction of the integrase (IN) gene-deleted vector designed *pNLΔINT* (Figure 7.2). Two restriction sites upstream and downstream of the IN gene were identified in the *pNL4-3mod* sequence (AgeI and AccB7I). PCR-directed mutagenesis was used to obtain a deletion of IN gene and to introduce a new Eco47III blunt-end restriction site for cloning exogenous IN genes. The external primers included the AgeI and AccB7I restriction sites (INT-AGE: 5'-CTAAAAGAACCGGTACATGGAGTGTATTATGAC-3' and INT-ACC: 5'-CACCTAGGACTAACTATACGTC-3'); the inner primers were designated to be one the reverse complement of the other and to contain: the original viral sequence in the 3' half, a blunt-end Eco47III site in the middle and again the viral sequence across the IN gene at the 5' end (INTECO-S: 5'-AAGGGGAAGCGCTTAGTAAAACACCATATG-3' and INTECO-AS: 5'-TTTACTAAGCGCTTCCCCTTTTAGCTGAC-3'). Under these conditions, two separate, but partly overlapping, PCR products incorporated the deletion of the IN gene and introduced a novel Eco47III in the frame site at the splice junction. The amplification products were purified from primers and used as templates in two different single-primer amplification reactions in order to obtain single-strand amplified products. These products were mixed, added to a T4 DNA polimerase polymerization reaction and finally amplified using the external primers. The PCR product was purified, restricted with AgeI and AccB7I, and ligated into the correspondingly cut *pNL4-3mod* vector. This molecular clone designated *pNLΔINT* bears the deletion of the IN gene, the introduction of a novel, unique Eco47III restriction site, and no other modification within the original molecular clone sequence, thus being replication-

competent after the introduction of the HIV-1 IN exogenous genes.

These three molecular vectors (*pNLΔRT, pNLΔPRO and pNLΔINT)* were further engineered with the green fluorescent protein (GFP), reporter gene, to yield a *nef*/GFP fusion protein to quantitatively measure viral replicative capacity (RC) . The GFP (from Aequorea victoria) was amplified using the primers GFPs (5'-GACGAGCTGAGCCAATGGTGAGCAGGGG-3 ') and GFPas (5'-TGCTGGCTCAGCTCAAGATCTGAGTC-3') containing BlpI restriction site. The amplification product was digested using this restriction enzyme. The molecular vectors were linearized with BlpI: an existing BlpI restriction site was located within *nef* gene. The new molecular vectors obtained were identified as follow: *pNLΔRTgfp, pNLΔPROgfp,* and *pNLΔINTgfp*.

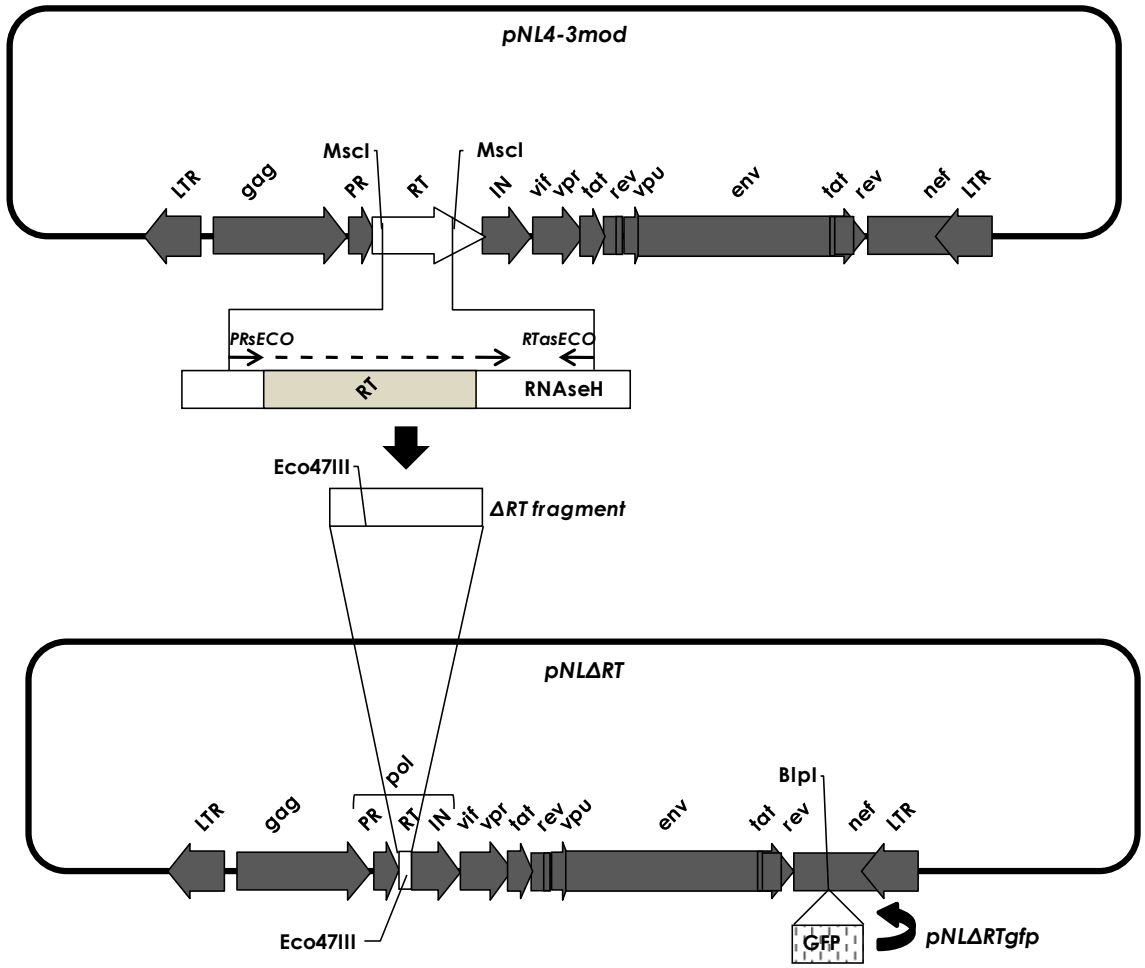

Figure 7.1: generation of *pNLΔRTgfp*. The sequence of *pNL4-3mod* RT gene (from the MscI restriction sites) was modified by PCR directed mutagenesis to obtain the ΔRT fragment. The fragment containing a new restriction site (Eco47III) was reinserted into *pNL4-3mod*. The GFP reporter gene was inserted into backbone to yield a *nef*/GFP fusion protein to quantitatively measure viral RC.

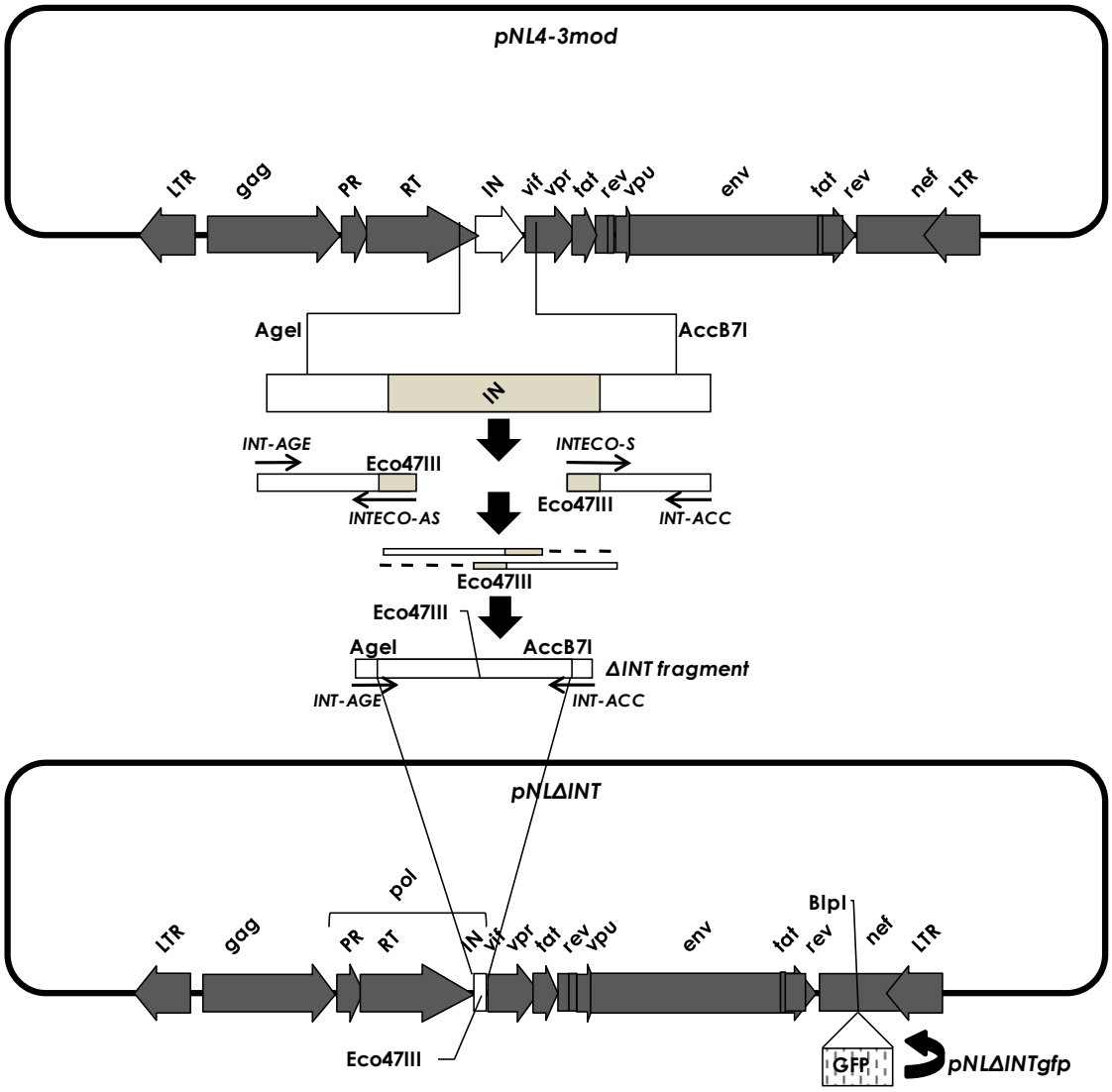

Figure 7. 2: generation of *pNLΔINTgfp*. The fragment of *pNL4-3mod* RT gene (from the AgeI to the AccB7I restriction sites) was modified by PCR directed mutagenesis to obtain the Eco47III restriction site containing ΔINT fragment. The mutagenized ΔINT fragment was reinserted into *pNL4-3mod*. The GFP reporter gene was inserted into backbone to yield a nef/GFP fusion protein to quantitatively measure viral RC.

7.2 Validation of recombinant phenotypic assay and correlation between p24 and RFV

In order to validate the recombinant phenotypic assay based on fluorescence reading, the full length sequence of the *pNL4-3mod* in the molecular vectors *pNLΔRTgfp, pNLΔPROgfp, and pNLΔINTgfp* was completed by cloning the specific regions amplified from *pNL4-3mod*. TZM cells were transfected with recombinant plasmids to produce virus particles which were subsequently quantify to standardize the infection in the permissive cell line. The virus from the recombinant clones showed a replication kinetic comparable to that from the control wild type *pNL4-3mod* (Figure 7.3). These results demonstrated that the strategy used was reliable and was applicable to the recombinant phenotypic analysis of the 3 respective genes.

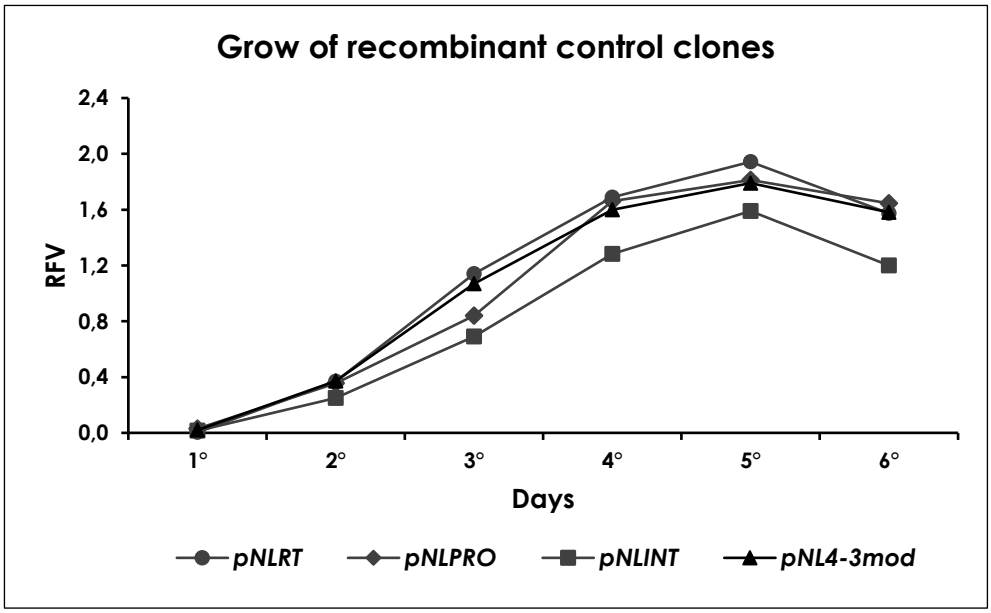

Figure 7.3: RFVs (Y axis) of recombinant control clones from the day 1 to day 6 (X axis) post infection of the U87/CXCR4 cell line;
pNLRT means *pNLΔRTgfp* with RT from *pNL4-3mod*;
pNLPRO means *pNLΔPROgfp* with PR from *pNL4-3mod*;
pNLINT means *pNLΔINTgfp* with IN from *pNL4-3mod*.

The RC of the recombinant viruses was computed after the infection of the U87/CXCR4 cell line either by measuring directly the relative fluorescence value (RFV) on the culture plate using the Fluoroskan Ascent or by dosing the p24 antigen using a chemiluminescent immunoassay in the supernatant of infected cells. Figure 7.4 shows the p24 values (X axis) and the RFV (Y axis) related to the validation tests described above. A strong correlation was observed between the values of p24 and RFVs as shown by Pearson correlation (r^2=0,7069; p<0,0001). Since the optimal agreement between the two measurement methods, the RFV method was selected to evaluate recombinant phenotypes as it was more flexible and less expensive than the p24 dosage and allowed to repeat measurements indefinitely on the same cultures.

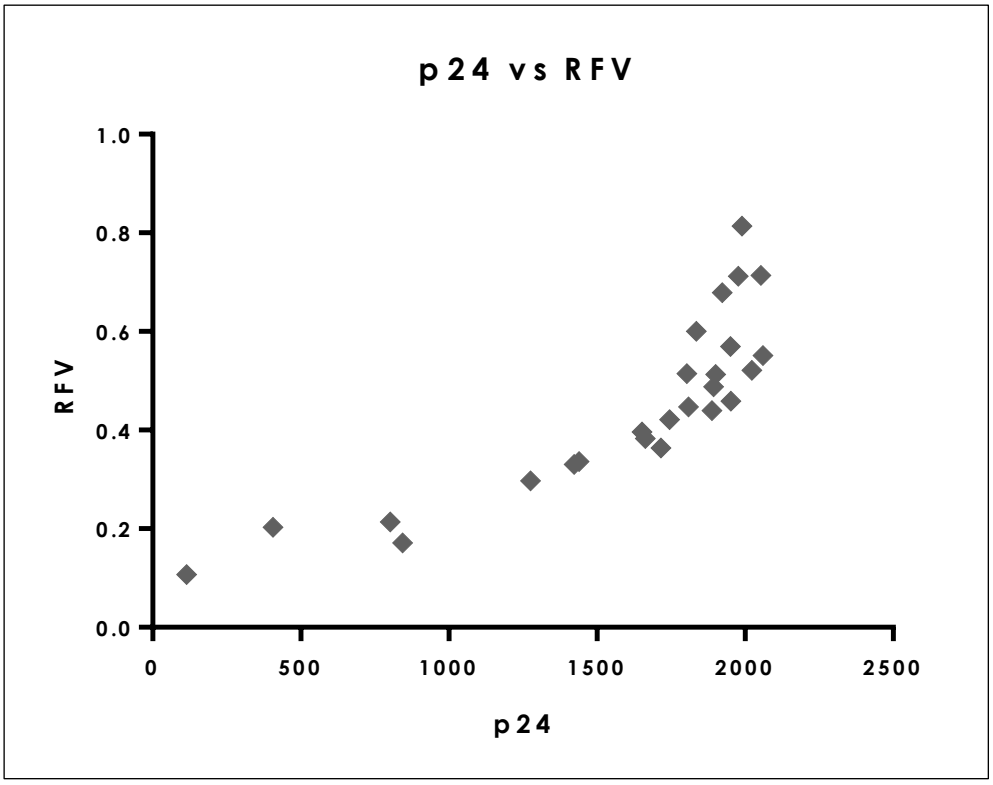

Figure 7.4: correlation between the value of p24 (X axis) and RFV (Y axis) as measure of RC of recombinant control clones after U87/CXCR4 infection.

7.3 Replicative capacity of HIV-1 strains from recently infected and chronically treated patients

7.3.1 Replicative capacity of RT recombinant phenotypes

40 HIV-1viremic patients were selected for the phenotypic study of the RT gene and were divided into four groups as described in materials and methods:

- Recent Infection Wild Type: recently infected patients (< 1 year) and naïve for antiretroviral treatment harboring a wild type virus
- Recent Infection Mutated: recently infected patients (< 1 year)and naïve for antiretroviral treatment harboring a virus with RT resistance mutations
- Non-recent Infection Wild Type: chronically treated patients harboring a wild type virus
- Non-recent Infection Mutated: chronically treated patients harboring a virus with RT resistance mutations.

In recent infections mutations against non-nucleoside reverse transcriptase inhibitor (NNRTI) were the most frequent: 4 patients with E138A/G, 2 patients with K103N, 2 patients harboring a virus with 2 resistance mutations (K101E + Y181C and K101E + E138K). Nucleoside reverse transcriptase inhibitor (NRTI) mutations were found only in 2 patients. One of these had a virus with one NRTI resistance mutations (M184V) and the other harbored a virus with combined NNRTI and NRTI mutations. Chronically treated patients (8/10) had a higher prevalence of NRTI mutations, frequently in combination with NNRTI mutations. The RT genes were amplified from plasma samples and cloned for a recombinant phenotypic analysis in *pNLΔRTgfp* molecular clone. After transfection of all clones on packaging cells, the supernatants were used to infect the U87/CXCR4 permissive cell line. Fluorescent emission of the reporter GFP was measured during *in vitro* replication of recombinant viruses from day 1 to

day 6 post-infection. The graphs (Figure 7.5) shows the RFV mean (Y axis) of four replicates for each recombinant molecular clone plotted against the days after infection (X axis), in 4 groups.

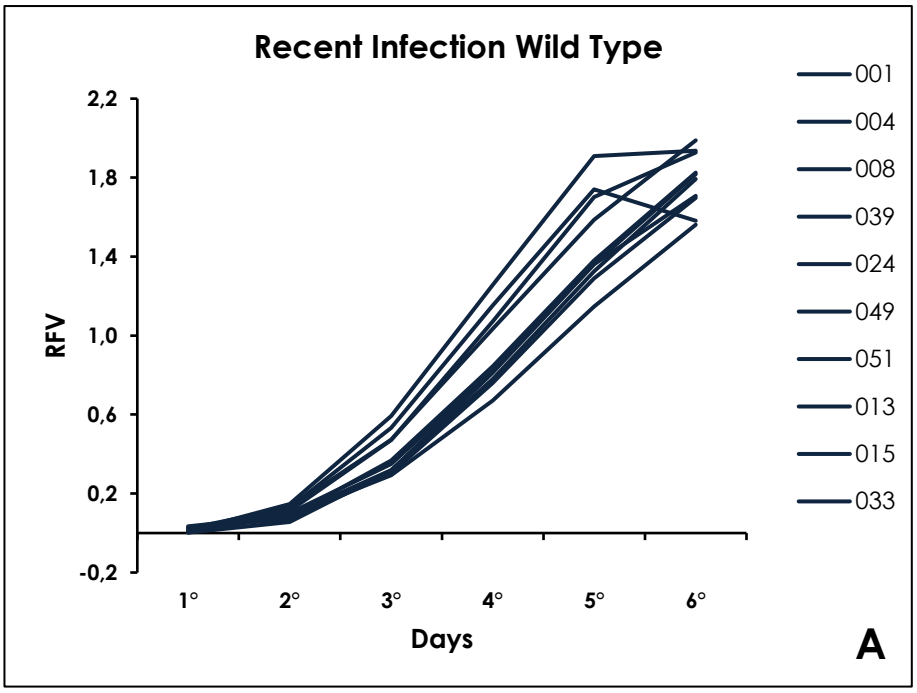

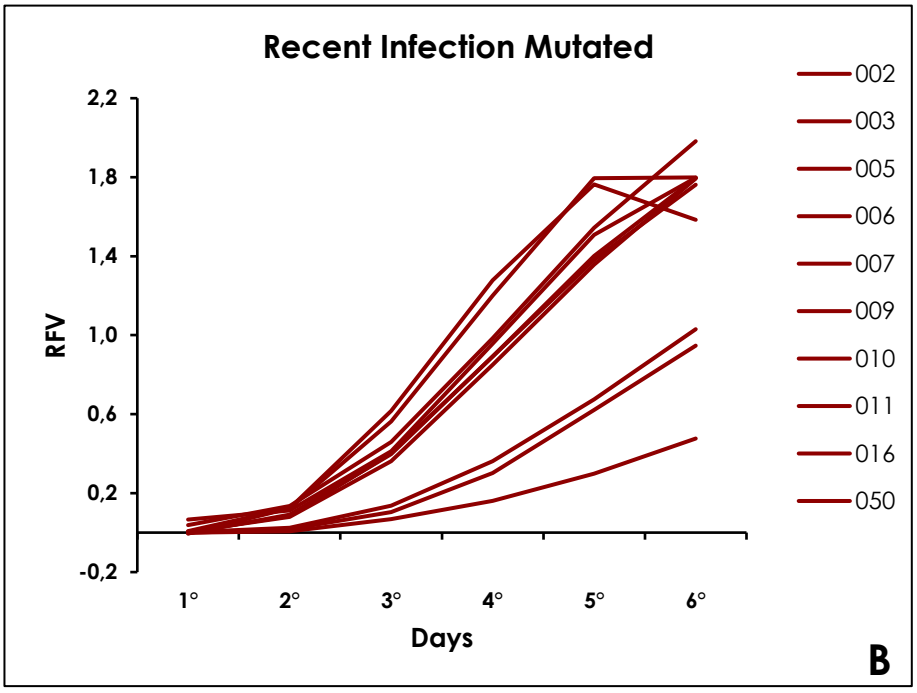

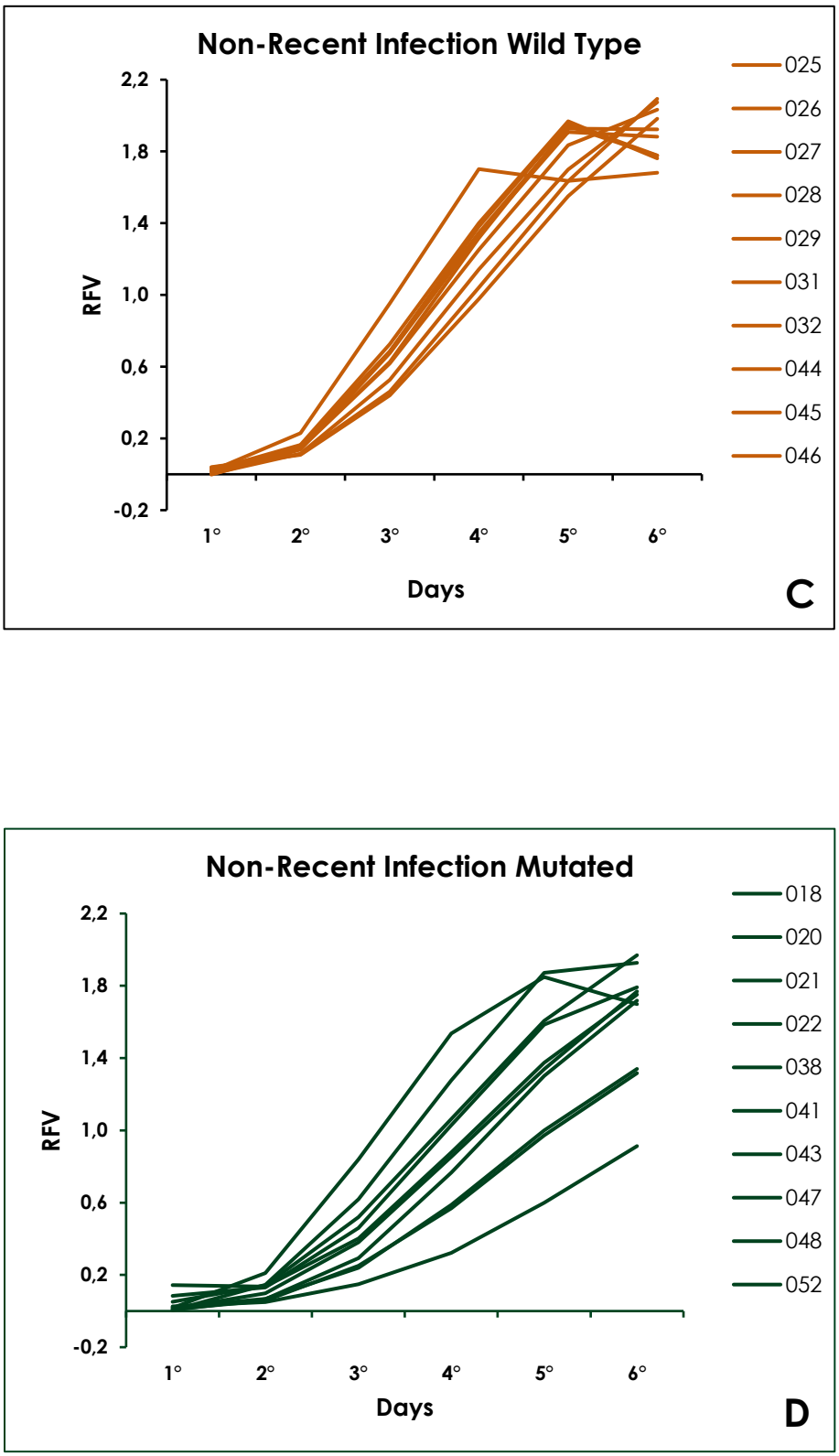

Figure 7.5: RFVs mean (Y axis) of all recombinant molecular clones in cell culture from the day 1 to day 6 (X axis) post infection: **A.** Recent Infection Wild Type-blue lines; **B.** Recent Infection Mutated-red lines; **C.** Non-Recent Infection Wild Type-orange lines; **D.** Non-Recent Infection Mutated-green lines.

The RFV values were proportional to the number of infected cells in the culture, and therefore, analyzed in kinetics, represented the virus's ability to infect new cells and the slope of the line between first and third day post infection was considered the best indicator of RC. RFVs increased from the first to the sixth day ranging from a minimum of -0,005 to a maximum of 2,093. The common characteristic was a decreasing grow rate 5 days after infection due to the saturation of the system. The histogram (figure 7.6) shows the slope values expressed as the X coefficient of the linear equation underlying the RFV increase for each isolate. Phenotypic tests showed a high degree of RC variability from patient to patient ranging from a minimum of 0,034 to a maximum of 0,467. The graph (figure 7.7) shows the median RC with interquartile range (IQR) of different groups: 0,1710 (IQR: 0,1408-0,2378) in Recent Infection Wild Type, 0,1885 (IQR: 0,0635-0,2268) in Recent Infection Mutated, 0,3165 (IQR: 0,2493-0,3413) in Non-recent Infection Wild Type and 0,1630 (IQR: 0,1170-0,2523) in Non-recent Infection Mutated. Mann-Whitney non-parametric test was used to compare RC in the 4 groups of patients. In recent infections, isolates bearing resistance mutations displayed a slightly increased RC compared to wild type isolates (0,1885 vs 0,1710; p=0,5298). On the contrary in non-recent infections the impact of resistance mutations in reducing RC was significant (0,1630 vs 0,3165; p=0,0089). Wild type isolates from recent infections were significantly less replicative than those from non-recent infections (0.1710 vs 0.3165; p=0,0015), while mutated isolates did not show differences in RC between recent and non-recent infections (0.1885 vs 0,1630; p=0,950).

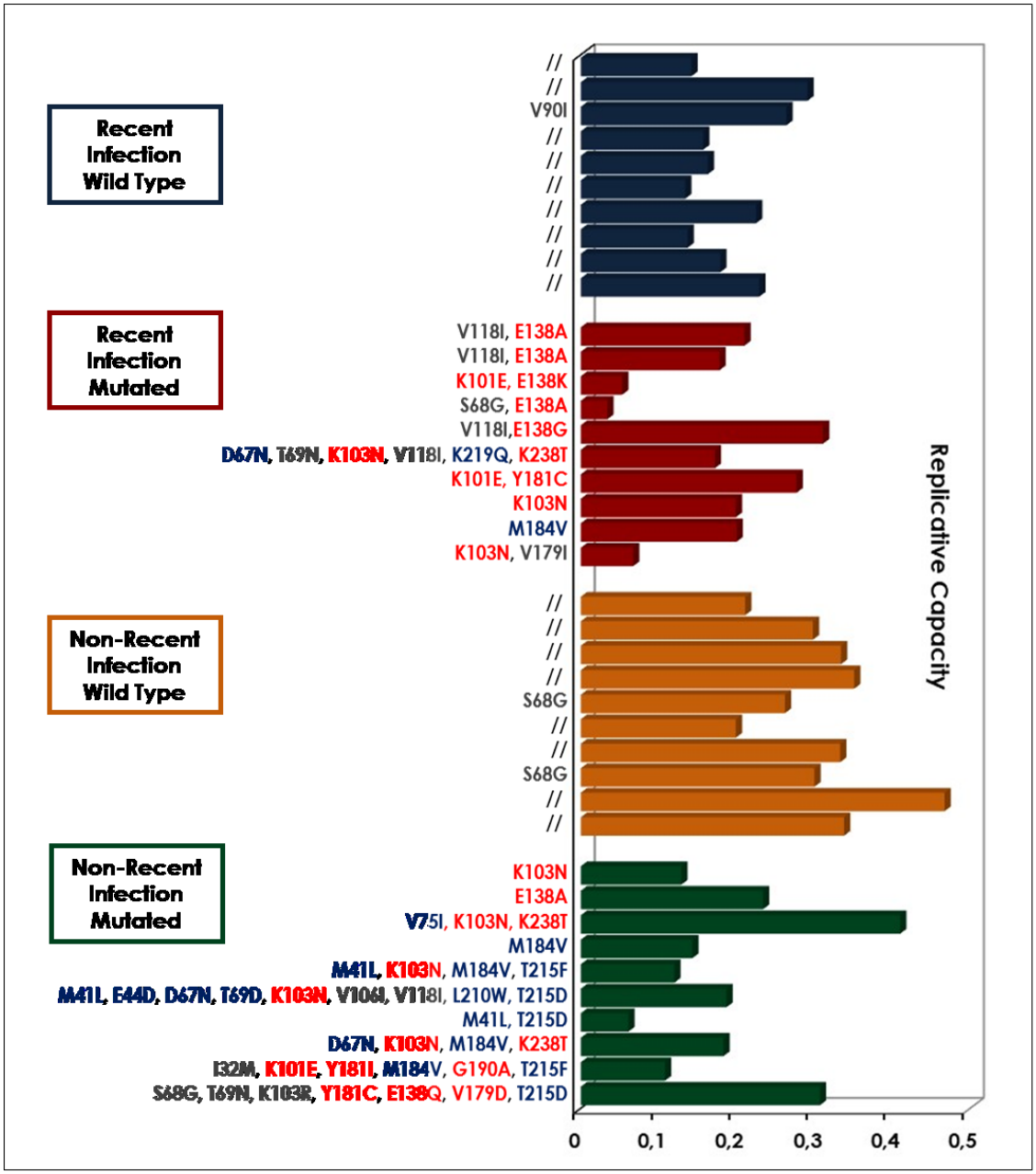

Figure 7.6: RC (X axis) of RT recombinant molecular clones from recently (wild type-blue, bearing resistance mutations-red) and non-recently (wild type-orange, bearing resistance mutations-green) infected patients and respective RT resistant mutations are listed for each recombinant clone (NNRTIs-red, NRTIs-blue and other mutations-grey).

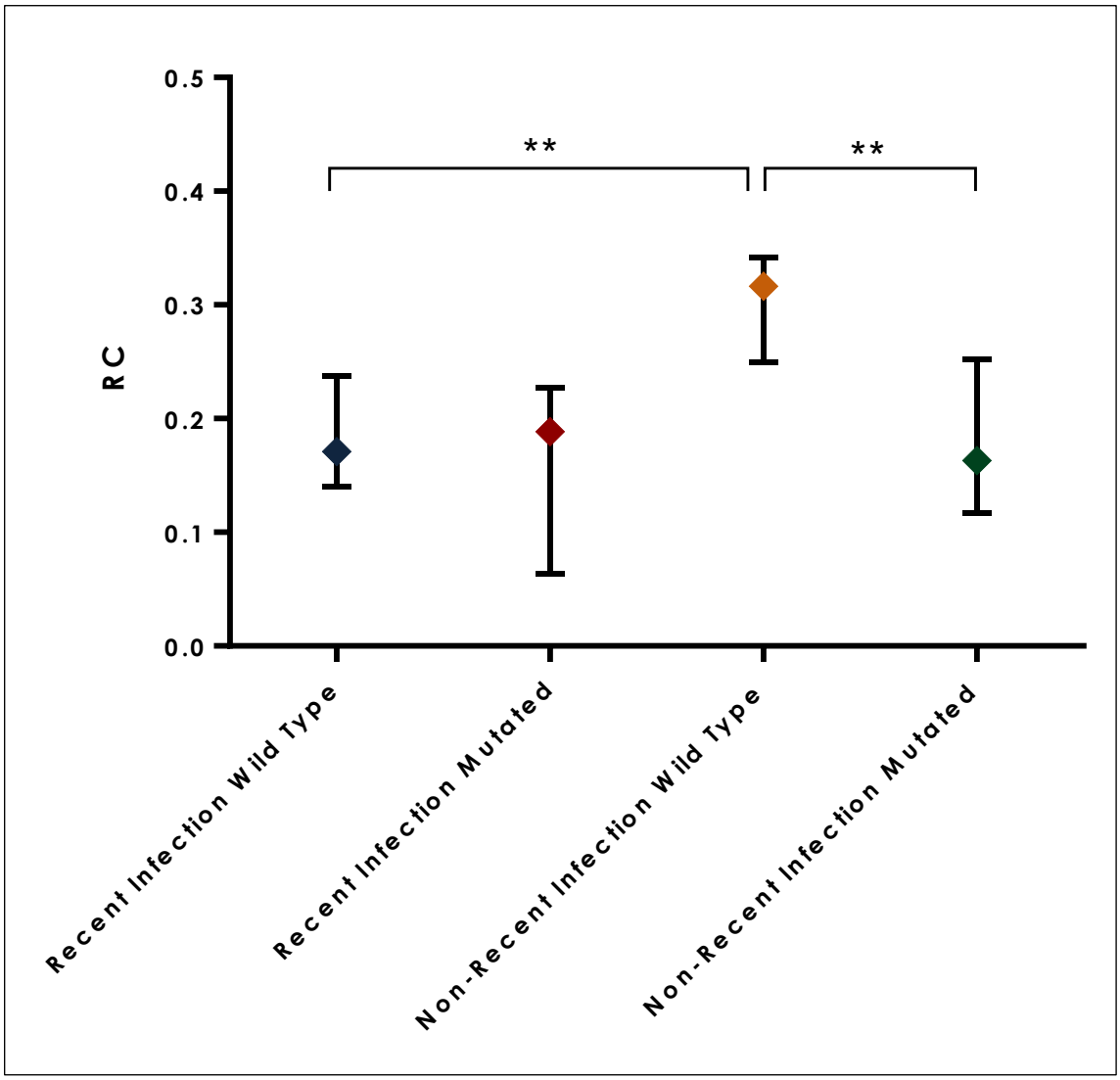

Figure 7.7: the median RC (Y axis) of RT recombinant clones with IQR of 4 different groups (X axis); recent infection wild type blue, recent infection mutated red, non-recent infection wild type orange and non-recent infection mutated green; ** shows significant difference (p<0,05) using Mann-Whitney non-parametric test.

7.3.2 Replicative capacity of PR recombinant phenotypes

The phenotypic significance and the impact of PR resistance mutations on the RC was evaluated on the following set of patients: Recent Infection Wild Type (4 patients), Recent Infection Mutated (2 patients), Non-Recent Infection Wild Type (6 patients) and Non-Recent Infection Mutated (6 patients) as described in materials and methods. The prevalence of transmitted drug resistance (TDR) for protease inhibitors (PIs) was lower compared to that of RT TDR. 2 of 20 recently infected patients enrolled for the study of RT, bore at least one PR resistance mutation such as L24I, M46I, I54V, T74P and V82A. Non-recently infected patients had a high prevalence of accessory mutations against PI, not detected in recently infected patients in addition to primary mutations. The PR genes were amplified from plasma samples and cloned for a recombinant phenotypic analysis in *pNLΔPROgfp* molecular clone. After transfection of all clones on TZM cells, the supernatants were used to infect U87/CXCR4 cells. Fluorescent emission of the reporter GFP was measured during *in vitro* replication of each recombinant molecular clone from day 1 to day 6 post-infection and RC was calculated as described. The figure 7.8 shows the individual RC values (A) and the median RC (B) with IQR of Recent Infection Wild Type, Recent Infection Mutated, Non-Recent Infection Wild Type, Non-Recent Infection Mutated. Values were 0,3685 (IQR: 0,3203-0,3838), 0,0695 (IQR: 0,0290-0,1100), 0,3825 (IQR: 0,3388-0,4030) and 0,2985 (IQR: 0,08275-0,3600) respectively. Isolates bearing PR resistance mutations displayed severely depressed RC compared to wild-type in recent infection and less severe decrease in non-recent infections. Globally, isolates bearing resistance mutations displayed a significantly depressed RC compared to wild type isolates (0,1990 [IQR: 0,05625-0,3413] vs 0,3755 [IQR: 0,3448-0,3960]; p=0,0085).

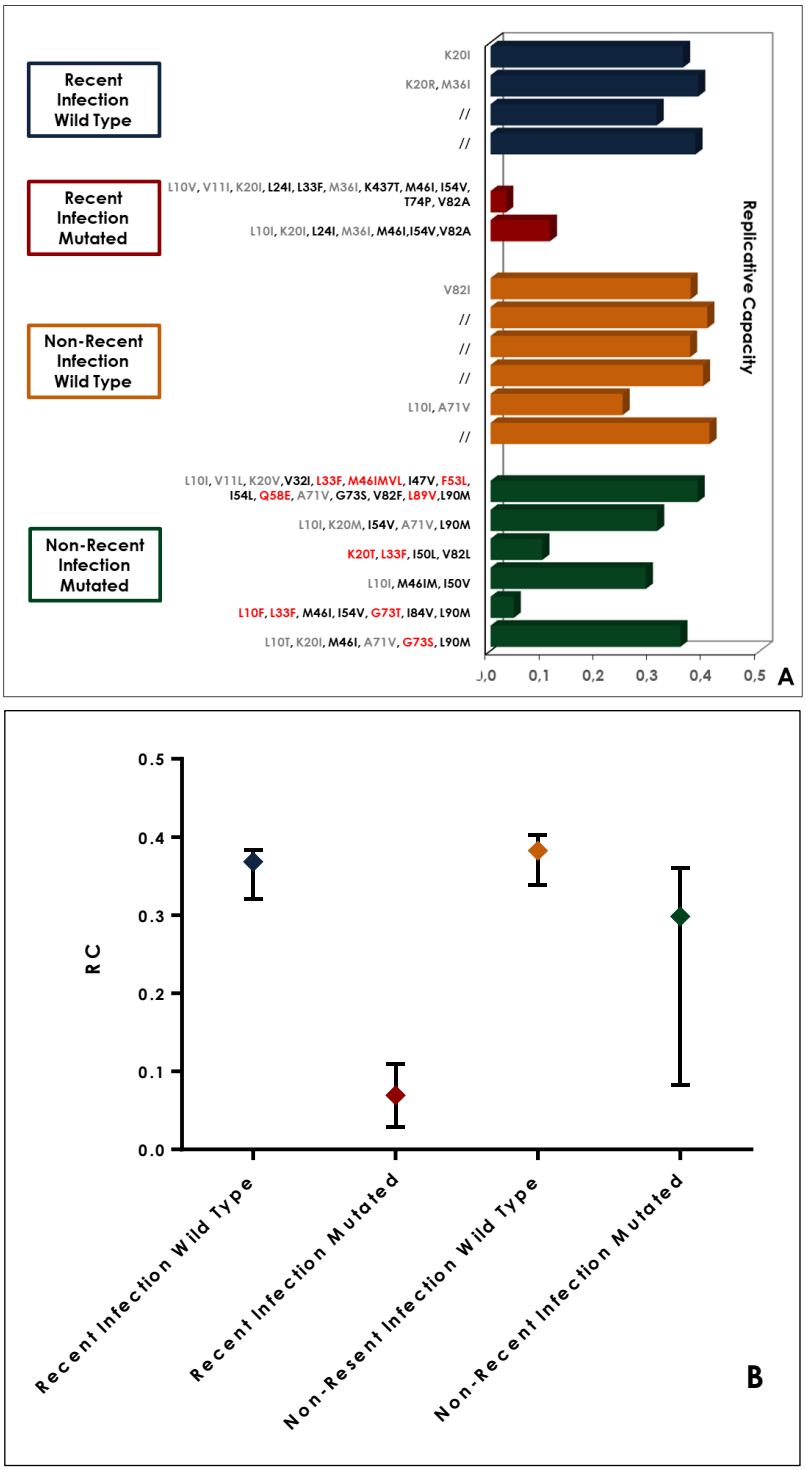

Figure 7.8: A. RC (X axis) of PR recombinant clones from recently (wild type-blue, bearing resistance mutations-red) and non-recently (wild type-orange, bearing resistance mutations-green) infected patients and respective PR resistant mutations are listed for each recombinant clone (PIs mutations-black, accessory mutations-red and other mutations-grey). **B.** the median RC (Y axis) of PR recombinant clones with IQR of 4 different group (X axis): recent infection wild type blue, recent infection mutated red, non-recent infection wild type orange and non-recent infection mutated green;

The RC of PR recombinant molecular clones and that of RT recombinant molecular clones from the same patients were compared to analyze the different impact of the respective mutations on RC and to clarify the phenotypic significance of PR resistance mutations on RC in this small cohort of patients. The figure 7.9 shows the RC calculated as a ratio between RC of each clone and RC of *pNL4-3mod*. PR resistance mutations had a deeper impact on RC compared with RT resistance mutations in the same patient. In recently infected patients (009 and 039) PR resistance mutations had a negative impact on RC (<0,300) as showed in figure 7.9E and F. On the contrary in non-recently infected patients (023 and 041) PR resistance mutations confer a higher RC ranging between 0,784 to 0,975 thus comparable to RC of *pNL4-3mod* (Figure 7.9O and P). In recently infected and non-recently infected patients, wild type PR could confer a higher RC then RT molecular clone respectively. Moreover in some non-recently infected patients (027, 032 and 029) RC was higher than RC of *pNL4-3mod*(Figure 7.9H, L and N)

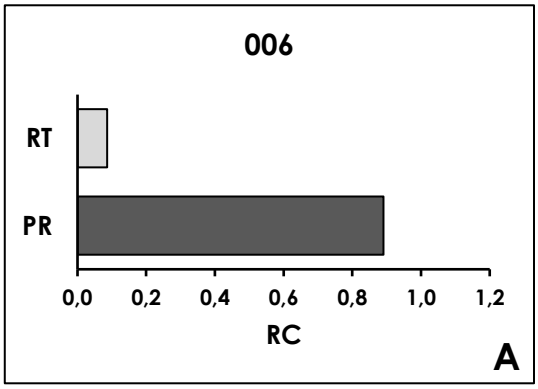

PRO	RT
K20I	S68G, E138A

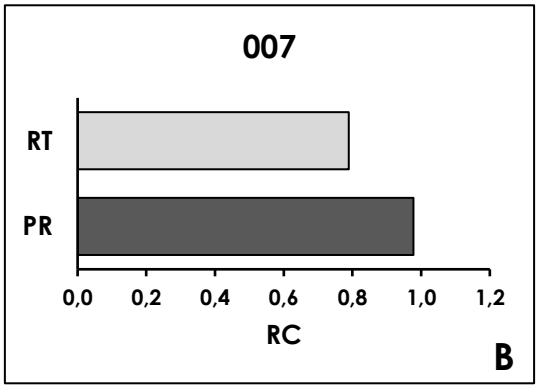

PRO	RT
K20R, M36I	V118I,E138G

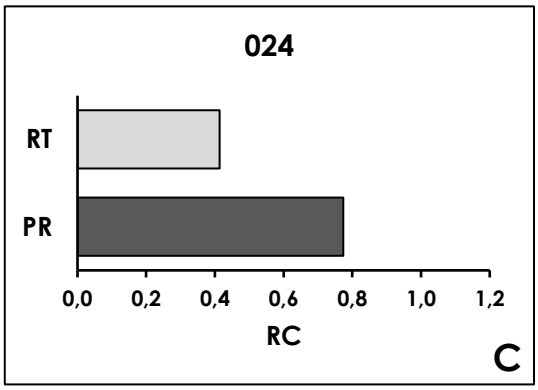

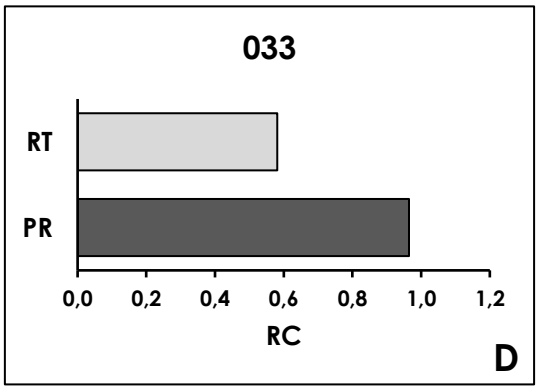

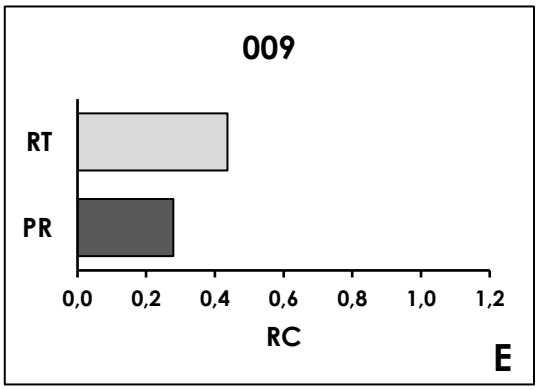

PRO	RT
L10I, K20I, L24I, M36I, M46I, I54V, V82A	D67N, T69N, K103N, V118I, K219Q, K238T

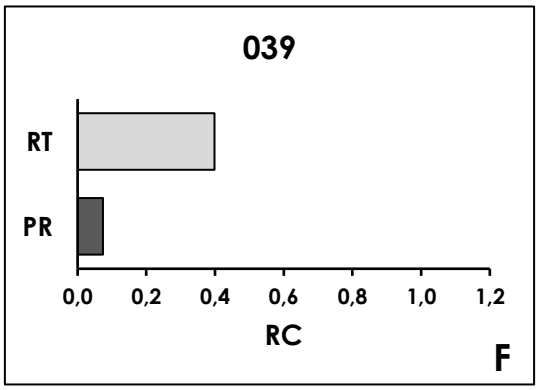

PRO	RT
L10V, V11I, K20I, L24I, L33F, M36I, K43T,M46I, I54V, T74P, V82A	-

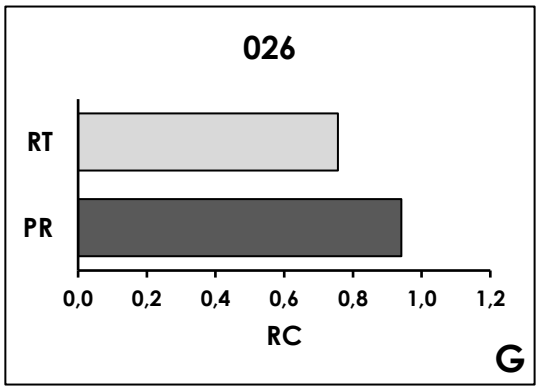

PRO	RT
V82I	-

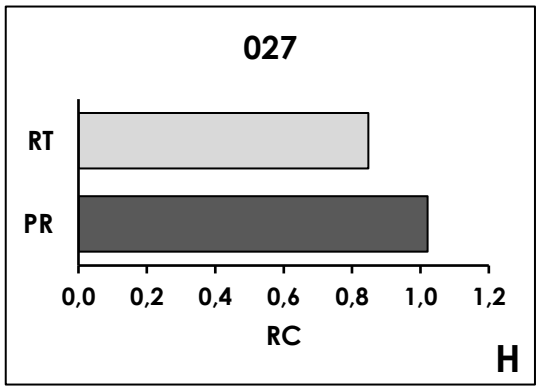

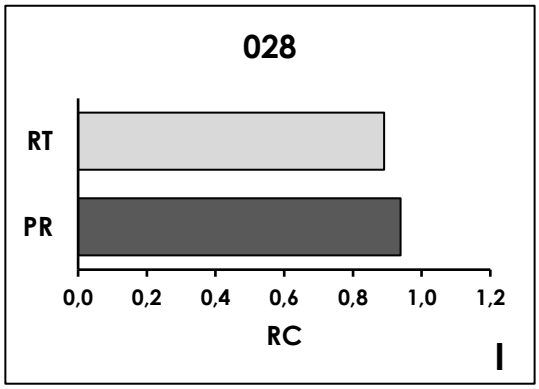

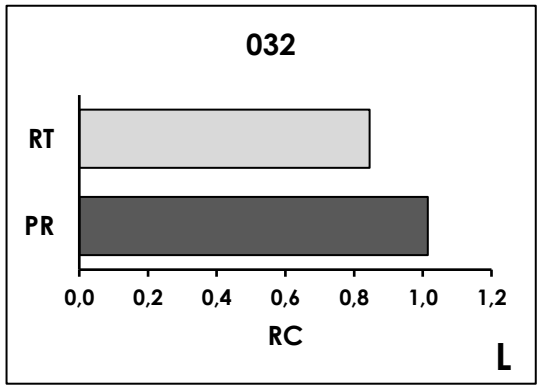

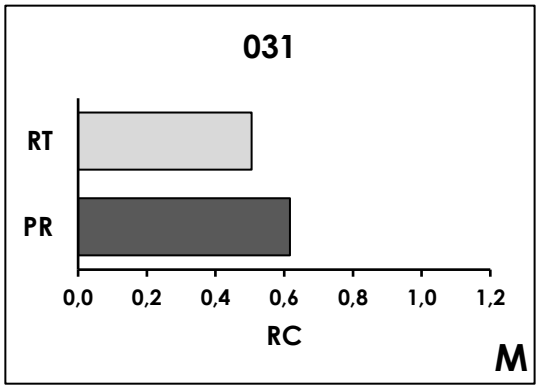

PRO	RT
L10I, A71V	-

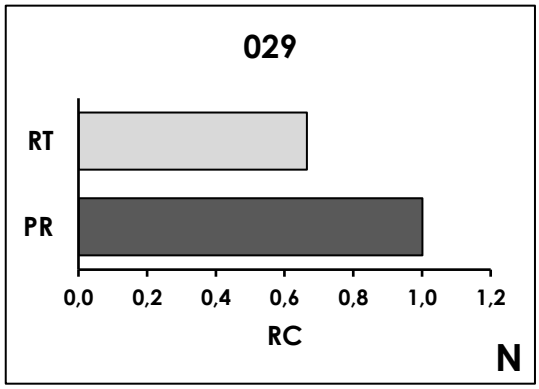

PRO	RT
-	S68G

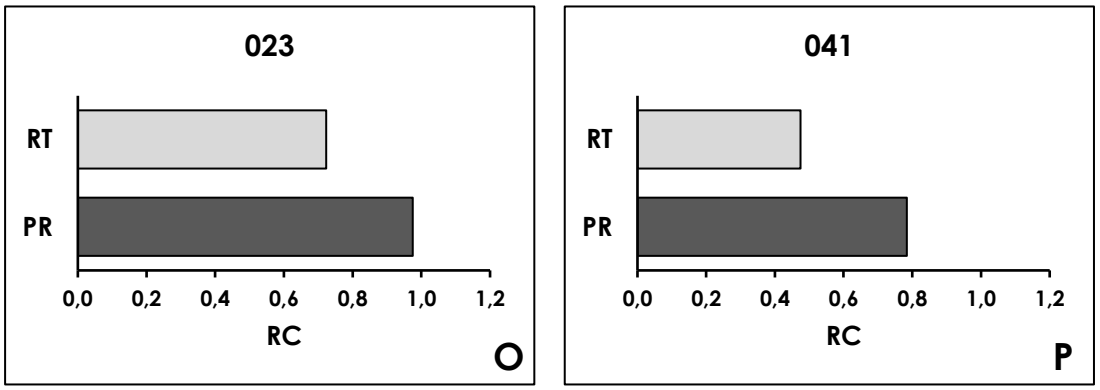

PRO	RT
L10V, V11L, K20V, V32I, L33F,M46IMVL, I47V, F53L, I54L, Q58E, A71V, G73S, V82F, L89V, L90M	M41L, K103N, T215CY

PRO	RT
L10I, K20M, I54V, A71V, L90M	M41L, E44D, D67N, T69D, K103N, V106I, V118I, L210W, T215D

Figure 7. 9: RC (X axis) showed in graphs was obtained from the ratio between RC of clones and *pNL4-3mod* of both RT (light gray) and PR (dark gray) recombinant phenotypic assays; **A. B. C. D.** wild type clones from recently infected patients; **E. F.** mutated clones from recently infected patients; **G. H. I. L. M. N.** wild type clones from non-recently infected patients; **O. P.** mutated clones from non-recently infected patients. The respective resistant mutations (black) and accessory or other mutations (gray) in both genes (PR and RT), if available, are listed in tables below each graph.

7.4 Replicative capacity and phenotypic sensitivity to antiretroviral compounds of HIV-1 strains from patients treated with raltegravir

7.4.1 Site-directed mutagenesis of the IN gene and viral phenotypes

5 patients treated with raltegravir, whose viral isolates naturally developed drug resistance mutations, were enrolled in the study to investigate the influence of the viral genetic background of the IN gene for the selection of a specific resistance pathway. Two patients, 036 and 054, developed the G140S+Q148H mutation pathway; two patients, 037 and 053, developed the N155H mutation pathway and one patient, 055, developed Y143R mutation pathway.
The wild type IN gene of these patients was amplified from plasma samples and cloned in the HIV molecular clone (*pNLΔINTgfp*) suitable for the phenotypic study of IN sequences. The sequences of wild type recombinant molecular clones were compared to the sequences of the viral quasispecies obtained from the plasma of the corresponding patients in order to select the most representative clones of the viral quasispecies in each patient. Subsequently, site directed mutagenesis was applied to the wild-type clones to reproduce the natural resistance pathway observed *in vivo* (G140S+Q148H or N155H) and the alternative mutations and pathways (Q148H, G140S, G140S+Q148H or N155H), generating a total of 5 recombinant molecular clones for each patient. In the case of patient 055, the resistant IN gene was directly amplified from plasma and cloned in the HIV molecular clone as it was the natural resistance pathway. The table 7.1 shows both the basal and resistant sequences for each patient and the amino acid differences between these sequences. The sequences of wild type and mutagenized molecular clones for each patient are also listed in the same table.

The sequences show, next to resistance mutations, a complete aminoacidic identity between the resistant sequences and the corresponding wild type molecular clones in sample 036, 053 and 055. Sample 054 and 037 differ from the resistant sequence for only one amino acid residue in position 72 and 125 respectively, present as variants in the basal sequence.

POS AA	50	59	72	74	75	84	97	112	113	119	124	125	126	134	135	136	**140**	**143**	**148**	151	154	**155**	157	165	201	206	208	211	212	215	221	222	229	230	231	232	234	254	255	283	284	290	292	293	294	295
pNL4-3mod	M	G	V	L	V	I	T	T	V	S	T	T	V	G	I	K	**G**	**Y**	**Q**	I	M	**N**	E	V	V	T	I	K	E	K	Q	N	D	S	R	D	V	N	S	S	R	H	E	K	I	S
036 basal sequence	M	G	I/V	L	V	I	T	T	I	S	A	T	V	G	I	K	G	Y	Q	V	I	N	E	I	I	T	I	K	E	K	Q	N	D	S	R	D	L	N	S	S	R	N	E	K/Q	L/F	S
036 clone	M	G	V	L	V	I	T	T	I	S	A	T	V	G	I	K	G	Y	Q	V	I	N	E	I	I	T	I	K	E	K	Q	N	D	S	R	D	L	N	S	S	R	N	E	K	L	S
036/Q148H clone	M	G	V	L	V	I	T	T	I	S	A	T	V	G	I	K	G	Y	H	V	I	N	E	I	I	T	I	K	E	K	Q	N	D	S	R	D	L	N	S	S	R	N	E	K	L	S
036/G140S clone	M	G	V	L	V	I	T	T	I	S	A	T	V	G	I	K	S	Y	Q	V	I	N	E	I	I	T	I	K	E	K	Q	N	D	S	R	D	L	N	S	S	R	N	E	K	L	S
036/N155H clone	M	G	V	L	V	I	T	T	I	S	A	T	V	G	I	K	G	Y	Q	V	I	H	E	I	I	T	I	K	E	K	Q	N	D	S	R	D	L	N	S	S	R	N	E	K	L	S
036/G140SQ148H clone	M	G	V	L	V	I	T	T	I	S	A	T	V	G	I	K	S	Y	H	V	I	N	E	I	I	T	I	K	E	K	Q	N	D	S	R	D	L	N	S	S	R	N	E	K	L	S
036 resistant sequence	M	G	V	L	V	M	T	T	I	S	A	T	V	G	I	K	S	Y	H	V	I	N	E	I	I	T	I	K	E	K	Q	N	D	S	R	D	L	N	S	S	S	N	E	K	L	S
054 basal sequence	M	G	I/V	L	V	I	T	T	I	S	N	V	V	G	I	K	G	Y	Q	V	L	N	E	I	V	T	I	K	E	K	Q	N/T	D	S	R	D	L	S	G	G/S	R	N	E	E/K	S/F	S
054 clone	M	G	V	L	V	I	T	T	I	S	N	V	V	G	I	K	G	Y	Q	V	L	N	E	I	V	T	I	K	E	K	Q	N	D	S	R	D	L	S	G	G	R	N	E	E	S	S
054/Q148H clone	M	G	V	L	V	I	T	T	I	S	N	V	V	G	I	K	G	Y	H	V	L	N	E	I	V	T	I	K	E	K	Q	N	D	S	R	D	L	S	G	G	R	N	E	E	S	S
054/G140S clone	M	G	V	L	V	I	T	T	I	S	N	V	V	G	I	K	S	Y	Q	V	L	N	E	I	V	T	I	K	E	K	Q	N	D	S	R	D	L	S	G	G	R	N	E	E	S	S
054/N155H clone	M	G	V	L	V	I	T	T	I	S	N	V	V	G	I	K	G	Y	Q	V	L	H	E	I	V	T	I	K	E	K	Q	N	D	S	R	D	L	S	G	G	R	N	E	E	S	S
054/G140SQ148H clone	M	G	V	L	V	I	T	T	I	S	N	V	V	G	I	K	S	Y	H	V	L	N	E	I	V	T	I	K	E	K	Q	N	D	S	R	D	L	S	G	G	R	N	E	E	S	S
054resistant sequence	I	G	I	L	V	I	T	T	I	S	N	V	V	G	I	K	S	Y	H	V	L	N	E	I	V	T	I	K	E	K	Q	N	D	S	R	D	L	S	G	G	R	N	E	K	F	S
037 basal sequence	M	G	V	L	V	I	T	T	I	P	T	M/V	M	G	V	K	G	Y	Q	V	M	N	E	V	I	T	L	K	E	K	Q	N	D	S	R	D	L	N	S	S	R	N	A	Q	F	G
037 clone	M	G	V	L	V	I	T	T	I	P	T	M	M	G	V	K	G	Y	Q	V	M	N	E	V	I	T	L	K	E	K	Q	N	D	S	R	D	L	N	S	S	R	N	A	Q	F	G
037/Q148H clone	M	G	V	L	V	I	T	T	I	P	T	M	M	G	V	K	G	Y	H	V	M	N	E	V	I	T	L	K	E	K	Q	N	D	S	R	D	L	N	S	S	R	N	A	Q	F	G
037/G140S clone	M	G	V	L	V	I	T	T	I	P	T	M	M	G	V	K	S	Y	Q	V	M	N	E	V	I	T	L	K	E	K	Q	N	D	S	R	D	L	N	S	S	R	N	A	Q	F	G
037/N155H clone	M	G	V	L	V	I	T	T	I	P	T	M	M	G	V	K	G	Y	Q	V	M	H	E	V	I	T	L	K	E	K	Q	N	D	S	R	D	L	N	S	S	R	N	A	Q	F	G
037/G140SQ148H clone	M	G	V	L	V	I	T	T	I	P	T	M	M	G	V	K	S	Y	H	V	M	N	E	V	I	T	L	K	E	K	Q	N	D	S	R	D	L	N	S	S	R	N	A	Q	F	G
037 resistant sequence	V	G	V	L	V	I	A	T	I	P	T	V	M	G	V	K	G	Y	Q	V	M	H	E	V	I	T	L	K	E	N	Q	N	C	S	K	D	L	N	S	S	R	N	A	Q	F	G
053 basal sequence	M	G	I	L	V	I	T	T	I	P	N	A	L	G	V	K	G	Y	Q	V	M	N	E/K	V	I	T	L	T	E	K	Q/H	N	D	N	R	E	L	N	S	S	R	Y	E	K	L	S
053 clone	M	G	I	L	V	I	T	T	I	P	N	A	L	G	V	K	G	Y	Q	V	M	N	E	V	I	T	L	T	E	K	Q	N	D	N	R	E	L	N	S	S	R	Y	E	K	L	S
053/Q148H clone	M	G	I	L	V	I	T	T	I	P	N	A	L	G	V	K	G	Y	H	V	M	N	E	V	I	T	L	T	E	K	Q	N	D	N	R	E	L	N	S	S	R	Y	E	K	L	S
053/G140S clone	M	G	I	L	V	I	T	T	I	P	N	A	L	G	V	K	S	Y	Q	V	M	N	E	V	I	T	L	T	E	K	Q	N	D	N	R	E	L	N	S	S	R	Y	E	K	L	S
053/N155H clone	M	G	I	L	V	I	T	T	I	P	N	A	L	G	V	K	G	Y	Q	V	M	H	E	V	I	T	L	T	E	K	Q	N	D	N	R	E	L	N	S	S	R	Y	E	K	L	S
053/G140SQ148H clone	M	G	I	L	V	I	T	T	I	P	N	A	L	G	V	K	S	Y	H	V	M	N	E	V	I	T	L	T	E	K	Q	N	D	N	R	E	L	N	S	S	R	Y	E	K	L	S
053 resistant sequence	M	G	I	L	V	I	T/A	T	I	P	N	A	L	G	V	K	G	Y	Q	V	M	H	E	V	I	T	L	T	E	K	Q	N	D	N	R	E	L	N	S	S	R	Y	E	K	L	S
055 basal sequence	M	G/V	I	L	V	I	T	V	I	S	G	A	V	N	I	T	G	Y	Q	V	M	N	E	V	I	S	L	K	A	K	Q	N	D	S	R	D	I	N	N	G	G	N	E	Q	S	S
055 clone	M	G	I	L	V	I	T	V	I	S	G	A	V	N	I	T	G	Y	Q	V	M	N	E	V	I	S	L	K	A	K	Q	N	D	S	R	D	I	N	N	G	G	N	E	Q	S	S
055/Q148H clone	M	G	I	L	V	I	T	V	I	S	G	A	V	N	I	T	G	Y	H	V	M	N	E	V	I	S	L	K	A	K	Q	N	D	S	R	D	I	N	N	G	G	N	E	Q	S	S
055/G140S clone	M	G	I	L	V	I	T	V	I	S	G	A	V	N	I	T	S	Y	Q	V	M	N	E	V	I	S	L	K	A	K	Q	N	D	S	R	D	I	N	N	G	G	N	E	Q	S	S
055/N155H clone	M	G	I	L	V	I	T	V	I	S	G	A	V	N	I	T	G	Y	Q	V	M	H	E	V	I	S	L	K	A	K	Q	N	D	S	R	D	I	N	N	G	G	N	E	Q	S	S
055/G140SQ148H clone	M	G	I	L	V	I	T	V	I	S	G	A	V	N	I	T	S	Y	H	V	M	N	E	V	I	S	L	K	A	K	Q	N	D	S	R	D	I	N	N	G	G	N	E	Q	S	S
055 resistance clone	M	G	I	M	I	I	T	V	I	S	G	A	V	N	I	T	G	R	Q	V	M	N	E	V	I	S	L	K	A	K	Q	N	D	S	R	N	I	N	N	G	G	N	E	Q	S	S
055 resistant sequence	M	G	I	M	I/V	I	T/A	V	I	S	G	A	V	N	I	T	G	R	Q	V	M	N	E	V	I	S	L	K	A	K	Q	N	D	S	R	D/N	I	N	N	G	G	N	E	Q	S	S

Table 7.1: amino acid sequences of the IN gene of each patient (basal and resistant sequence) and respective wild type and mutagenised sequence of recombinant molecular clones for each patient. 036 and 054, developed the G140S+Q148H mutation pathway; 037 and 053, developed the N155H mutation pathway; 055,developed Y143R mutation pathway *in vivo*. These sequences are compared to the *pNL4-mod* sequence.

7.4.2 Replicative capacity and drug sensitivity of IN recombinant phenotypes

All recombinant molecular clones were transfected in packaging cells (TZM cells), the supernatants were used to infect a permissive cell line (U87/CXCR4) in the absence and in the presence of different raltegravir (RAL) and dolutegravir (DTG) concentrations. RAL concentrations were: 0,1875 nM, 0,75 nM, 3 nM and 12 nM. For DTG, the same concentrations were tested with the addition of 48 nM. Fluorescent emission of the reporter GFP was measured during *in vitro* replication of four replicates for each recombinant molecular clone to calculate the RC. The RC was identified in the slope values expressed as the X coefficient of the linear equation describing cell growth dynamics between the first and the third day post infection. Each histogram (figure 7.10) shows the RC values (Yaxis) of five recombinant molecular clones of each patient for each concentration of RAL and DTG (X axis). The RC of the wild-type clones (blue histogram columns) was variable and inversely proportional to RAL and DTG concentration. The introduction of resistance mutations greatly reduced it, albeit again with a high degree of variability, depending on the mutational pattern. The mutation Q148H (red histogram columns) determined the maximum loss of RC in all clones (both with and without drugs, at all concentrations). The clone mutagenised with Q148H of patient 053 (who selected the N155H pathway *in vivo*) showed a higher RC compared to others clones with the same mutation (Figure 7.10G and H). The introduction of the G140S mutation (green histogram columns) reduced the RC in all patients. The RC reduction at various drug concentration was comparable to that of the wild type, suggesting that this mutation alone does not confer reduced susceptibility. All clones where Q148H was associated to the G140S secondary mutation (orange histogram columns), a complete recovery of RC was observed

at all concentrations of RAL and up to 3/12nM DTG, depending on the patient and irrespective of whether this resistance pathway was naturally selected by treatment. Conversely, the RC of N155H mutagenised clones (violet histogram columns) in 2 patients (054 and 055 who selected the G140S+Q148H and Y143R pathway *in vivo* respectively) was depressed compared to wild type and decreased with RAL and lower concentrations of DTG (despite still being higher than that of wild type clones at 12nM concentration of RAL) (Figure 7.10C, D I and L). Interestingly this mutations achieves the best results in terms of RC in the 2 patients (037 and 053) that selected the mutations *in vivo* (Figure 7.10E, F G and H). However, in all patients, including the latter, the best RC were observed with the G140S+Q148H association, while N155H depressed the RC more than this combination in all others (Figure 7.10A, B, C, and D). In patient 055 (who selected the Y143R pathway *in vivo*), the G140S+Q148H mutagenised clone (orange histogram columns) conferred a better RC at all drug concentrations compared to the N155H (violet histogram columns) and also to the Y143R /L74M combination itself (yellow histogram columns)(Figure 7.10I and L).

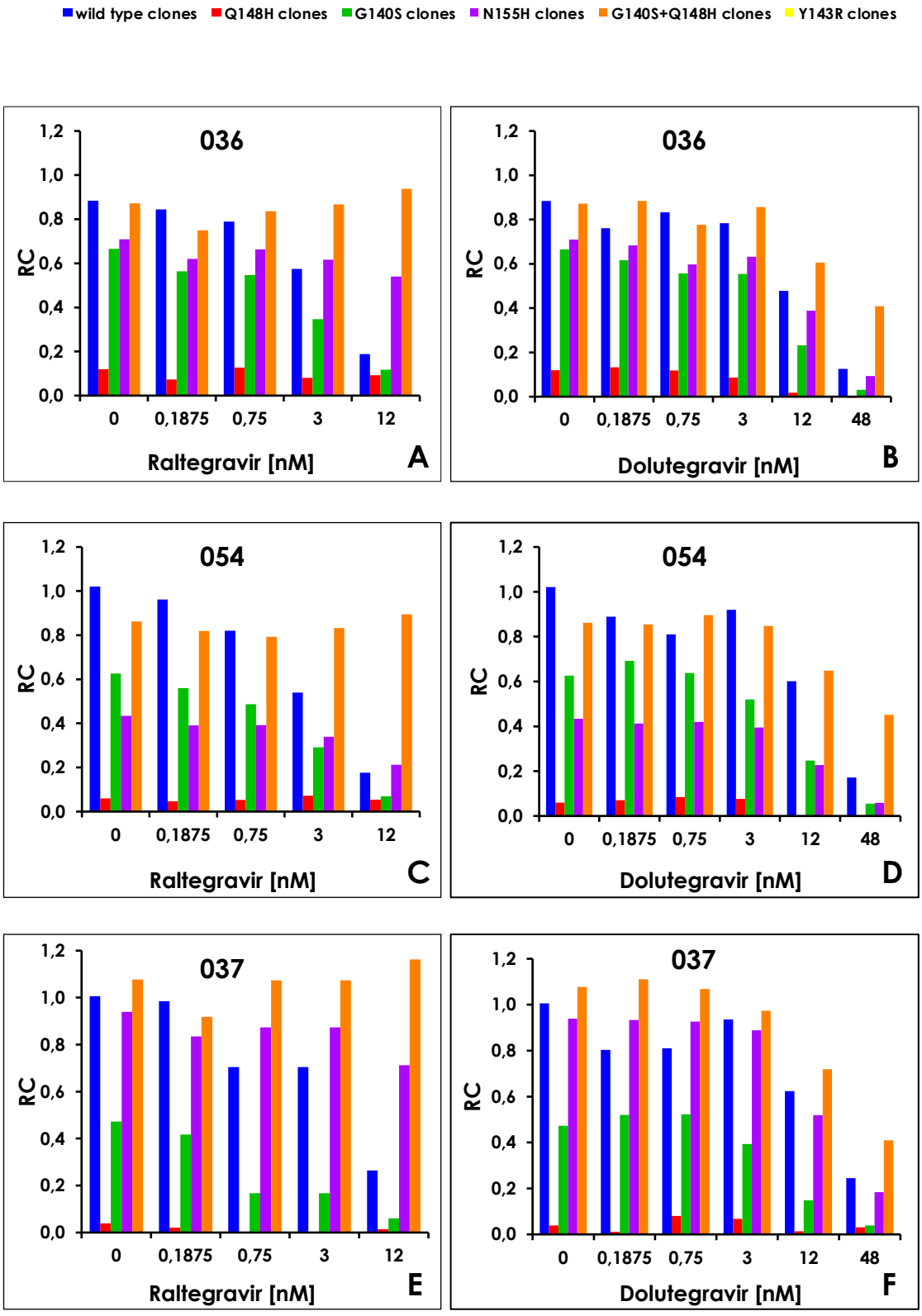
wild type clones
Q148H clones
G140S clones
N155H clones
G140S+Q148H clones
Y143R clones
036
RC
1,2
1,0
0,8
0,6
0,4
0,2
0,0
0
0,1875
0,75
3
12
Raltegravir [nM]
A
036
48
Dolutegravir [nM]
B
054
C
054
D
037
E
037
F

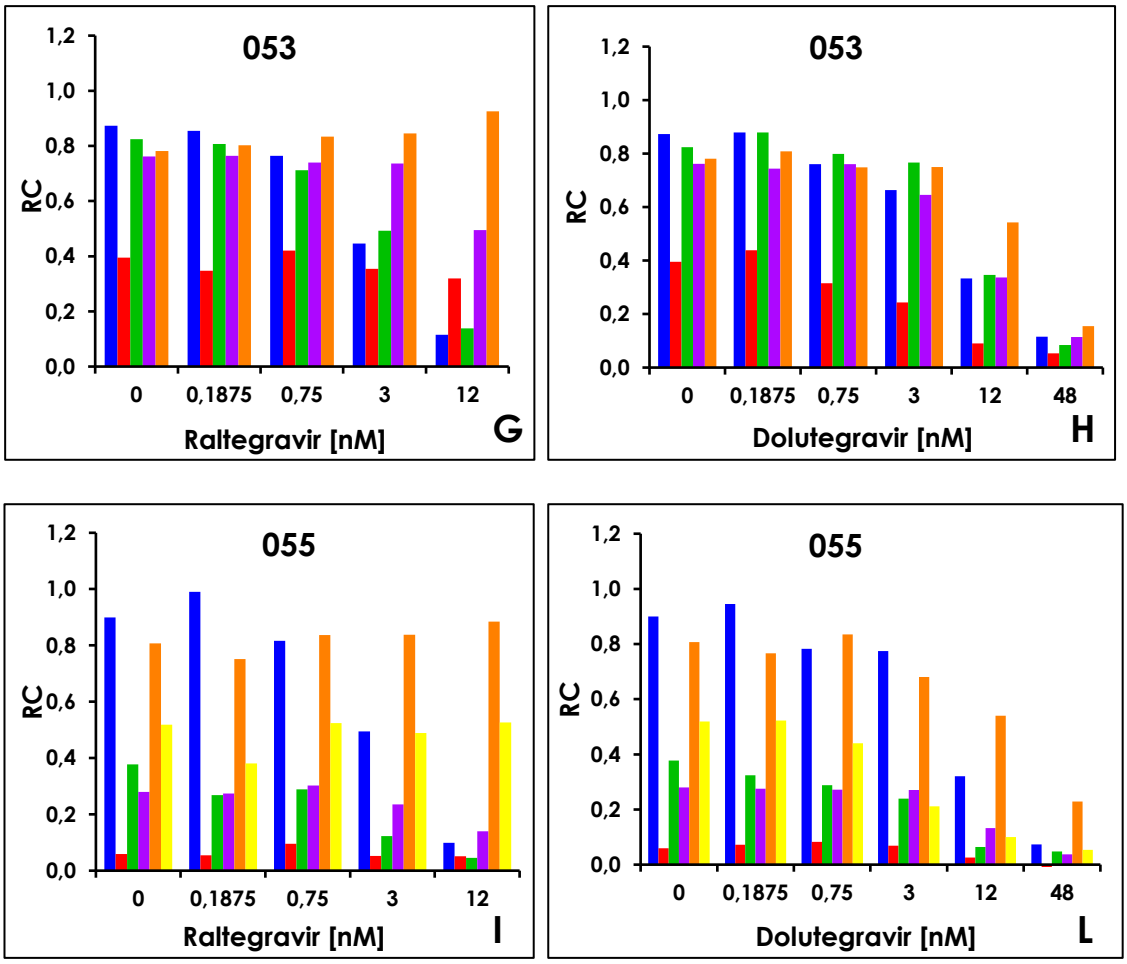

Figure 7.10: RC (Y axis) of recombinant molecular clones (wild type clone blue, Q148H clone red, G140S clone green, N155H clone violet, G140S+Q148H clone orange, Y143R clone yellow) for each patient for each concentration of RAL (on the left) or DTG (on the right) X axis); **A** and **B**: patient 036 who selected the G140S+Q148H pathway *in vivo;* **C** and **D**: patient 054 who selected the G140S+Q148H pathway *in vivo*; **E** and **F**: patient 037 who selected the N155H pathway *in vivo*; **G** and **H**: patient 053 who selected the N155H pathway *in vivo;* **I** and **L**: patient 055 who selected the Y143R pathway *in vivo*

The table 7.2 shows the Inhibitory Concentration capable of reducing replication by 50% (IC50) for each recombinant molecular clone and compound. In addition, for each patient the corresponding fold change (FC) was calculated as the ratio between the IC50 of molecular clone and wild type clone. Overall, the wild type clones and G140S mutagenised clones displayed a low median RAL IC50 (3,665 nM and 2,804 nM respectively) and median DTG IC50 (15,204 nM and 8,412 nM respectively) compared to the others mutagenised clones.
A high RAL IC50 was displayed also by all Q148H clones, while in all clones it conferred, on the contrary, a low DGT IC50. The combination G140S+Q148H in all clones conferred a higher RAL IC50 (median: >100nM) compared to N155H (median: 20,172 nM), albeit showing some variability among different clones. In patient 055 (who selected the Y143R /L74M combination *in vivo*), the RAL IC50 of this combination was >100nM, comparable to that of the G140S+Q148H. In the case of DTG, the combination G140S + Q148H in all mutagenised clones conferred a higher IC50 (median: 29,774 nM) compared to N155H (median: 14,584 nM) or Y143R (2.794 nM) mutagenised clones, no matter what patients pathway developed *in vivo*.

Recombinant Molecolar Clones	RALTEGRAVIR		DOLUTEGRAVIR	
	IC50 [nM]	FC	IC50 [nM]	FC
036	5,136	1,000	15,204	1,000
036/Q148H	45,228	8,807	5,235	0,344
036/G140S	3,700	0,720	8,412	0,553
036/N155H	34,756	6,768	14,925	0,982
036/G140S+Q148H	>100	>100	39,091	2,571
054	3,665	1,000	17,305	1,000
054/Q148H	>100	>100	7,559	0,437
054/G140S	2,804	0,765	9,509	0,549
054/N155H	11,264	3,074	14,584	0,843
054/G140S+Q148H	>100	>100	46,690	2,698
037	5,696	1,000	21,382	1,000
037/Q148H	0,201	0,035	62,510	2,923
037/G140S	0,970	0,170	8,164	0,382
037/N155H	35,239	6,186	17,285	0,808
037/G140S+Q148H	>100	>100	29,774	1,392
053	3,426	1,000	8,845	1,000
053/Q148H	41,396	12,084	4,803	0,543
053/G140S	4,284	1,250	11,135	1,259
053/N155H	20,172	5,889	11,733	1,327
053/G140S+Q148H	>100	>100	21,690	2,452
055	3,640	1,000	8,912	1,000
055/Q148H	33,660	9,247	10,572	1,186
055/G140S	1,902	0,523	4,396	0,493
055/N155H	12,053	3,311	13,502	1,515
055/G140S+Q148H	>100	>100	23,858	2,677
055/ Y143R	>100	>100	2,794	0,314
pNL4-3mod	5,098		7,169	

Table 7.2: IC50 (nM) and FC of RAL (on the left) and DTG (on the right) of wild type and mutagenised recombinant clones for each patient.

8. Discussion

8.1 Role of PR/RT in recent infections

Highly active antiretroviral therapy (HAART) has significantly improved the expectancy and the quality of life of people living with HIV-1. Since the approval of AZT to date, around 30 antiretrovirals were approved for clinical practice by FDA. The major goal of HAART is the stable suppression of viremia, but different factors such as suboptimal adherence to therapy, drug-drug interactions, and side effects can compromise the efficacy of an antiretroviral therapy (ART), leading to the development of drug resistance mutations.

Genotypic testing is a recommended tool to monitor HIV drug resistance in clinical practice and is necessary for managing decisions related to therapy initiation or regimen modification following treatment failure. This testing provides an indirect measure of susceptibility to antiretrovirals as algorithms are used to correlate resistance mutations to an estimated reduction of a drug's effectiveness.

Differently from genotypic testing, phenotypic testing allows the direct measurement in cell culture of drug susceptibility and replicative capacity (RC), in the absence and in the presence of a given compound, of any viral strain, independently from the complexity of its mutational pattern.

In the present study, a specific recombinant phenotypic assay was developed for the study of the reverse transcriptase (RT), protease (PR) and integrase (IN) genes. The assay is based on plasmid constructs containing the complete sequence of the viral genome (derived from *pNL4-3mod*), modified by the insertion of cloning cassettes for the genes of the enzymes targeted by antiretroviral drugs. The green fluorescent protein (GFP) gene was added to these constructs (as a fusion with the *nef* ORF), in order to allow straightforward measurement of the viral kinetics in cell cultures. The genetic determinants of RC are

distributed on multiple genes in the viral genome, however in some peculiar evolutionary situations such as antiviral therapy, the processivity of the genes targeted by treatment and subjected to a mutational pressure, could reduce viral replication and thus become the main determinant of RC. Resistance mutations modify the structure of these enzymes, causing both the reduction of the inhibitory action by the drugs and general loss of enzyme processivity. The genes harboring resistance mutations have a higher RC than the wild type in the presence of the drugs but they could lose overall processivity, limiting viral replication even in the absence of the compounds. This situation typically occurs in primary infection with viruses who have accumulated resistance mutations in the previous host (Transmitted Drug Resistance, TDR). A study on recent infections (Pingen M. *et al*., 2011) shows that in the absence of drug selective pressure in the new host, TDR viruses may:

1. revert rapidly to wild-type when drug resistance mutations severely reduce RC,
2. replace of TDR mutations by atypical amino acids that also improve viral RC,
3. persist either because mutations do not significantly affect viral RC or fix compensatory mutations.

As presently there is no clear demonstration of the phenotypic determinants that underlie these outcomes, the present study investigates the evolution of resistant variants after transmission to a new host, for the first time using phenotypic assays with the whole enzyme sequence to explore the potential role of viral RC in persistence of TDR mutations and to understand their evolutionary dynamic. The RC of viruses bearing resistance mutations in recent and non-recent infections was compared to that of wild type viruses isolated from the same categories of patients. In the present study the effect of RT and PR resistance mutations were analyzed separately.

8.1.1 Reverse transcriptase

As showed in the results section, phenotypic tests show a high degree of RC variability from patient to patient in recent infections, because the fitness cost of a particular resistance mutation is not constant and may vary among multidrug resistant isolates, depending on the genetic background of the enzyme sequence. However, collectively, isolates from recent infections bearing resistance mutations in the RT sequences show a RC comparable to that of wild type isolates. For this reason these resistant isolates have not been negatively selected and might have the same epidemic potential as wild type viruses. A high RC could explain the persistence of TDR mutations and an easy transmission of these viruses. These results substantiate with *in vivo* data the paradigm that fitness modulations may alter the persistence of resistance mutations, previously proposed and based on *in vitro* studies (Cong M.E. *et al*., 2007).

In recent infections mutations against non-nucleoside reverse transcriptase inhibitors (NNRTIs) were the most frequent: 4 patients were infected with a virus harboring E138A/G, 2 patients carrying K103N, 2 patients with virus carrying 2 resistance mutations (K101E +Y181C and K101E + E138K). The combination K101E + Y181C, conferring significant resistance to all NNRTIs, shows a high RC because these NNRTI resistance mutations revert only partially or persist during in vivo follow-up due to their high RC. Other NNRTI resistance mutations, particularly K103N, that causes high-level reduction in NVP and EFV susceptibility, have already been reported as having a moderate effect on RC. In fact, this mutation persists in most cases or disappears at a slower rate *in vitro* (Pingen M. *et al*., 2011). Our results show a low RC only in one patient, where K103N was associated with an accessory mutation (V179I) but average RC when present as single mutation or in association

with different nucleoside reverse transcriptase inhibitor (NRTI) mutations (K219Q and D67N).
In both cases described above(K103N or K101E + Y181C combination), these mutations confer high resistance to some inhibitors and do not significantly affect viral RC hence they could persist in new host. NNRTIs represent an important therapeutic tool and the ease with which these resistance mutations are transmitted could be a problem for their future use.
NRTI mutations were only in two patients, one was infected with a virus harboring M184V (that causes high level resistance to 3TC and FTC and low level resistance to ddI and ABC) and another, with a virus harboring combined NNRTI and NRTI resistance mutations (D67N, K103N, K219Q, K238T, low-level resistance to older NRTI, ABC and potentially TDF), both surprisingly displaying a good RC.
This is in contrast with previous results showing that M184V and TAMs significantly reduced the RC and do not persist for a long time in the absence of selective pressure. In particular, for M184, the difference between the wild type and the drug resistant variant is only one nucleotide change (ATG wild type > GTG variant); a virus containing only the M184V mutation can reduces RC (Harrison L. *et al*., 2010) and rapidly reverts to wild type in the absence of treatment (Yang V.L. *et al*., 2015).
These data predict that M184V might persist longer in some isolates than in others and may explain why this mutation has been found in some isolates after primary infection, while in other it was rapidly reverted (Cong M.E. *et al*., 2007). M184V is under-represented in recently infected patients(1/10 patients in this study) compared to non-recently infected patients (4/10 patients in this study) where it is often found in combination with M41L, D67N, T215F. M184V is a pivotal mutations for NRTI, as it affects most treatment options based on these compounds, including the most used TDF/FTC and TAF/FTC. TDR frequency of M184V remains slightly higher than 1%, in extended surveys

(Rossetti *et al.,* 2018) but the risk is that, thanks to favorable RC in some patients, its frequency could increase progressively, reducing treatment options and impairing the use of these combinations.
In non-recent infections, mutations that confer moderate or low RC, such as M41L and T215Y/F/D are also more represented in non-recent than in recent infections in the present study. Chronically treated patients (8/10) have a high prevalence of NRTI mutations (frequently in combination with NNRTI mutations). As expected, the phenotypic results attribute a significant lower RC to these mutated isolates compared to wild type isolates from non-recently infected patients.
An additional interesting and puzzling finding from this study is that wild type isolates from recent infections display a significantly lower RC than wild type isolates from non-recent infections. A possible explanation is that the immune system (in greater health in recent infections) selects viral strains with lower RC in these patients.

8.1.2 Protease

The RC conferred by the PR gene was also investigated. As described in the results section, the data reveal that the impact of PR resistance mutations on RC is much deeper than that of RT resistance mutations; in general RC is more conditioned by PR than by RT.
PR resistance mutations have a deep impact in decreasing RC both in recently and chronically infected patients. TDR to protease inhibitors (PIs) is generally rare and mainly attributable to the mutations M46I/L, V82ASL and L90M, contributing to resistance to a broad spectrum of PIs, with the exception of DRV (Rossetti B. *et al*., 2018). Persisting mutational profiles in recent infections from this study are characterized by the presence of several major PR resistance mutations, as well as rare secondary

mutations that phenotypically only partially compensate for the loss of RC, which remains low. Non-recently infected patients displayed a high prevalence of PR secondary mutations, not detected in recently infected patients, in addition to major resistance mutations, with a higher RC. Probably the absence of these secondary mutations is related to the loss of RC in recently infected patient.

8.2 Role of IN *in vivo* selection of resistance pathway

This study also includes a sub-study on the IN gene where similar IN-specific phenotypic resistance assays were used to analyze the RC in patients who failed treatment with integrase stand transfer inhibitors (INSTIs).
The introduction of INSTIs has been an important step for ART. Resistance against these compounds *in vivo* is generally associated with selection of one of three (alternative) primary mutations: Y143C/R, Q148K/H/R or N155H, representing three distinct and independent resistance pathways (Fun A. *et al*.,2018). The mechanisms that drives the selection of a specific pathway and the absence of overlap between these pathways are still poorly understood. Therefore the aim of the present study was to investigate the impact of the HIV-1 genetic background in the IN gene on the selection of a specific resistance pathway.
Recombinant viruses were generated containing the viral IN from the basal samples of 5 patients in whom raltegravir (RAL) resistance mutations subsequently developed through the three different pathways: 2 patients developed the G140S+Q148H resistance pathway, 2 developed the N155H resistance pathway and 1 developed the Y143R resistance pathway.
The replication kinetics, in the presence and in the absence of drugs, of the recombinant clones from each patient bearing

the naturally selected primary mutation (obtain by *in vitro* site-directed mutagenesis of the wild type sequence) was compared to that of clones bearing the primary mutation of the other pathways.
In the absence of INSTIs, resistant molecular clones are less fit than wild type clones, and the Q148H clones show the lowest RC compared to N155H or Y143R clones, regardless of the genetic background. The RC of Q148H based pathways was always restored by the presence of G140S.
Indeed, despite the higher resistance to INSTIs, strains carrying Q148H alone indeed are rarely observed as a dominant population in patients failing RAL treatment (Quercia R. *et al*, 2009). The N155H mutation conferred an inferior resistance to RAL, but reduced RC only moderately. Finally the Y143R pathway conferred good resistance to RAL, also at the expense of a depressed RC. Recombinant clones with the G140S/Q148H combination showed a higher RC both in the presence and in the absence of INSTIs, compared to the other mutational pathways, regardless of the genetic background, suggesting that the genetic background of HIV IN gene at baseline is not determinant for the selection of the naturally observed INSTI resistance mutational pathway in all of these patients. These findings, obtained with a phenotypic analysis, are easily reconciled with those obtained by deep sequencing of the viral quasispecies *in vivo* during the early phases of treatment failure. Fun A. and colleagues (Fun A. *et al.,*2018) investigated the prevalence of viral variants during the evolution of RAL resistance and their role in determining selection of a particular resistance pathway. They observed multiple resistance pathways that competed for dominance, frequently resulting in a switch of the dominant population over time towards the fittest variant or even multiple variants of similar fitness that can coexist in the viral population. A possible explanation on the selection of specific resistance pathway could be the so-called "hitchhiking" effect: a particular variant might have a fitness

advantage that is located outside the investigated region. They also concluded that the generation of a specific RAL resistant variant was not predisposed in the genetic background of the viral IN. The present study therefore provides a phenotypic explanation that the virus in different patients does not necessarily develop the resistance pathway more appropriate to its IN genetic background.

Our results and data from clinical trials and from other studies that analyze the impact of the different RAL resistance pathways on viral fitness by site-directed mutagenesis into molecular backbone (Hu Z. *et al*., 2010), suggest that in some patients the N155H pathway might emerge first due to its better RC and its highest selective advantage in than the single Q148H pathway. Moreover both substitutions result from single nucleotide changes, excluding the possibility that selection is biased by sequential nucleotide changes implying transient selection of an intermediate amino acid with a potential for altering viral fitness (Quercia R. *et al.*, 2009). With the addition of the G140S (or E138K/A) secondary mutation to Q148H pathway enjoys a substantial fitness advantage compared to other RAL resistant pathways and eventually becomes the dominant species in the viral population (Hu Z. *et al*., 2010)

Dolutegravir (DTG) is a next-generation INSTI with an increased genetic barrier to resistance respect to first-generation INSTIs such as RAL. Although limited data about *in vivo* selection of resistance to DTG have been reported, *in vitro* standard phenotypic assays show that DTG selects few mutations (L101I, T124A, S153FY), that confer only limited resistance to the drug (Saladini F. *et al*., 2019). In this study, phenotypic assays were used to investigate how the three described mutational pathways potentially decrease DTG activity. Different concentrations of DTG were tested *in vitro* against recombinant molecular clones carrying RAL resistance mutations. In this *in vitro* study DTG suppressed the growth of all recombinant molecular clones with a starting concentration of 12 nM.

Molecular clones with isolated Y143R, Q148H and N155H resistance mutations did not affect susceptibility to DTG as they did to RAL. By contrast, in our hands, the combination G140S/Q148H did affect DTG efficacy, albeit not at the extent observed for RAL. This is consistent with other data based on *in vitro* resistance selection using wild type HIV-1 (Seki T. *et al*., 2015), the Q148H confers negligible resistance to DTG and only the development of G140S as a secondary mutations leads to partial recovery in RC and partial resistance to DTG (Canducci F. *et al*., 2011); (Saladini F., personal communication 2018).

These results confirm that DTG has a high barrier to the development of resistance and even the presence of RAL resistance mutations does not profoundly affect DTG IC50, providing an explanation to the rarity of clinical DTG resistance and to its higher clinical efficacy (Laskey S.B. *et al*., 2016).

In conclusion the Q148 pathway may be initially hampered by the need to select both the primary resistance mutation and the compensatory mutations to achieve its best performance. In most patients the N155 or the Y143 pathways may be selected by chance and be provisional. Their replacement by the Q148H pathway has been indeed observed *in vivo* and it possibly occurs in more patients after a brief and undocumented appearance of the other mutational pathways.

Abbreviations

3TC: lamivudine
ABC: abacavir
ADR: acquired HIV drug resistance
AIDS: acquired immunodeficiency syndrome
APV: amprenavir
ARCA: Antiviral Response Cohort Analysis
ART: antiretroviral therapy
ATV: atazanavir
AZT: zidovudine
BIC: bictegravir
CA: CCR5 antagonist
CAB: cabotegravir
CNS: central nervous system
CPE: cytopathic effect
CRFs: circulating recombinant forms
d4T: stavudine
ddC: zalcitabine
ddI: didanosine
DHHS: department of health and human services
DLV: delavirdine
DMEM: dulbecco's modified eagle medium
dNTP: deoxyribonucleotide triphosphate
DOR: doravirine
DRV: darunavir
DTG: dolutegravir
EFV: efavirenz
ETR: etravirine
EVG: elvitegravir
FC: fold change
FCS: fetal calf serum
FDA: food and drug administration
FDC: fixed dose combination
FI: fusion inhibitor
FPV: fosamprenavir
FSU: countries of the former Soviet Union
FTC: emtricitabine
GFP: green fluorescent protein
HAART: highly active antiretroviral therapy
HIV: human immunodeficiency virus

HIVDB: Stanford HIV Drug Resistance Database
IAS-USA: international antiviral society-USA
IBA: ibalizumab-uiyk
IC50: 50% inhibitory concentration
IC95: 95% inhibitory concentration
IDV: indinavir
IN: integrase
INSTI: integrase strand transfer inhibitor
IQR: interquartile range
LB: Luria Bertani
LMICs: low- and middle-income countries
LPV: lopinavir
MCV: maraviroc
MSM: men who have sex with men
NFV: nelfinavir
NGS: next-generation sequencing
NNRTI: non-nucleoside reverse transcriptase inhibitor
NRTI: nucleoside and nucleotide reverse transcriptase inhibitor
NVP: nevirapine
OBT: optimized background therapy
PAI: postattachment inhibitor
PBMCs: peripheral blood mononuclear cells
PCR: polymerase chain reaction
PI: protease inhibitor
PR: protease
RAL: raltegravir
RC: replicative capacity
RFV: relative fluorescence values
RPV: rilpivirine
RT: reverse transcriptase
RTV: ritonavir
SQV: saquinavir
SSA: sub-Saharan Africa
SSEA: south and southeast Asia
T-20: enfuvirtide
TAF: tenofovir alafenamide fumarato
TAMs: thymidine analogue mutations
TDF: tenofovir
TDR: transmitted drug resistance
TPV: tripranavir
UNAIDS: joint united nations programme on HIV/AIDS

URFs: unique recombinant forms
WHO: world health organization

References

Adachi A, Gendelman HE, Koenig S, Folks T, Willey R, Rabson A, Martin MA. (1986). Production of acquired immunodeficiency syndrome-associated retrovirus in human and nonhuman cells transfected with an infectious molecular clone. J Virol. 59(2):284-91.

Ammaranond P, Sanguansittianan S. (2012). Mechanism of HIV antiretroviral drugs progress toward drug resistance. Fundam Clin Pharmacol. 26(1):146-61.

Anstett K, Brenner B, Mesplede T, Wainberg MA. (2017). HIV drug resistance against strand transfer integrase inhibitors. Retrovirology. 14(1):36.

Arenas M. (2015). Genetic Consequences of Antiviral Therapy on HIV-1. Comput Math Methods Med. 2015:395826.

Bagnarelli P, Fiorelli L, Vecchi M, Monachetti A, Menzo S, Clementi M.(2003) Analysis of the functional relationship between V3 loop and gp120 context with regard to human immunodeficiency virus coreceptor usage using naturally selected sequences and different viral backbones. Virology. 307(2):328-40.

Beccari MV, Mogle BT, Sidman EF, Mastro KA, Asiago-Reddy E, Kufel WD. (2019). Ibalizumab, a Novel Monoclonal Antibody for the Management of Multidrug-Resistant HIV-1 Infection. Antimicrob Agents Chemother. 63(6).

Brooks KM, Sherman EM, Egelund EF, Brotherton A, Durham S, Badowski ME, Cluck DB. (2019). Integrase Inhibitors: After 10 Years of Experience, Is the Best Yet to Come? Pharmacotherapy. 39(5):576-598.

Canducci F, Ceresola ER, Boeri E, Spagnuolo V, Cossarini F, Castagna A, Lazzarin A, Clementi M. (2011). Cross-resistance profile of the novel integrase inhibitor Dolutegravir (S/GSK1349572) using clonal viral variants selected in patients failing raltegravir. J Infect Dis. 204(11):1811-5.
Clutter DS, Jordan MR, Bertagnolio S, Shafer RW. (2016). HIV-1 drug resistance and resistance testing. Infect Genet Evol. 46:292-307.

Colafigli M, Torti C, Trecarichi EM, Albini L, Rosi A, Micheli V, Manca N, Penco G, Bruzzone B, Punzi G, *et al.* (2012). Evolution of transmitted HIV-1 drug resistance in HIV-1-infected patients in Italy from 2000 to 2010. Clin Microbiol Infect. 18(8):E299-304.

Collier DA, Monit C, Gupta RK. (2019). The Impact of HIV-1 Drug Escape on the Global Treatment Landscape. Cell Host Microbe. 26(1):48-60.

Cong ME, Heneine W, García-Lerma JG. (2007). The fitness cost of mutations associated with human immunodeficiency virus type 1 drug resistance is modulated by mutational interactions. J Virol. 81(6):3037-41.

Dau B, Holodniy M. (2009). Novel targets for antiretroviral therapy: clinical progress to date. Drugs. 69(1):31-50.

Dionne B. (2019). Key Principles of Antiretroviral Pharmacology. Infect Dis Clin North Am. 33(3):787-805.

Engelman AN. (2019). Multifaceted HIV integrase functionalities and therapeutic strategies for their inhibition. J Biol Chem.

Fabeni L, Alteri C, Di Carlo D, Orchi N, Carioti L, Bertoli A, Gori C, Forbici F, Continenza F, Maffongelli G, *et al.* (2017). Dynamics and phylogenetic relationships of HIV-1 transmitted drug resistance according to subtype in Italy over the years 2000-14. J Antimicrob Chemother. 72(10):2837-2845.

Franzetti M, De Luca A, Ceccherini-Silberstein F, Spagnuolo V, Nicastri E, Mussini C, Antinori A, Monno L, Vecchiet J, Fanti I,*et al.* (2018). Evolution of HIV-1 transmitted drug resistance in Italy in the 2007-2014 period: A weighted analysis. J Clin Virol. 106:49-52.

Franzetti M, Lai A, Simonetti FR, Bozzi G, De Luca A, Micheli V, Meraviglia P, Corsi P, Bagnarelli P, Almi P, *et al.* (2012). High burden of transmitted HIV-1drug resistance in Italian patients carrying F1 subtype. J Antimicrob Chemother. 67(5):1250-3.

Fun A, Leitner T, Vandekerckhove L, Däumer M, Thielen A, Buchholz B, Hoepelman AIM, Gisolf EH, Schipper PJ, Wensing AMJ, Nijhuis M. (2018). Impact of the HIV-1 genetic background and HIV-1 population size on the evolution of raltegravir resistance. Retrovirology.15(1):1.

Günthard HF, Calvez V, Paredes R, Pillay D, Shafer RW, Wensing AM, Jacobsen DM, Richman DD. (2019). Human Immunodeficiency Virus Drug Resistance: 2018 Recommendations of the International Antiviral Society-USA Panel. Clin Infect Dis. 68(2):177-187.

Harrison L, Castro H, Cane P, Pillay D, Booth C, Phillips A, Geretti AM, Dunn D, UK Collaborative Group on HIV Drug Resistance and the UK Collaborative HIV Cohort Study (UK CHIC). (2010). The effect of transmitted HIV-1 drug resistance on pre-therapy viral load. AIDS. 24(12):1917-22

Hemelaar J, Elangovan R, Yun J, Dickson-Tetteh L, Fleminger I, Kirtley S, Williams B, Gouws-Williams E, Ghys PD; WHO–UNAIDS Network for HIV Isolation Characterisation. (2019). Global and regional molecular epidemiology of HIV-1, 1990-2015: a systematic review, global survey, and trend analysis. Lancet Infect Dis. 19(2):143-155.

Hicks C, Gulick RM. (2009). Raltegravir: the first HIV type 1 integrase inhibitor. Clin Infect Dis. 48(7):931-9.

Hofstra LM, Sauvageot N, Albert J, Alexiev I, Garcia F, Struck D, Van de Vijver DAMC, Åsjö B, Beshkov D, Coughlan S, *et al*. (2016). Transmission of HIV Drug Resistance and the Predicted Effect on Current First-line Regimens in Europe. Clin Infect Dis. 62(5):655-663

Hu Z, Kuritzkes DR. (2010). Effect of raltegravir resistance mutations in HIV-1 integrase on viral fitness. J Acquir Immune Defic Syndr. 55(2):148-55.

Kandel CE, Walmsley SL. (2015). Dolutegravir- a review of the pharmacology, efficacy, and safety in the treatment of HIV. Drug Des Devel Ther. 9:3547-55.

Knipe DM, Howely PM. (2013). Fields Virology, sixth edition. ISBN-13: 978-1-4511-0563-6

Kuritzkes DR. (2004). Preventing and managing antiretroviral drug resistance. AIDS Patient Care STDS. 18(5):259-73.

Laskey SB, Siliciano RF. (2016). Quantitative evaluation of the antiretroviral efficacy of dolutegravir. JCI Insight. 1(19):e90033.

McCluskey SM, Siedner MJ, Marconi VC. (2019). Management of Virologic Failure and HIV Drug Resistance. Infect Dis Clin North Am. 33(3):707-742.

Menzo S, Rusconi S, Monachetti A, Colombo MC, Violin M, Bagnarelli P, Varaldo PE, Moroni M, Galli M, Balotta C, Clementi M. (2000). Quantitative evaluation of the recombinant HIV-1 phenotype to protease inhibitors by a single-step strategy. AIDS.14(9):1101-10.

Neijzen RW, Van Maarseveen EM, Hoepelman AI, Wensing AM, Bonora S, D'Avolio A, Mudrikova T. (2016). Continuous intravenous infusion of enfuvirtide in a patient with a multidrug-resistant HIV strain. Int J Clin Pharm. 38(4):749-51.

Nijhuis M, Deeks S, Boucher C. (2001). Implications of antiretroviral resistance on viral fitness. Curr Opin Infect Dis. 14(1):23-8.

Pandit NS, Chastain DB, Pallotta AM, Badowski ME, Huesgen EC, Michienzi SM. (2019). Simplifying ARV Therapy in the Setting of Resistance. Curr Infect Dis Rep. 21(10):38.

Paraskevis D, Hatzakis A. (2019). Global molecular epidemiology of HIV-1: the chameleon challenge. Lancet Infect Dis. 19(2):114-115.

Park TE, Mohamed A, Kalabalik J, Sharma R. (2015). Review of integrase strand transfer inhibitors for the treatment of human immunodeficiency virus infection. Expert Rev Anti Infect Ther. 13(10):1195-212.

Pingen M, Nijhuis M, de Bruijn JA, Boucher CA, Wensing AM. (2011). Evolutionary pathways of transmitted drug-resistant HIV-1. J Antimicrob Chemother. 66(7):1467-80.

Quercia R, Dam E, Perez-Bercoff D, Clavel F. (2009). Selective-advantage profile of human immunodeficiency virus type 1 integrase mutants explains *in vivo* evolution of raltegravir resistance genotypes. J Virol. 83(19):10245-9.

Ramkumar K, Neamati N.(2010). Raltegravir: The evidence of its therapeutic value in HIV-1 infection. Core Evid. 4:131-47.

Rhee SY, Blanco JL, Jordan MR, Taylor J, Lemey P, Varghese V, Hamers RL, Bertagnolio S, de Wit TF, Aghokeng AF *et al.* (2015). Correction: Geographic and Temporal Trends in the Molecular Epidemiology and Genetic Mechanisms of Transmitted HIV-1 Drug Resistance: An Individual-Patient- and Sequence-Level Meta-Analysis. PLoS Med. 12(6):e1001845.

Rhee SY, Grant PM, Tzou PL, Barrow G, Harrigan PR, Ioannidis JPA, Shafer RW. (2019). A systematic review of the genetic

mechanisms of dolutegravir resistance. J Antimicrob Chemother. 74(11):3135-3149.

Rossetti B, Di Giambenedetto S, Torti C, Postorino MC, Punzi G, Saladini F, Gennari W, Borghi V, Monno L, Pignataro AR, *et al.* (2018). Evolution of transmitted HIV-1 drug resistance and viral subtypes circulation in Italy from 2006 to 2016. HIV Med. 19(9):619-628.

Saladini F, Giannini A, Boccuto A, Dragoni F, Appendino A, Albanesi E, Vicenti I, Zazzi M. (2019). Comparable *in vitro* activity of second-generation HIV-1 integrase strand transfer inhibitors (INSTIs) on HIV-1 clinical isolates with INSTI resistance mutations. Antimicrob Agents Chemother. pii: AAC.01717-19.

Saladini F, Giannini A, Boccuto A, Dragoni F, Appendino A, Albanesi E, Vicenti I, Zazzi M. (2018). Comparable predicted and phenotypic susceptibility to dolutegravir and bictegravirin first generation INSTI resistant HIV. Oral communication at 2rd National Congress of the Italian Society for Virology "SIV-ISV".

Schauer GD, Huber KD, Leuba SH, Sluis-Cremer N.(2014). Mechanism of allosteric inhibition of HIV-1 reverse transcriptase revealed by single-molecule and ensemble fluorescence. Nucleic Acids Res.
42(18):11687-96.

Seki T, Suyama-Kagitani A, Kawauchi-Miki S, Miki S, Wakasa-Morimoto C, Akihisa E, Nakahara K, Kobayashi M, Underwood MR, Sato A, *et al*. (2015). Effects of raltegravir or elvitegravir resistance signature mutations on the barrier to dolutegravir resistance *in vitro*. Antimicrob Agents Chemother. 59(5):2596-606.

Shah BM, Schafer JJ, Desimone JA Jr. (2014). Dolutegravir: a new integrase strand transfer inhibitor for the treatment of HIV. Pharmacotherapy. 34(5):506-20.

Smyth RP, Davenport MP, Mak J. (2012). The origin of genetic diversity in HIV-1. Virus Res. 169(2):415-29.

Tang MW, Shafer RW. (2012). HIV-1 antiretroviral resistance: scientific principles and clinical applications. Drugs. 72(9):e1-25.

Warnke D, Barreto J, Temesgen Z. (2007). Antiretroviral drugs. J Clin Pharmacol. 47(12):1570-9.

Wensing AM, Calvez V, Günthard HF, Johnson VA, Paredes R, Pillay D, Shafer RW, Richman DD. (2017). Update of the Drug Resistance Mutations in HIV-1. Top Antivir Med. 24(4):132-133.

Xu Y, Peng X, Peng X, Ji S, Chen B, Wang L, Lu X, Xie T, Sun T, Wang H, *et al*. (2018). Characterization of HIV-1 subtypes and transmitted drug resistance among treatment-naïve HIV-infected individuals in Zhejiang, China, 2014-2017. Arch Virol.163(8):2233-223.

Yang WL, Kouyos RD, Böni J, Yerly S, Klimkait T, Aubert V, Scherrer AU, Shilaih M, Hinkley T, Petropoulos C, *et al.* (2015). Persistence of transmitted HIV-1 drug resistance mutations associated with fitness costs and viral genetic backgrounds. PLoS Pathog.11(3):e1004722.

Zhang X, Ding X, Zhu Y, Chong H, Cui S, He J, Wang X, He Y. (2019). Structural and functional characterization of HIV-1 cell fusion inhibitor T20. AIDS. 33(1):1-11.

Web References

https://www.who.int/en/news-room/fact-sheets/detail/hiv-aids
https://www.unaids.org/sites/default/files/media_asset/unaids-data-2018_en.pdf
https://www.who.int/hiv/data/en/
https://www.who.int/en/news-room/fact-sheets/detail/hiv-aids
https://www.unaids.org/en/resources/documents/2017/20170720_Global_AIDS_update_2017
https://www.who.int/hiv/data/en/)
https://aidsinfo.nih.gov/understanding-hiv-aids/infographics/25/fda-approval-of-hiv-medicines
https://www.accessdata.fda.gov/drugsatfdadocs/label/2017/022145s036,203045s013,205786s004lbl.pdf
https://www.accessdata.fda.gov/drugsatfda_docs/label/2018/204790s016s018lbl.pdf
https://www.accessdata.fda.gov/drugsatfda_docs/label/2018/204790s016s018lbl.pdf
https://www .who.int/hiv/ pub/drugresistance/ hivdr-report-2019/en/
https://hivdb.stanford.edu/page/surveillance-map/
http://www.dbarca.net
https://spread.crp-sante.lu/public/tdr
http://hivdb.stanford.edu